

# The Messenger



No. 140 – June 2010

Summaries of all E-ELT instrument concept studies  
20 years of FORS operations  
CRIRES search for exoplanets  
Support for Chile earthquake victims



# Twenty Years of FORS Science Operations on the VLT

Gero Rupprecht<sup>1</sup>  
 Hermann Bönnhardt<sup>2</sup>  
 Sabine Moehler<sup>1</sup>  
 Palle Møller<sup>1</sup>  
 Ivo Saviane<sup>1</sup>  
 Bodo Ziegler<sup>1</sup>

<sup>1</sup> ESO

<sup>2</sup> Max-Planck-Institut für Sonnensystemforschung, Katlenburg-Lindau, Germany

Celebrating the double jubilee of ten years in operation of FORS1 and FORS2, this article summarises, from an insider's point of view, the history of the FORS instruments, arguably the most prolific on ESO's Very Large Telescope. The FORS story began in the early 1990s and FORS1 was the first VLT user instrument to be commissioned. Both FORS instruments have undergone considerable evolution and quickly parted from the original concept of being identical twins. They have both made major contributions to scientific research and have helped shape VLT operations. In 2009, FORS1 was retired, but FORS2 continues, fusing the best of both.

The first of April 1999 marks the day science operations started on the Very Large Telescope (VLT), with Unit Telescope 1 (UT1, Antu) only. Two instruments were installed on Antu: ISAAC, (the Infra-red Spectrometer And Array Camera) designed and built by ESO, and FORS1, (the first FOcal Reducer/low dispersion Spectrograph) created by VIC, the VLT Instrument Consortium, composed of the observatories of Heidelberg, Göttingen and Munich (Germany). Exactly one year later, FORS2 took up duty on Paranal on UT2 Kueyen. Since then the FORS twins (Figure 1) have provided astronomers with a wealth of observational data of excellent quality. The successful teamwork of the two FORS instruments came to an end on 1 April 2009 with the retirement of FORS1 after exactly ten years of operations. FORS2 reached the ten-year mark one year later, so on 1 April of this year, the two FORS instruments together had racked up a total of 20 years of successful science operations.



Figure 1. The FORS twins, in separate UTs.

## Some pre-history

The origins of what became FORS date back a long way. The report of the Working Group on Imaging and Low Resolution Spectroscopy (VLT Report No. 52) in July 1986 recommended building “a set of general purpose focal reducers at one Nasmyth focus on each of the (four) array elements” (that is, the UTs). The only direct legacy of this far-reaching recommendation are the twin FORS instruments. In June 1989 ESO issued the VLT Instrumentation Plan asking for comments and expressions of interest from European institutes. In response to the ESO call, a consortium was formed by Immo Appenzeller of the Landessternwarte in Heidelberg as Principal Investigator, with Rolf Kudritzki of the University of Munich and Klaus Fricke of the University of Göttingen as co-Investigators. This consortium intended to submit a proposal for the medium-high resolution spectrograph, now known as UVES. ESO, however, finally decided to build this instrument internally, so the consortium changed course at short notice and entered the competitive tender with a bid for the focal reducer/low dispersion spectrograph instead! The bid was successful, against one competing proposal, and after lengthy contract negotiations involving the project institutes, their host universities and, by the end, three different German federal states as well as several federal ministries, the contract with ESO was signed in December 1991. The contract foresaw ESO paying for the FORS

hardware and the provision of the detector systems; in addition the consortium invested substantially in its infrastructure in support of the FORS project and about 130-person years of work until the completion of the project. At the final acceptance of the FORS instruments by ESO, the FORS consortium even stayed under budget. In return for its effort, the consortium was granted 66 nights of guaranteed observing time to be spent on science programmes using the two FORS instruments in visitor mode.

A highly motivated team of astronomers and engineers jumped to the task of designing the first VLT science instrument, and the Preliminary Design Review took place in April 1992. Originally it was planned to build two identical copies of FORS and equip them with identical sets of filters and grisms. During the Final Design Phase it was, however, decided to purchase only one set of the expensive polarisation optics; the Wollaston prism and the linear and circular retarder plate mosaics being among the largest ever made, at least for astronomical applications. The money saved was instead invested in high-resolution collimator optics, which avoided vignetting out to the corners of the CCD and, in addition, also paid for the Mask Exchange Unit (MXU), later incorporated in FORS2.

The Final Design Review was passed at the end of 1994. In 1996 system integration and tests started in an assembly hall rented at DLR (Deutsches Zentrum für





Figure 2. Provisional Acceptance in Europe of FORS1 at DLR Oberpfaffenhofen in June 1998. From left to right: front row Heinz Kotzowski, Immo Appenzeller, Sandro D'Odorico, Bernard Muschielok, Walter Seifert, Wolfgang Hummel. Middle row: Guy Monnet, Roberto Gilmozzi, Thomas Szeifert. Back row: Harald Nicklas, Rolf Kudritzki, Gerd Wieland, Gero Rupprecht, Reinhold Häfner, Wolfgang Meisl, Achim Hess. *Tempus fugit ...*

was quickly but carefully dismantled again, disassembled and painstakingly dried and cleaned using huge amounts of optical paper! The reason for this "flood" was a burst cooling hose inside the telescope adapter/rotator. After replacement of the hose, FORS1 was re-mounted and saw its true first light during the night of 15 to 16 September 1998 (Appenzeller et al., 1998).

Luft- und Raumfahrt) in Oberpfaffenhofen. It was here that an accident happened during a handling operation, and the fully equipped collimator section of FORS1, in total about 600 kg of mechanics, optics and electronics, fell from the crane. Rumours spread quickly that someone had been killed, which fortunately turned out not to be true. Nobody had been hurt, not even the optics, the only damage was to the metal housing and the floor of the DLR integration hall. Now ordering all major instrument parts twice paid off: within three weeks the damaged part had been replaced by the corresponding piece from FORS2 and a replacement ordered, which arrived by the time it was needed for the assembly of FORS2! After extensive tests, Preliminary Acceptance of FORS1 in Europe was declared by ESO in July 1998 (see Figure 2) and the instrument was shipped to Paranal for installation at the VLT.

light (see Tarengi et al., 1998) had occurred just weeks before. In September, on-site assembly and testing in the Auxiliary Telescope Hall (which was itself still under construction) was finished and FORS1 was attached to the Antu Cassegrain focus. In the hours preceding what was supposed to become the FORS1 first light on the night sky, one of us discovered, to everybody's horror, that there was water inside the instrument! FORS1

It turned out that the instrument was in optimum focus when mounted, and the stars showed an image quality of 0.6 arc-seconds in the very first image taken with the instrument on sky! The first exposures of an interesting celestial object resulted in the famous image of spiral galaxy NGC 1232, which, one year later, the readers of *Sky and Telescope* magazine voted to be among the ten most inspiring astronomical images of the 20th century (Figure 3)!

### Commissioning

Upon arrival of FORS1 and the integration team on site in August 1998, Paranal was still a full-blown construction site. You could only enter the Control Building wearing a hard hat — there were no proper ceilings, the rooms that later became offices had no windows, there were no sanitary facilities available, etc.! UT1 was still undergoing commissioning — first



Figure 3. Named one of the most inspiring astronomical images of the 20th century: the FORS1 first light image of the galaxy NGC 1232.

A further (and final!) water incident during the second commissioning run, again due to a hose in the telescope adapter, earned FORS1 the nickname “Yellow Submarine” among the mountain crew. This had no effect, however, on the excellent relationship between the FORS consortium team and the colleagues on Paranal who gave superb support to the commissioning activities. One important commissioning task involved the verification on the telescope of the specified image motion due to telescope tilt and instrument rotation. To accomplish the task, the mechanics specialist from the instrument team spent several nights laboriously driving FORS through endless measurement cycles that confirmed the finite element prediction and first assessments at a telescope simulator in Europe: image motion is so small, below a quarter of a CCD pixel in two hours for the standard collimator, that FORS is known to be the only focal reducer type instrument to allow the image distortion by weak lensing around remote galaxy clusters to be measured. After two weeks of Science Verification in January 1999, FORS1 was finally handed over to ESO for operation at the VLT. As a last step, now performed by ESO, the instrument was “Paranalised”, i.e. its operation and control scheme were tuned to fully match the observatory operation environment and science operations concept. During the VLT inauguration ceremony in March 1999, a few weeks before science operations began, FORS1 delivered some of the sharpest ground-based images ever taken without special techniques, such as adaptive optics or speckle imaging: 0.25 arcseconds full width at half maximum in *I*-band — a very promising start indeed!

One side effect of being the first instrument on the VLT was the need to record all night activities, so the FORS team invented the structure of the night logs, which is still basically the same today, although the night astronomer can now rely on software tools to fill them, which the team did not have at their disposal back in 1999.

On 1 April 1999 Massimo Tarenghi, the first director of the VLT, declared that from now on Paranal was no longer a construction site, but a working observatory

and FORS1, together with ISAAC, opened the science operations period at the VLT. In September 1999 its twin, FORS2 arrived on Paranal and entered regular service on UT2 Kueyen in April 2000 (without the embarrassment that FORS1 had to go through). Although this had not been foreseen, both FORS instruments changed telescopes several times in the following years to optimise the use of the UTs as telescopes came online one after the other. Every Cassegrain focus of the VLT has by now successfully hosted at least one FORS at some time, a testimony to the precision with which the UTs were built to be identical, and to the robustness of the FORS instruments at the VLT!

#### Upgrades and the FORS merger

Earlier than originally expected, new CCDs with a better red sensitivity became available, so work on the replacement of one of the original TEK 2k × 2k detectors started when FORS2 was barely on the telescope. The Garching Optical Detector Team provided a CCD mosaic with two MIT 2k × 4k (15 μm pixel) chips complete with a new FIERA controller, and the system was successfully commissioned in October 2001. It has been in continuous science operations on FORS2 since April 2002, only recently interrupted sometimes when the blue-sensitive FORS1 CCD is mounted. Upgrading FORS1 with a blue-sensitive CCD mosaic took much longer: a mosaic of blue sensitive e2v CCDs with the same format as the red system on FORS2 was ready for commissioning only in early 2007. Since the retirement of FORS1 in 2009 it has been offered in visitor mode on FORS2.

In addition to the replacement of the detectors, ESO improved the efficiency of both FORS instruments by acquiring a number of highly efficient Volume Phased Holographic Grisms (VPHG) as well as various high throughput broad- and medium-band filters.

The need to free a VLT Cassegrain focus for X-shooter (Vernet et al., 2009), the first of the second generation VLT instruments, sealed the fate of FORS1. The decision was to keep FORS2 operational since it is younger and is operationally

more versatile due to the MXU. From the electro-mechanical point of view both FORS instruments are almost identical, so it was possible, with only a small effort, to transfer the polarimetry optics (Wollaston prism and the two retarder plate mosaics) from FORS1 to FORS2, to calibrate and commission this important mode and to offer it from Period 83 onwards with FORS2.

#### FORS: popular, productive and highly cited

From the very first period on the VLT, FORS1 was the most popular instrument in terms of requested observing time, and it was only surpassed in popularity by UVES at the time FORS2 came online and the demand for FORS time could be divided between the two instruments (Figure 4). The demand for both FORS instruments remained high until the day of FORS1 decommissioning. This is also reflected in their productivity. In Figure 5 we plot the number of refereed publications per year as a function of the time after the instrument came into operation. It is clearly seen that FORS1 and UVES were the two most productive instruments for the first five years of their careers, while FORS2 takes third position. Both FORS instruments together had produced 1161 refereed papers by the end of 2009 with a total of 40 783 citations.

Only after FORS2 was upgraded did FORS1 drop in popularity, as many users moved to FORS2 instead. The publication rate is, to some extent, a result of how much time was allocated. Looking instead at the publication efficiency, i.e. publication rate per allocated night, ISAAC and FORS2 currently produce roughly 0.75 refereed papers per observing night, UVES produces 0.9, while FORS1, during its last few periods, produced about 1.0 paper per night and was the most publication-efficient VLT instrument so far.

If we look at the number of citations of VLT papers, it is symptomatic that at least one of the two FORS instruments was involved in eight of the ten most cited VLT papers. The most-cited papers are those of large collaborations that include all major telescopes — the Hubble

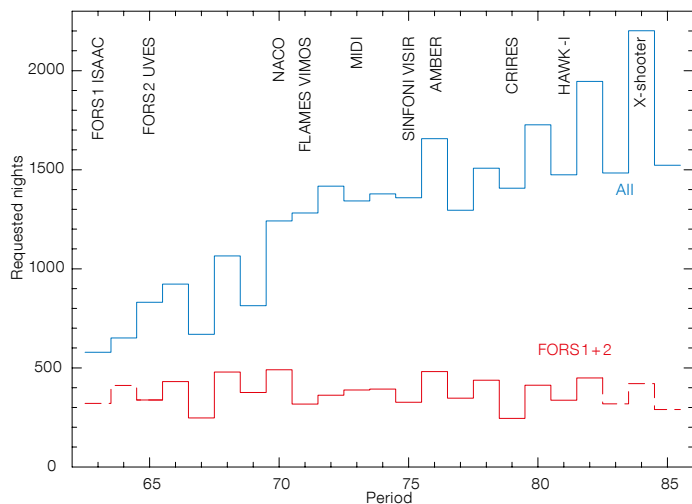


Figure 4. Breakdown of nights requested for all VLT and VLTI instruments (blue) and FORS (red — solid line both FORS instruments, dashed line for only one FORS).

to the South Galactic pole also contained a quasar at  $z = 3.4$ . Several papers exploited this deep field investigating for example evolving luminosity functions and star formation rates. However, the FDF project was, from the start, also a spectroscopic campaign obtaining about 700 spectra of high-redshift galaxies to study, for example, their metal enrichment and mass evolution.

As already mentioned the FORS instruments are the only focal reducers to allow measurements of weak gravitational lensing. Bradac et al. (2005) used FORS data of a very massive X-ray cluster to perform a combined analysis of both strong lensing (multiple images of background sources) and weak lensing (distortion of background sources) effects to determine the cluster's mass. They used the high resolution collimator of FORS1 to achieve an internal astrometric accuracy of 0.01 to 0.015 arcseconds.

Both FORS instruments were involved in the first conclusive demonstration that long-duration, energetic gamma-ray bursts (GRBs) are associated with the deaths of massive stars (also known as hypernovae). Hjorth et al. (2003) used long-slit spectra of GRB030329 obtained with FORS1 and FORS2 over a period of four weeks after the detection of this high-redshift GRB to fit the light curve of the underlying supernova. Analysis of these observations strongly favoured the collapsar model for typical GRBs.

FORS1 in particular contributed significantly to the study of asymmetry effects in Type Ia supernovae, employing its spectro-polarimetric (PMOS) mode. Electron scattering in the ejecta of a supernova polarises its light and polarimetry therefore allows information about possible asymmetries in the ejecta to be derived. Wang et al. (2007) presented observations of 17 Type Ia supernovae, twelve of which were observed with FORS1 in its PMOS mode. They clearly show significantly higher polarisation in some emission lines compared to the continuum. This points towards a chemically clumpy structure of the outermost ejecta. Such clumpiness introduces a certain amount of randomness into the modelling of supernovae and may thus affect their use as standard candles.

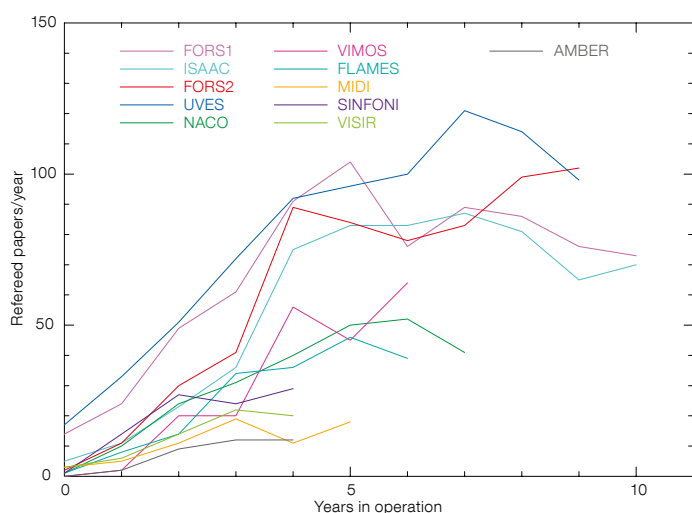


Figure 5. Number of refereed papers per year for all VLT and VLTI instruments in operation since 2005.

Space Telescope, Keck and the VLT. Typically those are produced by high-redshift supernova projects with up to almost 2000 citations. The most-cited paper exclusively involving the VLT currently has 643 citations and was based on data taken with both FORS1 and FORS2 (Hjorth et al., 2003; see also the science highlights below).

### Science highlights

As befits a multi-mode instrument like FORS, it has contributed to a broad range of science topics, some of which will be briefly reported below. Considering the huge number of publications and citations, it is obvious that the papers discussed below present a very limited

sample. We have tried to select publications that illustrate the wide variety of science topics addressed with FORS.

One of the first major scientific ventures by the FORS consortium was an imaging campaign for the FORS Deep Field (FDF; Appenzeller et al., 2004), with a sky coverage substantially larger than the Hubble Deep Field (HDF), see Figure 6. Across several semesters, many members of the three observatories of the FORS consortium spent several nights on Paranal, enjoying the desert life, since the Residencia had not yet been built. In the end, about 72 hours of integration time were spent on UBGRI images reaching limiting magnitudes similar to the Hubble Deep Field. The resulting catalogue of 8753 objects in this  $7 \times 7$  arcminute region close



**Figure 6.** Colour-composite of the FORS Deep Field formed by combining *UBgR* filter images (Appenzeller et al., 2004).

Moving from extragalactic to closer targets, in 1999 FORS1 also obtained the first spectra of globular cluster white dwarfs, the brightest of which have typical *V* magnitudes of 24–25. The high background added by myriads of brighter stars close by, most of them on the main sequence, made these observations a real challenge. Using FORS1 multi-object spectroscopy data observed with the high resolution (HR) collimator from 1999–2001, Moehler et al. (2004) verified for the first time that the average mass of hot globular cluster white dwarfs differs significantly from the average mass of field white dwarfs. Their detection of only hydrogen-rich white dwarfs was the first indication that the number of hydrogen-rich vs. helium-rich white dwarfs differs between field and globular cluster stars, which raises questions about our understanding of white dwarf evolution.

Coming even closer to home the FORS instruments also pointed their optics to extrasolar planets, and more specifically to transiting planets. Moutou et al. (2004) used FORS2 with its HR collimator to achieve a spatial resolution of 0.125 arcseconds and observed OGLE-TR-132b during a transit. With these data they achieved an unprecedented relative photometric precision of 0.0012 mag, which allowed them to constrain the previously rather uncertain planetary parameters, despite the very shallow minimum of the light curve.

The outskirts of our own planetary system, the trans-Neptunian region, has also been explored with the FORS instruments. In fact most of the visible spectra of Trans-Neptunian Objects (TNOs) that exist in the astronomical archives were collected with one of the FORS instruments, and there are several indications for features attributable to alteration by water seen in these spectra: an intriguing detection indeed, since it may imply the existence of liquid or gaseous water in these objects for a couple of million years at a solar distance where it was not expected to exist.



### Operations and future prospects

When the VLT started science operations in 1999, the way the VLT was operated differed in many aspects from the La Silla model. The concept of observation blocks (OBs) was quite new, as was the excellent pointing precision of the UTs and the fact that you never needed to worry about focusing the instrument or the telescope — it was all designed and built into the system! But it was necessary to gain experience in building efficient OBs, otherwise one could waste a lot of precious observing time (one second of tele-

scope time on the VLT costs roughly one euro) with unnecessary instrument reconfiguration or telescope presets.

Although the optical concept of FORS looks quite simple, the technical realisation resulted in a complex instrument. Each FORS instrument contains more than 50 motors, most of them small precision motors driving, for instance, multislits with sub-arcsecond accuracy, but also some big ones used to turn heavy filter and grism wheels or to exchange collimators the size of a small telescope. Nevertheless both instruments hold

top positions on Paranal regarding reliability, thanks to the careful design, engineering, manufacture and testing done by the FORS consortium more than a decade ago. As true multi-mode instruments with a large number of available filters and grisms, the FORS instruments also present a particular challenge to the operations team at Paranal — every evening the correct set of components must be inserted and the necessary sequence of calibration OBs executed in the morning. This is now supported by software tools whose development was triggered by the difficulties our first Paranal post-docs encountered when they tried to stitch together the calibration sequences from the entries in faulty paper log sheets written by tired astronomers during the night!

Considering the long way we have come since then and the huge success achieved by the FORS instruments, it is understandable that many users did not like the decision to mothball FORS1 to give way to the new X-shooter. But we are looking forward to many exciting FORS2 observations and results in the years to come — after all, what would the VLT be without a sturdy, reliable imaging/low resolution spectrograph like FORS?

#### Acknowledgements

The authors are, or were at some time, members of the FORS Instrument Operations Team (IOT), and we would like to thank all the colleagues who contributed to the design, construction, commissioning and operation of these marvellous instruments.

First of all we thank the members of the FORS consortium under the leadership of Immo Appenzeller and his co-Investigators Klaus Fricke and Rolf Kudritzki, and all colleagues in Heidelberg (Walter Fürtig, Wolfgang Gässler, Claus Hartlieb, Roland Östreicher, Walter Seifert, Otmar Stahl), Göttingen (Klaus Beuermann, Frank Degenhardt, Ulrich Dünsing, Rainer Harke, Harald Nicklas, Harald Schink, Torsten Toeteberg, Walter Wellem) and Munich (Reinhold Häfner, Hans-Joachim Hess, Wolfgang Hummel, Walter König, Karl-Heinz Mantel, Wolfgang Meisl, Franz Mittermaier, Bernard Muschielok, Ludwig Schäffner, Karl Tarantik, Peter Well) for delivering and commissioning the FORS twins.

Sincere thanks go to Norma Hurtado and Julio Navarrete, who skilfully steered the UTs through most of the commissioning nights, and to Jason Spyromilio for his constant support, critical sympathy and inspiring humour during the commissioning runs.

The ESO FORS team provided invaluable input during the whole design and construction phase, based on their long experience in building ESO instruments: Sebastian Deiries, Sandro D'Odorico, Olaf Iwert, Heinz Kotzlowski, Jean-Louis Lizon, Walter Nees, Gianni Raffi, Roland Reiß, Rein Warmels, but in particular Bernard Delabre for his ideas concerning the optical layout. Science Operations with FORS has rested in different hands during the past

decade, thanks therefore to Emmanuel Jehin, Kieren O'Brien, Emanuela Pompei and Thomas Szeifert for their exceptional effort to keep the FORS instruments at the forefront of astronomical instrumentation, and to our current and former fellow members of the IOT. But no matter how good and reliable an instrument is — there will always be some problems with hard- and software. All are resolved quickly by the Paranal INS team, notably Miguel Riquelme and Pedro Baksai, as well as Carlo Izzo (for the pipeline), who therefore contributed decisively to the reputation of the FORS instruments as being amongst the best and most reliable instruments near and far — many thanks!

Last, but not least, we thank the staff in the ESO Garching library for providing the data for the citation statistics, and in OPO for providing the proposal statistics.

#### References

- Appenzeller, I. et al. 1998, *The Messenger*, 94, 1
- Appenzeller, I. et al. 2004, *The Messenger*, 116, 18
- Bradac, M. et al. 2005, *A&A*, 437, 49
- Hjorth, J. et al. 2003, *Nature*, 423, 847
- Moehler, S. et al. 2004, *A&A*, 420, 515
- Moutou, C. et al. 2004, *A&A*, 424, L31
- Tarengni, M. et al. 1998, *The Messenger*, 93, 4
- Wang, L., Baade, D. & Patat, F. 2007, *Science*, 315, 212

#### Links

For technical details on FORS see <http://www.eso.org/sci/facilities/paranal/instruments/fors/>.



A recent FORS image showing the massive young Galactic star cluster NGC 3603. Located at about 8 kpc, NGC 3603 is the nearest giant HII region. This colour image (7 × 7 arcminutes) was formed from FORS2 exposures taken through V, R and I filters. See release eso1005 for more details.



# A New Lenslet Array for the NACO Laser Guide Star Wavefront Sensor

Markus Kasper<sup>1</sup>  
 Gerard Zins<sup>2</sup>  
 Philippe Feautrier<sup>2</sup>  
 Jared O'Neal<sup>1</sup>  
 Laurence Michaud<sup>2</sup>  
 Patrick Rabou<sup>2</sup>  
 Eric Stadler<sup>2</sup>  
 Julien Charton<sup>2</sup>  
 Claudio Cumani<sup>1</sup>  
 Alain Delboulbe<sup>2</sup>  
 Christoph Geimer<sup>1</sup>  
 Gordon Gillet<sup>1</sup>  
 Julien Girard<sup>1</sup>  
 Nicolas Huerta<sup>1</sup>  
 Pierre Kern<sup>2</sup>  
 Jean-Louis Lizon<sup>1</sup>  
 Christian Lucuix<sup>1</sup>  
 David Mouillet<sup>2</sup>  
 Thibaut Moulin<sup>2</sup>  
 Sylvain Rochat<sup>2</sup>  
 Christian Sönke<sup>1</sup>

<sup>1</sup> ESO

<sup>2</sup> Laboratoire d'AstrOphysique de Grenoble, France

In February 2010, a new  $14 \times 14$  lenslet array was installed in the NAOS–CONICA (NACO) visible wavefront sensor. Compared to the previously available array, this new array has a shorter focal length and hence a field of view that is large enough for the extended laser guide star (LGS) spot. This successful upgrade results in improved adaptive optics correction delivered by NACO with the LGS.

Since 2007 NACO and SINFONI have regularly operated using a laser guide star on the VLT Unit Telescope 4 (UT4) (see Organisation Release eso0727). Theoretically, the performance of NAOS with an LGS should be close to the performance with a bright natural guide star (NGS), reduced by the unavoidable cone-effect of about 20% loss in  $K$ -band Strehl ratio. Considering a NACO–NGS peak performance of 50–60%  $K$ -band Strehl ratio in good observing conditions, one could expect Strehl ratios around 40% with the LGS. However, the Strehl ratios obtained so far were around 20–25% with the  $7 \times 7$  lenslet array.



Figure 1. *JHK* composite image of the globular cluster Omega Cen with a field of view of  $27 \times 27$  arcseconds and containing about 3000 stars.

One reason for this deficiency is that the LGS effective magnitude (NGS photon noise equivalent) corresponds to a star with  $V \sim 12$  mag. Hence, the adaptive optics (AO) no longer operates in the regime where it is limited by fitting error, but rather in the photon and detector noise-limited regime, thus hampering the achievable Strehl ratios. Even in favourable seeing conditions, the previously available  $14 \times 14$  lenslet array could not be used because of its small field of view (FoV) of 2.3 arcseconds per sub-aperture. This small FoV cuts the edges of the LGS spots and the corresponding truncation errors led to poor correction performance.

In May 2009, a contract for the replacement of the current visible wavefront sensor (WFS)  $14 \times 14$  lenslet array by one that has a shorter focal length, and hence larger field of view, was commenced by ESO and the Laboratoire d'AstrOphysique de Grenoble (LAOG), the institute that was in charge of building the original NAOS visible WFS. This new array has a FoV that is twice as large, with 4.6 arcseconds per sub-aperture, and was expected to significantly improve the correction performance in good observing

conditions when accurate wavefront sensing can be obtained with the LGS.

A major challenge for this project was to disturb regular observation with NACO as little as possible. So the installation and alignment of the new array at ESO Headquarters in Garching had to strictly follow a short and well-defined schedule that made the upgraded visible WFS available again in February 2010, only one and a half months after it had been dismantled and shipped to Garching just before Christmas 2009. Re-installation at UT4 started in the last days of January 2010, and the first night available for commissioning was 5 February.

During the commissioning nights, it quickly became clear that the new lenslet array brought the expected gain in performance, with the achievement of  $K$ -band Strehl ratios up to 35% and image quality around 80 milliarcseconds (mas) full width at half maximum (FWHM) in good observing conditions. Also, the operation with the new lenslet array is virtually identical to that with the previous arrays, so the upgrade is largely transparent for the users. The globular cluster Omega Centauri was observed for five



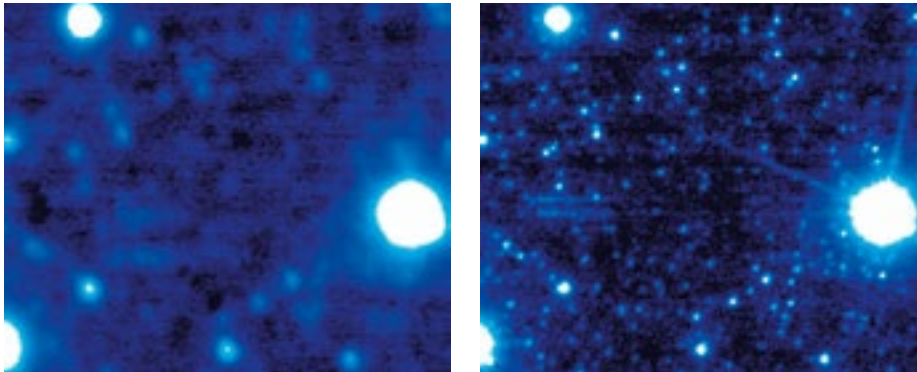


Figure 2. *K*-band close-up of the centre of Omega Cen, demonstrating the gain in sensitivity of the LGS AO (right) over the seeing-limited image (left).

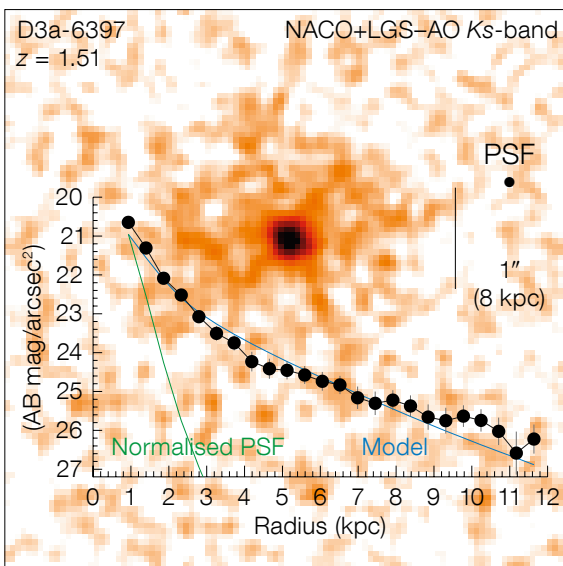


Figure 3. *Ks*-band map of the  $z = 1.51$  galaxy D3a-6397. The surface brightness profile of the galaxy is shown as inset and compared to a stellar PSF and a model fit. Image and data processing by Natascha Förster Schreiber, Ric Davies (both MPE) and Giovanni Cresci (Arcetri).

minutes in each of the *J*-, *H*- and *K*-bands; Figure 1 shows a *JHK* colour composite and Figure 2 demonstrates the gain in resolution and sensitivity (about 3 magnitudes in that case) provided by the LGS AO. The angular resolution is better than 100-mas FWHM over the whole 27-arcsecond FoV. The Strehl ratio in the image centre is better than 30% in the *K*-band, and better than 17% and 12% in the *H*- and *J*-bands respectively. The bright star in the centre was used as a tip-tilt guide star.

In order to test the sensitivity of the new mode, the high- $z$  galaxy D3a-6397 was observed for 78 minutes total in the *Ks* filter. The FWHM of the point spread function of the data, as determined from two stars within the NACO FoV, is approx-

imately 0.15–0.19 arcseconds, and the variations across the FoV are consistent with anisoplanatism. The image quality at the location of the science target (on-axis) could therefore be very close to, or indeed diffraction-limited (FWHM of about 0.11 arcseconds). This corresponds to a linear physical resolution of about 1 kpc at the redshift of the D3a-6397 of  $z = 1.5$ . The  $3\sigma$  limiting magnitude in a point-source aperture of diameter 0.26 arcseconds in *Ks* (AB) is  $\sim 24.8$  mag. The NACO *Ks*-band image clearly reveals a steep inner light profile and fainter emission is detected out to radii  $\sim 10$  kiloparsec (kpc). The surface brightness distribution can be well represented by a central unresolved (point-like) component and an underlying exponential disc component of effective radius of  $\sim 7$  kpc.

#### Acknowledgements

This intervention was successful thanks to the efficient planning and professional expertise provided by the LAOG project team as well as a high level of dedication from ESO staff during the critical period early in 2010. The authors would like to thank the UT4 telescope and instrument operator Cristian Herrera, and the Paranal laser specialists Juan Beltran and Jose-Luis Alvarez who made sure the laser was working at high power during the whole commissioning, as well as Natascha Förster Schreiber, Ric Davies (both MPE) and Giovanni Cresci (Arcetri) for the reduction and analysis of the D3a-6397 data.

# The High Order Test Bench: Evaluating High Contrast Imaging Concepts for SPHERE and EPICS

Patrice Martinez<sup>1</sup>  
Emmanuel Aller-Carpentier<sup>1</sup>  
Markus Kasper<sup>1</sup>

<sup>1</sup> ESO

The High Order Test bench (HOT) is an adaptive optics facility developed at ESO to test high contrast imaging instrument technologies and concepts. HOT reproduces realistically in the laboratory the conditions encountered at a telescope, including turbulence, high order adaptive optics correction and coronagraphy. Experiments carried out with HOT will be discussed mainly in the context of the SPHERE instrument.

Around the end of 2011, the SPHERE instrument (Beuzit et al., 2008) for the ESO Very Large Telescope (VLT), dedicated to direct imaging and spectroscopy of self-luminous giant planets, will be on its way for integration and tests at the Laboratoire d'Astrophysique de Grenoble (LAOG), followed by installation at Paranal. The High Order Test bench (HOT) is a high-contrast imaging adaptive optics bench developed at ESO in collaboration with Durham University and Arcetri with the support of the European Framework Programme 6 Opticon JRA1. It is a key tool for enabling technologies and concepts, and probing crucial aspects of high contrast imaging instruments such as SPHERE or EPICS (for the European Extremely Large Telescope). HOT reproduces realistically in the laboratory the

conditions encountered at a telescope (for example, the VLT), including turbulence generation, a high order adaptive optics system and near-infrared (NIR) coronagraphs. We present recent results obtained with HOT, efficiently combining extreme adaptive optics, coronagraphy and differential imaging techniques (spectral and polarimetric). Results will be particularly discussed in the context of SPHERE.

### Design and characteristics of HOT

Direct detection and characterisation of faint objects around bright astrophysical sources is challenging due to the high flux ratio and small angular separations. For instance, self-luminous giant planets are typically  $10^6$  times fainter than the parent star in the NIR. Virtually all

high contrast instrument concepts for large ground-based telescopes dedicated to the search for extrasolar planets use a combination of a high order (or eXtreme) adaptive optics (XAO) system and advanced starlight cancellation techniques such as coronagraphy. While an XAO system corrects the scattered light for optical aberrations introduced by the atmospheric turbulence and the instrument, a coronagraph reduces the starlight diffracted by the telescope in the image plane.

HOT is a high contrast imaging adaptive optics bench, which implements an XAO system, star and turbulence generator, mimicking conditions at a telescope realistically, and provides a large panel of coronagraphs. It provides ideal conditions to study XAO and coronagraphy. HOT is installed at ESO Headquarters on the

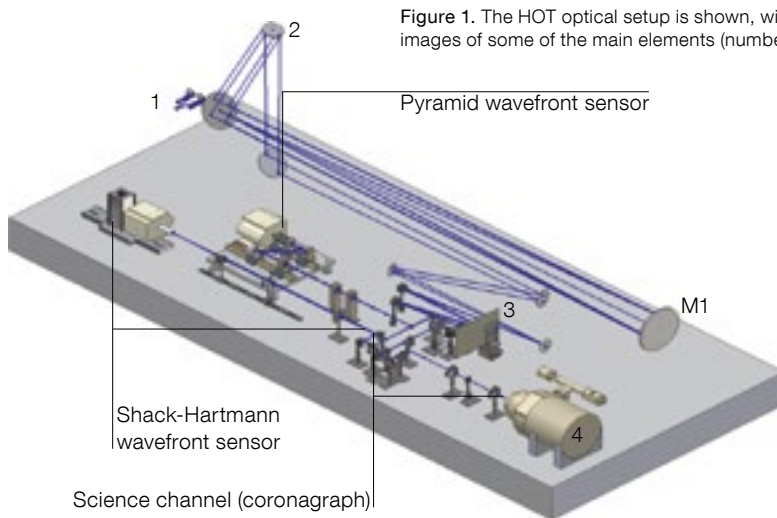
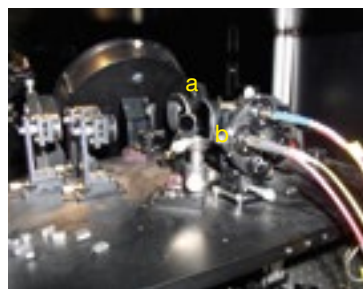


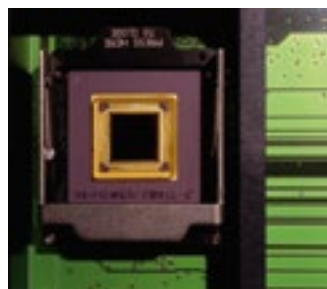
Figure 1. The HOT optical setup is shown, with images of some of the main elements (numbered).



1 Turbulence generator  
a Screens  
b Source



2 Bimorph deformable mirror  
VLT-pupil



3 Electrostatic deformable mirror



4 Infra-red test camera





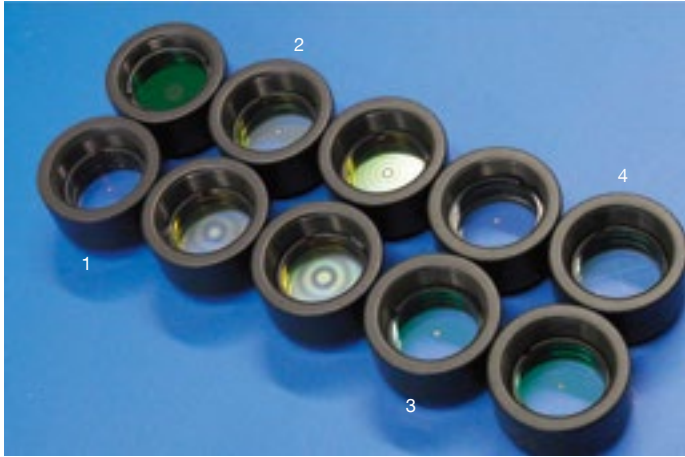


**Figure 2.** A selection of the various coronagraphic masks manufactured for HOT are shown.

- 1 Apodised Pupil Lyot Coronagraph (APLC)
- 2 Band-Limited Coronagraphs (BLC)
- 3 Lyot Coronagraphs (LC)
- 4 Four-Quadrant Phase Mask (FQPM)

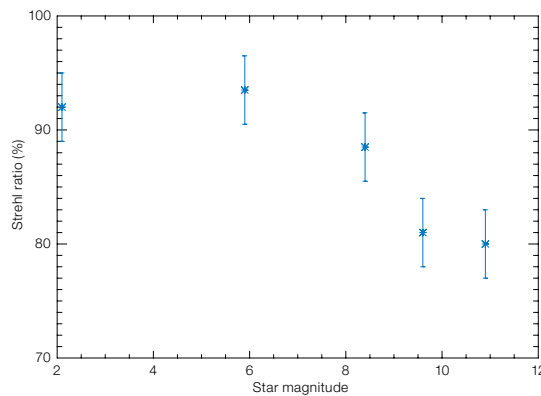
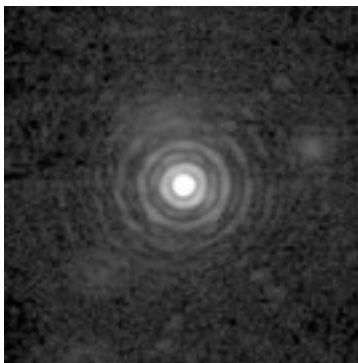


**Figure 3.** Left: XAO corrected PSF in *H*-band under 0.5-arcsecond seeing, Strehl ratio > 90%. Right: Strehl ratio performance as a function of the *H*-band stellar magnitude.

**Table 1.** A comparison of the main parameters of HOT and SPHERE (13 m/s wind speed assumes Paranal standard atmospheric conditions).

	Parameter	HOT	SPHERE
General	Seeing (arcseconds)	0.5	–
	Wind velocity (m/s)	1.3	~ 13
AO System	AO speed frequency (Hz)	80	1200
	AO system bandwidth (Hz)	3.5	100
	Deformable mirror actuators	32 × 32	41 × 41
	SHWFS subapertures	31 × 31	40 × 40
	Pixels per subaperture	4 × 4	6 × 6
	Inter-actuator pitch (μm)	340	4500
	Mechanical stroke (μm)	1.53	5
IR Path	AO cut-off frequency (arcseconds)	0.6	0.8
	Pupil plane diameter (mm)	3	18
	Pupil-stop plane diameter (mm)	3	10
APLC	F number	F/48	F/40
	Mask diameter (λ/D)	4.5	4.0/5.2
	Inner working angle (arcseconds)	0.09	≤ 0.1

Multi Application Curvature Adaptive Optics (MACAO) test bench (the MACAO test bench was initially developed for the assembly, integration and testing of the ESO multi-application curvature AO systems for the VLT Interferometer), and includes several critical components as shown in Figure 1:

- a turbulence generator with phase screens to simulate real seeing conditions;
- a VLT-pupil mask installed on a tip-tilt mount;
- a 60-bimorph large stroke deformable mirror correcting for static aberrations;
- a 32 × 32 micro-deformable mirror — an electrostatic MEMS (micro-electronic-mechanical system) device correcting for dynamic turbulence;
- a beam splitter transmitting the visible light to a wavefront sensor (WFS), either with a Shack–Hartmann WFS (SHWFS), or a pyramid concept WFS (PWFS), while the infrared light is directed towards the coronagraph and the Infrared Test Camera (ITC) that employs a 1k × 1k pixel HAWAII detector; and
- the ESO SPARTA real-time computer.

All the optics are set up on a table with air suspension in a dark room and are fully covered with protection panels that form a nearly closed box.

After the generation of the dynamical aberrations, the output f/16.8 beam is transformed into an f/51.8 beam by a spherical on-axis mirror (M1), and directed towards the pupil plane located at about 1010 mm above the table level, with its axis tilted at 13.26°, as in the VLT Coudé train. Then relay optics prior to the beam splitter make use of flat and spherical mirrors to produce an f/50 telecentric beam. All the relay optics in the IR-path include IR achromatic doublets. The SHWFS, developed by the University of Durham, provides a plate scale of 0.5 arcseconds/pixel with 31 × 31 subapertures, each one sampled by 4 × 4 pixels of a 24 μm pixel L3-CCD (Andor camera, readout noise < 1e<sup>-</sup>). The SHWFS real-time computer is an all-CPU architecture. The PWFS built by Arcetri is formally equivalent to the Large Binocular Telescope wavefront sensor optical design, and consists of a double refractive pyramid modulated by a tip-tilt mirror,

combined with an L3CCD-camera. Two pupil samplings are available depending on the final camera lens; a low sampling mode ( $31 \times 31$  subapertures); and a high sampling mode with  $48 \times 48$  subapertures. The PWFS uses a dedicated all-CPU real-time computer.

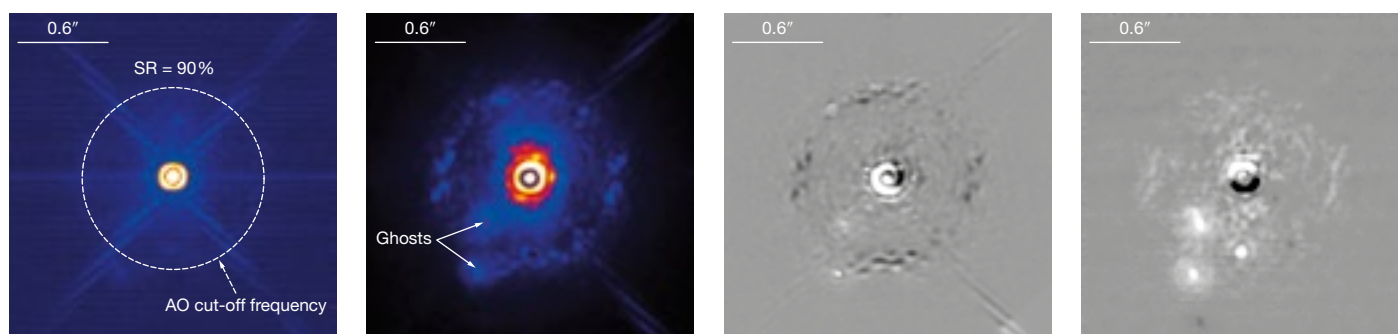
In collaboration with the Paris Observatory (LESIA), several coronagraph concepts were manufactured for HOT (as shown in Figure 2): Apodised Pupil Lyot Coronagraph (APLC); Band-Limited Coronagraphs (BLC); Lyot Coronagraphs (LC); and a Four-Quadrant Phase Mask (FQPM). All of them, except for the BLC, are SPHERE-like coronagraphs. In its standard operational coronagraphic mode, HOT uses an APLC that combines pupil apodisation and a hard-edge opaque focal plane mask.

Although HOT was not meant to be a SPHERE demonstrator, it is, in some aspects, similar to SPHERE. In Table 1 we compare HOT and SPHERE at different levels of their design.

### AO closed-loop results

During all experiments presented in the following, the XAO system was operating with the SHWFS, under 0.5 arcsecond seeing with 1.3 m/s wind speed. The SHWFS closed-loop runs at 80 Hz using 600 modes for the modal reconstruction on an 8-metre pupil. In these conditions, we were able to demonstrate that XAO

Figure 4. From the left to the right: *H*-band AO-corrected and apodised PSF, raw APLC image, SDI image, and PDI image. The arbitrary false colour distribution and image dynamic have been chosen to enhance the contrast for the sake of clarity.



can produce very well-corrected images, delivering *H*-band Strehl ratios above 90 % (see Figure 3) at high flux (stellar magnitude 5). Evolution of the Strehl ratio as a function of the stellar magnitude obtained with HOT is presented in Figure 3 (right).

### Coronagraphic runs

Point spread function (PSF) and APLC raw images recorded during the experiment in *H*-band are shown in Figure 4. The AO-corrected and apodised PSF (left) reveals the diffraction pattern of the VLT pupil owing to the high 90 % Strehl ratio. As a consequence of the apodiser presence, the intensity of the PSF wings is reduced; otherwise the wing of the PSF would be better defined in the image according to the level of the AO-correction. The AO cut-off frequency identified in the image with a dashed-white circle is localised as expected at 0.6 arcseconds. Its position in the field is clearly identified in the coronagraphic image owing to the slope of the intensity in the speckle field at 0.6 arcseconds offset from the centre. Outside the inner domain defined by the AO cut-off frequency, the AO system cannot measure or correct the corresponding spatial frequencies. The APLC image demonstrates starlight attenuation, and exhibits atmospheric speckles with lower intensity in the AO-correction domain. For the sake of clarity, ghosts originating from reflections in the optical system have been identified with white arrows. A radial trend in speckle intensity is observable in the image: speckles closer to the centre of the image are brighter. The central part of the APLC image is dominated by diffraction residuals and pinned speckles. These pinned

bright speckles localised at the position of the diffraction rings, originate from random intensity fluctuations — residual speckles produced by aberrations left after the AO correction — amplified by the coherent part of the wave. Contrasts of  $1 \times 10^{-3}$  at 0.1 arcseconds, and  $9 \times 10^{-5}$  at 0.5 arcseconds have been demonstrated with the APLC. All the various coronagraphs available on HOT (Figure 2) have been tested in the same way, and deliver roughly similar performances.

### Spectral and polarimetric differential imaging runs

Ground-based instruments with adaptive optics, such as SPHERE, require significant speckle attenuation to achieve star-planet contrast of  $10^{-4}$ – $10^{-7}$ . Instrumental errors and errors in the wavefront due to imperfect optics are expected to produce a limiting speckle noise floor. Among the instrumental speckle suppression techniques prepared for SPHERE, the Spectral Differential Imaging (SDI) and the Polarimetric Differential Imaging (PDI) techniques can be tested on HOT. These techniques rely on either the spectral characteristics of the planet (e.g., methane absorption feature) or the polarimetric *a priori* assumptions on the planet signal (i.e. light reflected by a planet is polarised, typically by about 10 %, while the stellar light is almost unpolarised).

In its current design, HOT does not allow simultaneous images to be taken since the IR-path is made with only one optical channel, so a sequential series of two images has to be made. Therefore SDI runs are carried out as a non-simultaneous spectral differential imaging mode. SDI is carried out using subtraction of



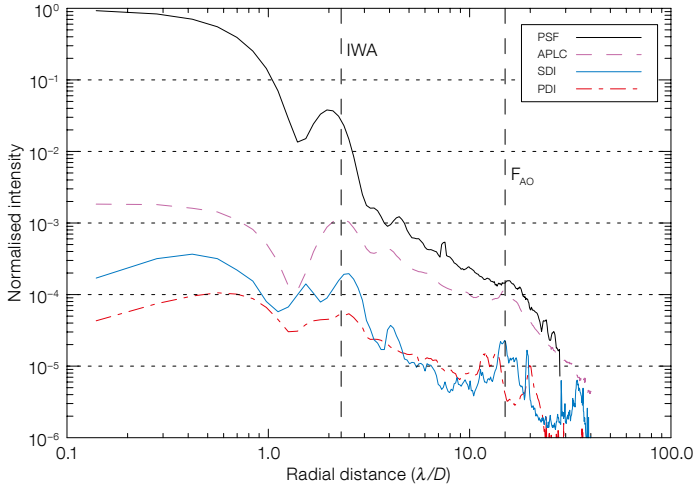


**Figure 5.** Azimuthally averaged contrast profiles: PSF (black), raw coronagraphic image (purple), SDI (1 $\sigma$ , blue), and PDI (1 $\sigma$ , red). IWA stands for the coronagraph inner-working angle, i.e. angular separations beyond which science can be carried out.

sequential coronagraphic images made with closely spaced narrowband filters around 1.6  $\mu\text{m}$  (H1 filter centred at 1.56  $\mu\text{m}$  with FWHM 55 nm, and H2 filter centred at 1.60  $\mu\text{m}$ , FWHM 64 nm), while a PDI run is performed by the subtraction of two coronagraphic images with orthogonal polarisation states using a NIR linear polariser.

We have carried out these differential-imaging tests under 0.5 arcsecond seeing, efficiently corrected by the AO system to a 90 % Strehl ratio. Figure 4 presents in  $H$ -band (from left to right) the PSF, the APLC coronagraphic image, and finally the SDI and PDI images. Corresponding contrast profiles are presented in Figure 5. SDI and PDI yield very similar performance (the PDI image exhibits an additional ghost, originating from the polariser components). In both cases, the improvement over that of the raw APLC image contrast is about a factor 22 at 0.1 arcsecond offset and 20 at 0.5 arcseconds. Images exhibit quasi-static speckles that

are, in principle, stable on timescales of minutes to hours. At this level of contrast a fair agreement with SPHERE simulations (Boccaletti et al., 2008) is already demonstrated. Investigations are being carried out to identify the source of limitation in the delivered contrast in SDI/PDI images (e.g., speckle stability, calibration issues, etc.).

In the SPHERE instrument, in order to push the detection threshold further down, calibration procedures such as the use of a reference star, or the comparison between two angular positions (angular differential imaging technique, ADI) will be implemented, with the goal of delivering a  $10^{-5}$  and  $5 \times 10^{-7}$   $5\sigma$  detectability at 0.1 and 0.5 arcsecond offsets respectively. The results obtained with HOT and presented above provide confidence for achieving such challenging contrast requirements. The  $1\sigma$  contrast obtained in the laboratory at 0.1 and 0.5 arcseconds (prior to application of the ADI technique) translated to a  $5\sigma$  contrast is two orders

of magnitude (a factor of 25 and 45 respectively) away from the corresponding SPHERE goal requirements (after SDI and ADI) at the same angular separation. Table 2 compares SPHERE, the Gemini Planet Image (GPI) and the High Contrast Instrument for the Subaru next generation Adaptive Optics (HiCIAO) contrast goals to that obtained with HOT. GPI and HiCIAO are the US and Japanese counterparts of SPHERE developed for the Gemini and Subaru telescopes respectively. Accounting for system differences, the agreement between these experimental results and the expectations from SPHERE, or GPI at similar level of contrast, is fairly good, while HiCIAO contrast goals are already met.

### From SPHERE to EPICS

Among the various experiments carried out with HOT, we were able to demonstrate that XAO can produce very well-corrected images, delivering  $H$ -band Strehl ratios above 90 %. SHWFS and PWFS have been compared, including their behaviour with respect to different error sources during calibration, showing an advantage for PWFS (Aller Carpentier et al., 2008; Pinna et al., 2008). We have successfully developed and validated a new technical solution for manufacturing components with spatially varying transmission (e.g. APLC, BLC), the so-called microdot masks (Martinez et al., 2009). These masks have now been selected for SPHERE, solving issues raised by a previous approach.

Accounting for the system differences (e.g., deformable mirror (DM) actuator number), we have demonstrated a fairly good agreement between experimental coronagraphic results and the expectation from SPHERE (Martinez et al., 2010). Finally, a speckle-nulling technique, using a single DM to sense and correct the static speckles directly in the coronagraphic image is being implemented and tested with HOT, opening up the possibility of reaching higher contrast by overcoming the limit imposed by remnant speckles in the coronagraphic image.

A new pupil mask (E-ELT-like) has been recently installed on HOT in place of the VLT one. With this configuration we have

**Table 2.** Contrast goals ( $5\sigma$ ) of several planet-finder instruments compared to results obtained with HOT.

System	Inner Working Angle (IWA) (arcseconds)	Contrast at 0.1 arcseconds	Contrast at 0.5 arcseconds	Telescope
HOT (w/ SDI or PDI)	0.09	$2.5 \times 10^{-4}$	$2.2 \times 10^{-5}$	–
HiCIAO (w/ SDI)	0.1	$2.0 \times 10^{-4}$	$2.0 \times 10^{-5}$	Subaru
SPHERE (w/ SDI & ADI)	$\leq 0.1$	$10^{-5}$	$5.0 \times 10^{-7}$	VLT
GPI (w/ SDI & ADI)	0.2	–	$10^{-7}$	Gemini

demonstrated the ability of the APLC to accommodate the large central obscuration and configuration of the spider arms, as well as testing another promising concept, the Dual Zone phase mask (DZ) in collaboration with the Marseille Observatory (LAM). The DZ is a potential second generation SPHERE corona-graph. All these experiments provide useful information and feedback for both the SPHERE and EPICS consortia. SPHERE is currently under construction and due at the VLT in 2011, so in the near future HOT will obviously be more oriented towards EPICS. For instance, the baseline XAO wavefront sensor of the EPICS instrument for the E-ELT is a roof-pyramid concept. This modified PWFS has been extensively studied by simulation and demonstrates improved behaviour (Korkiakoski & Vérinaud, 2010).

A proof-of-concept is at this stage necessary, and HOT could provide the required environment to design and implement such a sensor. Among the other potential experiments that can be performed with HOT, the so-called “island effect” is of a great interest: the partial or complete coverage of the wavefront sensor sub-apertures by the dark zones created by the secondary mirror supports (spider arms) on the pupil. This issue is particularly important in the case of the E-ELT, and can easily be addressed by experiment with HOT.

The High Order Test bench is thus a unique and versatile ESO key tool to enable technologies and concepts, and to address crucial aspects of the forthcoming and future generation of high contrast imaging instruments.

#### Acknowledgements

The activities outlined in this paper have been funded as part of the European Commission through the Sixth Framework Programme (FP6) and Seventh Framework Programme (FP7), and the Opticon Joint Research Activity JRA 1.

#### References

- Aller Carpentier, E. et al. 2008, Proc. SPIE, 7015, 108  
 Aller Carpentier, E. et al. 2010, Proc. 1st AO4ELT conference, eds. Y. Clénet et al., EDP Sciences  
 Beuzit, J.-L. et al. 2008, Proc. SPIE, 7014, 18  
 Boccaletti, A. et al. 2008, Proc. SPIE, 7015, 177  
 Martinez, P. et al. 2009, The Messenger, 137, 18  
 Martinez, P. et al. 2010, PASP, accepted  
 Pinna, E. et al. 2008, Proc. SPIE, 7015, 143  
 Korkiakoski, V. & Vérinaud, C. 2010, Proc. 1st AO4ELT conference, eds. Y. Clénet et al., EDP Sciences



Colour-composite image of the central part of the young Galactic stellar cluster RCW 38 formed from *J*, *H* and *K<sub>s</sub>* filter images taken with the VLT NACO adaptive optics instrument. The image, which is about 1 arcminute in size, is centred on the binary O star RCW 38 IRS2 and reveals many lower mass protostar candidates. See eso0929a for more details.

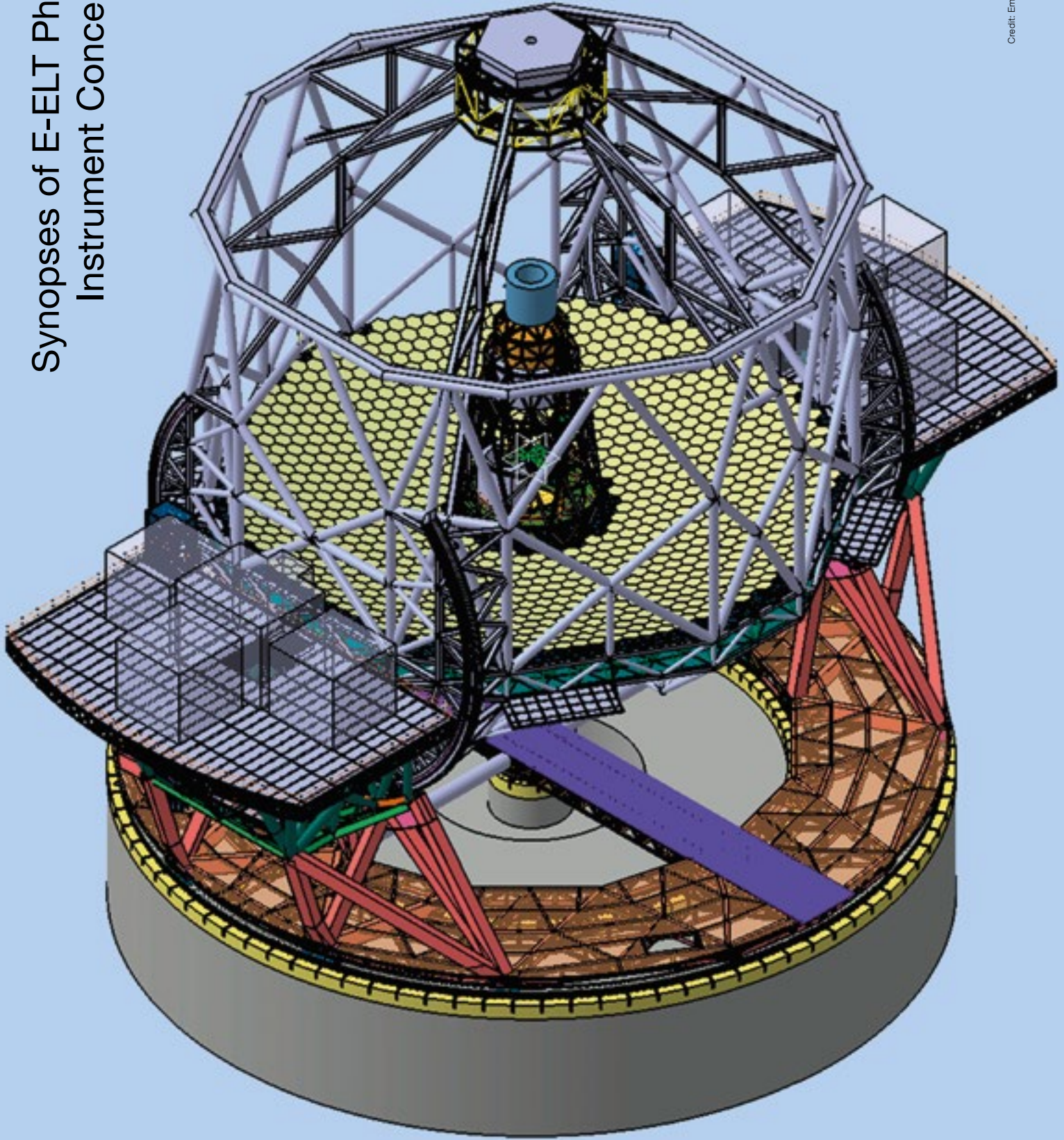




The AEM consortium has recently completed the full assembly of the first two European antennas within their camp at the ALMA Operations Support Facility (OSF). The picture shows the complete AEM antenna 2, which will start functional and commissioning testing in the coming months.



# Synopses of E-ELT Phase A and Instrument Concept Studies



A CAD view of the main structure of the European Extremely Large Telescope.



# An Introduction to the E-ELT Instrumentation and Post-focal Adaptive Optics Module Studies

Sandro D’Odorico<sup>1</sup>  
 Suzanne Ramsay<sup>1</sup>  
 Norbert Hubin<sup>1</sup>  
 Juan Carlos Gonzalez<sup>1</sup>  
 Filippo Maria Zerbi<sup>1</sup>

<sup>1</sup> ESO

The following eleven articles provide short summaries of the conceptual design studies for the European Extremely Large Telescope instruments and post-focal adaptive optics modules. The background and scope of these studies is outlined in this introduction.

As part of the study for the 42-metre European Extremely Large Telescope (E-ELT), ESO initiated ten conceptual design studies into the instruments and post-focal adaptive optics (AO) modules that could deliver the science case for the telescope. This extraordinary effort was undertaken in more than forty institutes in ten member states and Chile, involving several hundred engineers and scientists. There were eventually eleven studies, as one concept, for the multi-object spectrograph OPTIMOS, was split into two separate studies. The eleven studies varied in duration from 15 to 30 months, and therefore in the depth of the study (see Table 1 for an overview). All the studies had the common goals of exploring the science case for the instrument, determining whether it was technically feasible and could be delivered at a reasonable cost and timescale, and identifying any preparatory R&D work required. For the two post-focal AO modules, the scientific performance was demonstrated in collaboration with the instrument teams that plan to exploit those AO modules.

The studies were formally organised along similar lines to all ESO instrument projects: a statement of work and technical specification was agreed and signed at a “Kick-off” meeting and the study concluded with the delivery of a final report and a formal review. The final reports consisted of 10–20 documents specified in the statement of work and were in total 500–1000 pages in length. The reports covered all major aspects of the instrument design including: a science case and analysis of the scientific performance; an operation and maintenance plan; a verification matrix including information on compliance with the telescope interfaces; a system design covering optomechanical design, detector systems, cryogenic or thermal design, instrument control electronics and software; a management plan for the design and construction of the instrument including R&D plans, risk analysis, schedule and budget. The review, coordinated by the Instrumentation Project Office of the E-ELT Programme, was conducted by a board consisting of ESO experts in all these areas and including an external reviewer from a non-ESO member state. Members of the E-ELT Science Working Group (SWG) also participated as observers and were able to question the teams. All of the studies were considered successfully closed: the high quality of the delivered reports show the strength of the instrument development capabilities in the European astronomical community and the great interest in the E-ELT project.

The articles following are a snapshot of the instrument concepts written by the Principal Investigators (PIs) of the studies at this important phase for ESO and the E-ELT project. With strictly limited space they can only give a flavour of the science cases, the technical concept and the expected performance of each

instrument. A straightforward comparison of the quoted performance of different instruments in the bands in common has to be made with great caution. It requires a full understanding of the many underlying assumptions, such as AO performance or image quality in general, integration time and sky subtraction strategy, assumed light distribution of the sources and instantaneous spectral coverage. Anyone who is interested in more information on a particular study should contact the corresponding PI.

The next step is the development of an instrumentation plan for the first generation of instruments at the telescope. This plan will form part of the construction proposal for the E-ELT Project to be presented to the ESO Council at the end of 2010 and will outline the capabilities for the instruments to be delivered within the first ten years of telescope operations. The instrument concepts presented here provide a basis for this plan, but there will not necessarily be a one-to-one correspondence between these studies and the instruments that will be built or the consortia that will build them. There will be a need to simplify and improve some of the instrument concepts according to the results of the reviews and there will be the possibility to reshape the consortia in order to distribute the effort, with the possibility for new partners to step in.

For a telescope with such a highly innovative design as the E-ELT, the proof of the feasibility of the instruments to carry out the ambitious science programme was a crucial step. Thanks to the successful effort by the PIs of the studies and to their teams, we can now look forward with confidence and great anticipation to the final design and construction phases of the project.

**Table 1.** An overview of the instrument studies for the E-ELT instruments and post-focal adaptive optics modules in alphabetical order.

Name	PI	Institutes	ESO Responsible	Kick-off	Final Review
ATLAS	T. Fusco (ONERA)	ONERA, LESIA, GEPI, LAM, UK ATC	J. Paufique	19/09/08	02/02/10
CODEX	L. Pasquini (ESO)	ESO, INAF–OATS and OA Brera, IAC, IoA Cambridge, Obs. Genève.	N/A	16/09/08	23/02/10
EAGLE	J.-G. Cuby (LAM)	LAM, GEPI, LESIA, ONERA, UK ATC, Univ. Durham	S. Ramsay	27/09/07	27/10/09
EPICS	M. Kasper (ESO)	ESO, LAOG, INAF–OAPd, LESIA, NOVA ASTRON, Uni. Utrecht, ETHZ, ONERA, Univ. Oxford, FIZEAU, LAM	N/A	24/10/07	16/03/10
HARMONI	N. Thatte (Oxford)	Univ. Oxford, CRAL, CSIC–DAMIR, IAC, UK ATC	J. Vernet	1/04/08	28/01/10
MAORY	E. Diolaiti (INAF–OABo)	INAF–OABo and Univ. Bologna, ONERA, INAF–OAPd, INAF–OAA, INAF–IASFB0	E. Marchetti	09/11/07	10/12/09
METIS	B. Brandl (Leiden)	NOVA Leiden and ASTRON, MPIA, CEA Saclay, KU–Leuven, UK ATC	R. Siebenmorgen	07/05/08	17/12/09
MICADO	R. Genzel (MPE)	MPE, MPIA, USM, INAF–Padova, NOVA ASTRON, Leiden, Groningen, LESIA	A. Richichi	28/02/08	30/10/09
OPTIMOS–DIORAMAS	O. Le Fèvre (LAM)	LAM, STFC RAL, INAF IASF–Milano and OATs, Obs. Genève, IAC, Obs. Haute Provence	S. Ramsay	03/11/08	30/03/10
OPTIMOS–EVE	F. Hammer (GEPI)	GEPI, NOVA ASTRON, RUN, Uni. Amsterdam, STFC RAL, INAF–OATs and Brera, NBI Copenhagen	S. Ramsay	03/11/08	30/03/10
SIMPLE	L. Origlia (INAF–OABo)	INAF–OABo, Arcetri, Roma, Univ. Bologna, UAO, TLS, PUC	H. U. Käufel	30/10/08	04/03/10

# ATLAS: An Advanced Tomographic Laser-assisted Adaptive Optics System

Thierry Fusco<sup>1</sup>

<sup>1</sup> ONERA, Châtillon, France

Team members:

Jean-Philippe Amans<sup>1</sup>, Yann Clenet<sup>2</sup>, Mathieu Cohen<sup>1</sup>, Eric Gendron<sup>2</sup>, Damien Gratadour<sup>2</sup>, Norbert Hubin<sup>3</sup>, Pascal Jagourel<sup>1</sup>, Serge Meimon<sup>4</sup>, Vincent Michau<sup>4</sup>, Cyril Petit<sup>4</sup>, Jérôme Paufigue<sup>3</sup>, Clélia Robert<sup>4</sup>, Hermine Schnetler<sup>5</sup>

<sup>1</sup> GEPI, <sup>2</sup> LESIA, <sup>3</sup> ESO, <sup>4</sup> ONERA, <sup>5</sup> UK ATC

ATLAS is a generic laser tomographic adaptive optics system for the E-ELT. Based on modular, relatively simple, and yet innovative concepts, it aims at providing diffraction-limited images in the near-infrared for close to 100 percent sky coverage.

The E-ELT will provide scientific instruments with high light-gathering power and high angular resolution. It will be equipped with adaptive optics systems for real-time compensation of turbulence and windshake effects. Various adaptive optics systems are currently under consideration. In order of increasing performance and complexity these are:

- Ground layer AO (GLAO) providing a small but uniform correction in a wide field (typically 5 to 10 arcminute diameter) with close to 100 % sky coverage;
- Single conjugated AO (SCAO) providing a good correction over a small field (typically a few tens of arcseconds), but with an extremely poor sky coverage (less than 1%);
- Laser tomography AO (LTAO), with performance close to that of SCAO over a slightly larger field of view (FoV) and with a much higher sky coverage (close to 100 %), due to the availability of E-ELT laser guide stars;
- Multi-mirror adaptive optics systems such as multi-conjugate AO (MCAO) and multi-object AO (MOAO), which will allow the E-ELT to be corrected for atmospheric turbulence.

As an intermediate solution, the planned LTAO topology to be used in ATLAS has shown a significant gain in performance compared to SCAO in terms of sky coverage, while keeping the complexity of the overall design relatively low compared to that of MCAO/MOAO. An added advantage of ATLAS is its potential “wide bandpass” in the third dimension, namely the spectral range. ATLAS provides a science field free from optical elements and obscuration, while transmitting a large range of wavelengths. This feature will enable

instruments to analyse astronomical objects over a wide wavelength range.

ATLAS has been designed to be compatible with several potential scientific instruments (HARMONI, METIS and SIMPLE). The requirements for an additional instrument, which can be attached directly to the ATLAS rotating part (instrument mass to be less than 3 tonnes) were also considered. The ATLAS specifications are therefore a mix of generic considerations defined by ESO (at the start of the Phase A study) and more specific requirements derived by working directly with the instrument teams (Fusco et al., 2010). By considering all the requirements and constraints, the team succeeded in designing a baseline concept that is modular, relatively simple, and innovative, while relying on existing mature technologies.

## Science drivers

ATLAS (being defined as a generic LTAO module) has no science drivers *per se*; nevertheless several key science drivers have been identified after interaction with the ATLAS client instrument teams. Hence, the wavefront-corrected focal plane delivered by ATLAS and the E-ELT can be utilised by the following Nasmyth-mounted instruments: a single field near-infrared (NIR) spectrograph (HARMONI); a mid-infrared camera-spectrograph (METIS); a high spectral resolution NIR Spectrograph (SIMPLE); and potentially a large FoV NIR

camera (MICADO). In addition, it has been shown that the ATLAS final design (see below), will be able to deliver four out of the nine prominent E-ELT science cases (circumstellar discs, black holes and active galactic nuclei, dynamical measurement of Universe’s expansion and metallicity of the low density intergalactic medium) and complies partially with the requirements of four others (Kissler-Patig 2010).

## Instrument design concept

ATLAS can be mounted at any of the Nasmyth focal stations (straight through and lateral ports). It implements an advanced laser tomography topology to calculate the corrections that will be applied by the E-ELT Telescope Control System (TCS) to the M4 adaptive mirror and the M5 field stabilisation mirror. ATLAS uses the six laser guide stars (LGS) provided by the E-ELT laser launch telescope and two natural guide stars (NGS) to sense the wavefront error of the incoming beam by implementing six identical LGS wavefront sensor (WFS) channels and two identical NGS WFS channels. The LGS WFS channels are used to sense the high-order wavefront errors while the NGS WFS channels are used to measure the low order modes. ATLAS can deliver a clear central 30-arcsecond FoV free from optics to the Nasmyth focal stations. An extended FoV of 60 arcseconds, which may be partially vignetted (by the two NGS pick-off arms) is available. In its present layout (see Figure 1), ATLAS

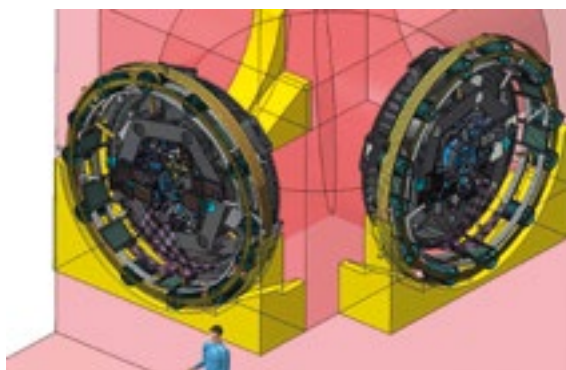


Figure 1. Upper: ATLAS optomechanical implementation at the direct and lateral Nasmyth port of the E-ELT. Lower left: one of the two NGS-WFS modules. Lower right: one of the six LGS-WFS modules.

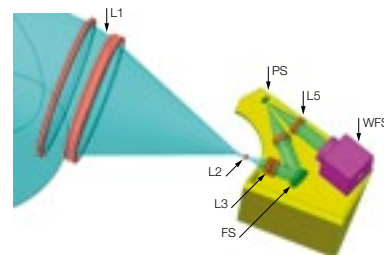
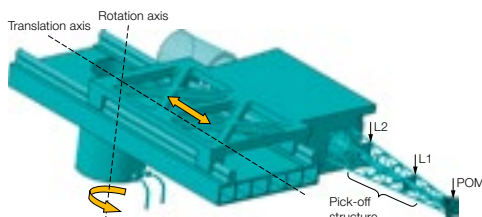


Table 1. Performance of ATLAS for median atmospheric conditions (0.8-arcsecond seeing, isoplanatic angle of 2.08 arcsecond). The relevant performance data for HARMONI, SIMPLE and METIS have been highlighted.

Lambda (nm)	440	550	640	750	900	1250	1650	2200	3500	4800	10500
Ensquared Energy (%)											
Width (in mas)	10	0.1	0.7	2.1	5.2	10.3	21.1	26.1	26.4	17.8	13.7
	20	0.3	1.2	3.2	7.4	15.1	32.1	42.5	48.5	45.6	37
	40	0.8	2.2	4.7	9.6	18.2	37.8	53.6	63.8	62.8	61
	60	1.7	3.6	6.6	11.9	22.4	40.5	56.3	67.8	75.9	69.1
	100	4.3	7.1	10.7	16.4	25.6	44.8	59.5	71.7	81.3	84.6
SR (%)		0	0.1	0.6	1.9	5.5	18.8	35.3	52.7	75.6	90.5
FWHM (mas)		211	8.9	8.1	8	8.2	9	10.1	12.1	17.6	23.7

does not introduce any additional optics along the line of sight to the instrument. Thus, there are no additional losses due to restrictions coming from the coatings or glass absorption, nor additional thermal background.

In particular, the following critical points have been very carefully addressed:

- Tomographic reconstruction process. This is the key element of the system (true for any laser-assisted wide-field AO system on the E-ELT). Complex trade-offs have been made to find the best solution and balance between the complexity of the control algorithm, its robustness and the cost of computation. The whole process will be based on a regularised pseudo-open loop control (Gilles, 2005) and a clever separation between NGS and LGS control loops. The LGS measurement will rely on Shack–Hartmann WFS with centroiding measurements using a correlation scheme.
- Improvement of the sky coverage. This has been achieved by the design of a new NGS WFS concept, fully optimised for maximising the sky coverage in the context of a laser-assisted AO system (Meimon et al., 2010a). The performance has been fully simulated and the predicted sky coverage is close to 100%. This is an exceptional sky coverage performance achieved by using existing components and a straightforward optomechanical design. The ATLAS sky

coverage is one of its most attractive selling points (Meimon et al., 2010b).

- Simplification of the optomechanical design. As stated before, the pursuit of a simple system has led the team to make radical choices in terms of the design allowing us to minimise:
  - the number of large optical elements (the largest optical element is 400 mm);
  - the number of moving mechanisms; and
  - space and weight.

### Performance

The ATLAS system fulfils the ESO specifications and reaches a Strehl ratio (SR) of 52.7% for median seeing conditions (0.8 arcsecond) in K-band, up to 56.8% in good seeing conditions (0.6 arcsecond). In case of bad seeing conditions (1.1 arcsecond) the performance remains very decent with an SR around 35%. A summary of ATLAS performance in terms of ensquared energy and SR is given in Table 1. It is important to highlight the huge gain brought by ATLAS with respect to GLAO both in terms of ensquared energy and full width at half maximum (FWHM), as shown in Figure 2.

Even though ATLAS will not reach the ultimate performance of an SCAO system (50% instead of 70%) on bright stars (typically magnitude

- < 13), it will ensure this performance and thus a diffraction-limited point spread function (PSF) for NIR bands over more than 98% of the whole sky. It will also provide a very sharp PSF (< 10 milliarcseconds (mas) from J-band down to V-band. Such results are achievable thanks to a good LGS-tomographic topology combined with a very accurate correction of the tip-tilt / defocus on axis using off-axis natural guide star(s). We benefit from:
  - the very favourable ratio of the outer scale of turbulence to telescope diameter (most of the time < 1), which significantly reduces the turbulent jitter;
  - a dedicated low-order focal plane sensor optimised for very faint guide stars (up to magnitude 19 typically);
  - an optimised Kalman filter control law which allows temporal prediction to be made in order to correct telescope windshake well;
  - a dedicated correction in the NGS direction (using a 30 × 30 array of micro-deformable mirrors located in the WFS arms and the LGS tomographic data) in order to obtain a diffraction-limited PSF on the WFS arms in H- to Ks-bands (and thus an improved signal-to-noise ratio on NGS WFS); and
  - the use of two NGS channels, combined with an optimised spatial reconstruction process in order to interpolate the on-axis tip-tilt / defocus measurements from the NGS off-axis (up to 60 arcseconds).

The full sky coverage estimation scheme is based on a random generation of stellar fields following the Besançon model. A selection of star–star couples is made following a general strategy based on a balance between residual anisoplanatic, temporal and noise errors. Sky coverage is extremely dependent on the outer scale of turbulence ( $L_0$ ) as well as on the readout noise (RON) of the IR detector. For the nominal values of the study (i.e. a 25-metre  $L_0$  and  $6e^-$  RON), a sky coverage of 98% for the whole sky (larger than 97% for Galactic latitude < 60° and larger than 92% for Galactic latitude ≥ 60°) has been computed.

### References

- Fusco, T. et al. 2010, Proc. 1st AO4ELT conference, eds. Y. Clénet et al., EDP Sciences  
Gilles, L. 2005, Applied Optics, 44, 6, 993  
Kissler-Patig, M. 2010, Proc. 1st AO4ELT conference, eds. Y. Clénet et al., EDP Sciences  
Meimon, S. et al. 2010a, Optics Letter, submitted.  
Meimon, S. 2010b, SPIE Astronomical Instrumentation, San Diego, June 2010

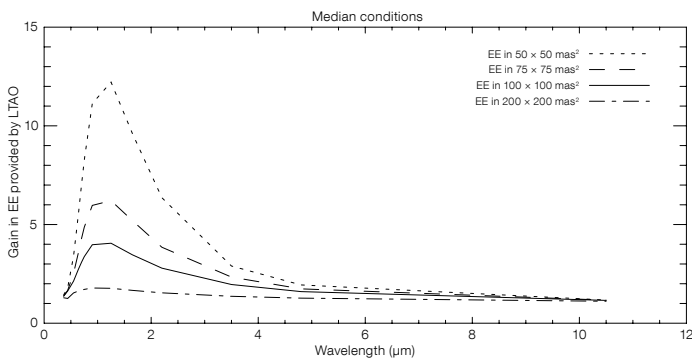


Figure 2. Gain brought by ATLAS with respect to a GLAO system for various imaging wavelengths and various box sizes (for the ensquared energy computation). Median atmospheric conditions (0.8-arcsecond seeing, isoplanatic angle of 2.08 arcsecond) have been considered.



# CODEX: An Ultra-stable High Resolution Spectrograph for the E-ELT

Luca Pasquini<sup>1</sup>  
 Stefano Cristiani<sup>2</sup>  
 Ramón García-López<sup>3</sup>  
 Martin Haehnel<sup>4</sup>  
 Michel Mayor<sup>5</sup>

<sup>1</sup> ESO

<sup>2</sup> INAF–Osservatorio di Trieste, Italy

<sup>3</sup> Instituto de Astrofísica de Canarias, Spain

<sup>4</sup> Institute of Astronomy, Cambridge, United Kingdom

<sup>5</sup> Observatoire de Genève, Switzerland

Team members:

Gerardo Ávila<sup>1</sup>, George Becker<sup>2</sup>, Piercarlo Bonifacio<sup>3</sup>, Bob Carswell<sup>4</sup>, Roberto Cirami<sup>3</sup>, Maurizio Comari<sup>3</sup>, Igor Coretti<sup>3</sup>, Gaspare Lo Curto<sup>1</sup>, Hans Dekker<sup>1</sup>, Bernard Delabre<sup>1</sup>, Miroslava Dessauges<sup>5</sup>, Paolo di Marcantonio<sup>3</sup>, Valentina D’Odorico<sup>3</sup>, Artemio Herrero<sup>2</sup>, Garik Israelian<sup>2</sup>, Olaf Iwert<sup>1</sup>, Jochen Liske<sup>1</sup>, Christophe Lovis<sup>5</sup>, Antonio Manescau<sup>1</sup>, Denis Mégevand<sup>5</sup>, Paolo Molaro<sup>3</sup>, Dominique Naef<sup>5</sup>, María Rosa Zapatero Osorio<sup>2</sup>, Francesco Pepe<sup>5</sup>, Rafael Rebolo<sup>2</sup>, Marco Riva<sup>6</sup>, Paolo Santin<sup>3</sup>, Paolo Spanò<sup>8</sup>, Fabio Tenegi<sup>2</sup>, Stéphane Udry<sup>5</sup>, Eros Vanzella<sup>3</sup>, Matteo Viel<sup>3</sup>, Filippo Maria Zerbi<sup>6</sup>

<sup>1</sup> ESO, <sup>2</sup> IAC, <sup>3</sup> INAF–Trieste, <sup>4</sup> IoA, <sup>5</sup> Obs. de Genève, <sup>6</sup> INAF–Brera

CODEX is the proposed optical high resolution spectrograph for the E-ELT. Designed to make the most of the unique light-gathering power of the E-ELT and to obtain superb stability, CODEX will open up a new parameter space in astrophysical spectroscopy. The wide-ranging science case has a large discovery potential in stellar, Galactic and extragalactic astronomy as well as in fundamental physics.

## Science drivers

The concept and science case for an ultra-stable high resolution spectrograph at a giant telescope was first analysed in the context of an OWL study (Pasquini et al., 2005). It was found that photon-hungry high-precision spectroscopy will particularly benefit from the enormous light-collecting power of the E-ELT and will enable some new, truly spectacular science. In the Phase A study for CODEX, a science case and instrument design have been fully developed. Five scientific showcases that highlight the abilities of CODEX and cover a wide range of subject areas are presented; a more exhaustive description of CODEX capabilities is on the web<sup>1</sup>.

– *Detecting and measuring the cosmological redshift drift of the Lyman-alpha forest* — a

*direct measurement of the accelerating expansion of the Universe.* The cosmological redshifts of spectroscopic features originating at large distances are the signature of an expanding Universe. As the expansion rate changes with time, a corresponding change in redshift is expected. This is a very small effect, but measurable with CODEX if the collective signal in a large number of absorption features is monitored for 30 years (see Figure 1). The most favourable target is the multitude of absorption features making up the Lyman-alpha forest in quasar absorption line spectra.

- *Detection of Earth twins in the habitable zone of solar-type stars.* The search for extra-solar Earth-like planets that could sustain life catches the imagination of scientists as well as that of the general public. The 2 cm/s accuracy of CODEX constitutes a factor of about 20 improvement compared to current instruments. With this accuracy it will be possible to assemble and study sizeable samples of Earth-like planets in the habitable zone of their parent stars (see Figure 2).
- *Galactic archaeology: unravelling the assembly history of the Milky Way with nucleochronometry.* How did galaxies assemble and come to look the way they do? Much has been learned from our own Galaxy, which we can study in fine detail. Weak features of rare isotopes in stellar spectra can be studied to new limits with CODEX, and nucleochronometry — the equivalent of dating materials on the Earth using radioactive nuclides — will become an accurate quantitative tool yielding precise age determinations of stars.
- *Probing the interplay of galaxies and the intergalactic medium from which they form.* The formation of the first autonomous sources of radiation, stars and black holes, led to the heating, reionisation and pollution of the intergalactic medium (IGM) with metals. The sensitivity of CODEX to trace amounts of metals in the low density IGM thus opens a window into this important period in the history of the Universe, enabling the study of the interplay of galaxies and the IGM from which they formed in unprecedented detail.
- *Testing fundamental physics — taking the test of the stability of fundamental constants to new limits.* It has long been speculated that the fundamental constants vary in space or time or both. The discovery of such variations would be a revolutionary result leading to the development of new physics. The current evidence for small variations of the fine structure constant on cosmological timescales from studies of QSO absorption line spectra is intriguing but rather controversial. CODEX will enable tests of the stability of fundamental constants to greatly improved new limits.

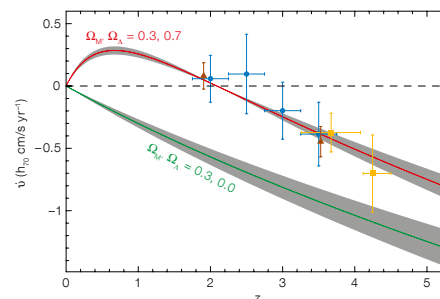


Figure 1. Monte Carlo simulations of three different implementations of a redshift drift experiment. Plotted are values and errors of the “measured” velocity drift  $\dot{v}$ , expected for a total experiment duration of 30 yr and a total integration time of 4000 h. See Liske et al. (2008) for more details.

A high Strehl ratio imager at the E-ELT will be capable of directly detecting some of the more massive planets discovered by CODEX. The combination of these instruments will provide the E-ELT community with a full characterisation of the planetary orbits as well as atmospheres, true masses and temperature. CODEX will also follow up Earth-sized exoplanet candidates discovered by space missions and ground-based transit searches. Confirmation of the planetary origin of the photometric transit and accurate measurements of the mass of the transiting body require a radial velocity (RV) precision of a few  $\text{cm s}^{-1}$ , which CODEX will provide. Gaia will provide accurate physical stellar parameters enabling the positions of stars in the Hertzsprung–Russell diagram to be compared with those derived by CODEX from nucleochronometry and asteroseismology. Also high-redshift molecular rotational absorption lines discovered by ALMA and H I 21 cm absorption detected by SKA can be compared to optical metal lines observed with CODEX to constrain various combinations of constants involving the fine structure constant ( $\alpha$ ), the proton-to-electron mass ratio ( $\mu$ ) and the proton  $g$ -factor.

## Instrument design concept

The top-level technical specifications have been derived from the requirements set by the main science cases (see Table 1). Given the high-precision aim of the instrument, the spectrograph should be located at the coudé focus, as this is the quietest (mechanically and thermally) environment available. At the coudé focus a guiding and tip-tilt correcting system accurately centres the object light into the 500  $\mu\text{m}$  diameter fibre core, which guides the light into the spectrograph vessel. In the fibres the light is scrambled in order to make the output signal independent of variations at the

**Figure 2.** Expected planet population detected by Doppler spectroscopy with HARPS on the ESO 3.6-metre (precision  $1 \text{ ms}^{-1}$ ; left), ESPRESSO on the VLT (precision  $10 \text{ cms}^{-1}$ ; middle) and CODEX on the E-ELT (precision  $1 \text{ cms}^{-1}$ ; right). CODEX is required to detect Earth-like planets in the habitable zone of solar-type stars (green rectangle).

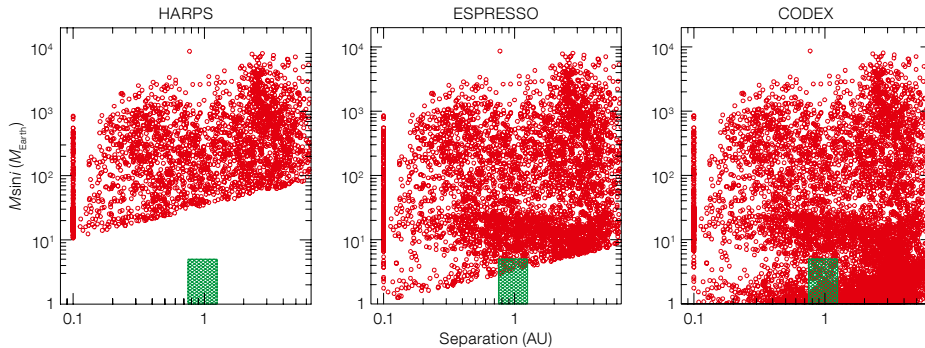
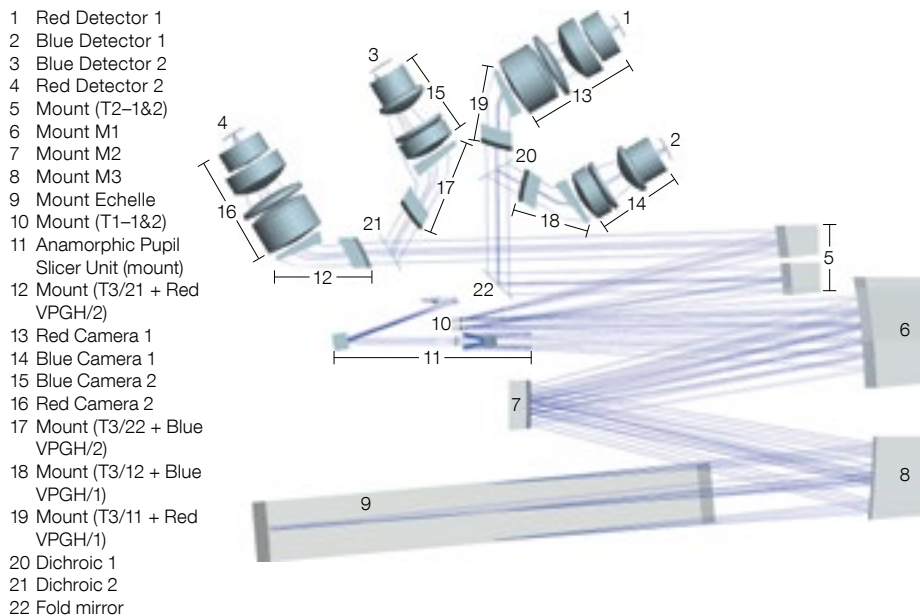


**Table 1.** Brief summary of CODEX characteristics.

Aperture on the sky	0.82 arcsecond, with a $500 \mu\text{m}$ fibre
Wavelength range	370–710 nm, in two arms: Blue 370–500 nm; Red 490–710 nm
Doppler precision	$< 2 \text{ cms}^{-1}$ over 30 years
Wavelength precision	$< 1 \text{ ms}^{-1}$ (absolute)
Resolving power	120 000 for square fibre, $\sim 135$ 000 for circular fibre
Echelle	R4, 41.6 l/mm, 1700 $\times$ 200 mm, 4 $\times$ 1 mosaic
Detector focal plane	Four CCDs (9k $\times$ 9k $10 \mu\text{m}$ pixels) (2 in Blue Camera, 2 in Red Camera)
Total efficiency	28.8 % (max.), 14.5 % (min.) slit losses not included

**Figure 3.** Optomechanical design of CODEX is shown.



entrance. In the spectrograph the pupil is made highly anamorphic and sliced into six parts, which pass through the 1.7-metre long echelle and the collimating system of the spectrograph, after which they are divided into two separate paths (Blue and Red). Each path is imaged onto two cameras, each equipped with  $9 \times 9 \text{ cm}$  CCDs. Figure 3 shows the optomechanical concept. The cross-dispersed format enables the whole range, 380–710 nm, to be

covered simultaneously with 60 echelle orders and 4-pixel sampling per resolution element. Two fibres will be available, one for the object and one for the sky or simultaneous calibration. The fibres are separated by 30 pixels on the detector, which is also the minimum separation between adjacent orders.

The mechanical concept of CODEX builds on the HARPS (Mayor et al., 2003) experience to

obtain the highest mechanical and thermal stability. The thermal environment is designed to be progressively more stable with 10 mK variations within the spectrograph and 1 mK variations at the CCD. No movable parts are allowed in the spectrograph vessel. The optical system is mounted on three optical benches, enclosed in a large vacuum vessel. A full scientific pipeline and a very competitive set of analysis tools will be part of the set of deliverables, allowing the main science goals of CODEX to be achieved.

## Performance

The uniqueness of CODEX stems from the combination of photon-collecting capability, high resolving power and unprecedented Doppler precision. We have analysed the causes of instability in HARPS and they have been extensively addressed in our R&D programme.

- Any instability of the reference source will translate directly into radial velocity errors. The commonly used Th–Ar lamps are not sufficient for the required precision. Laser frequency combs would be the ideal calibrators. A development in collaboration with MPQ has produced very encouraging results in tests with HARPS (Wilken et al., 2010).
- The input from the astronomical source must be kept very homogeneous and stable, and a combination of accurate centring and scrambling is required. Our R&D programme on fibres has shown that square fibres produce high scrambling with minimal loss of light.
- Photons from the simultaneous calibration and from the astronomical objects are not detected by the same CCD pixels. Differential motions between pixels in the detector can produce RV errors. By testing the HARPS detectors we have shown that thermal control of the cryostat can reduce this effect to insignificant levels.

The expected signal-to-noise ratio (including slit losses of 20 %) is of 86 for  $V = 19$  and 12 for an object with  $V = 22$  with one-hour long observations. More than one billion potential targets will therefore be available to the CODEX user community.

## References

- Pasquini, L. et al. 2005, *The Messenger*, 122, 10  
 Liske, J. et al. 2008, *MNRAS*, 386, 1192  
 Mayor, M. et al. 2003, *The Messenger*, 114, 20  
 Wilken, T. et al. 2010, *MNRAS*, 405, L16

## Links

- <sup>1</sup> <http://www.iac.es/proyecto/codex/>

# EAGLE: An Adaptive Optics Fed, Multiple Integral Field Unit, Near-infrared Spectrograph

Simon Morris<sup>1</sup>  
Jean-Gabriel Cuby<sup>2</sup>

<sup>1</sup> Department of Physics, University of Durham, United Kingdom

<sup>2</sup> Laboratoire d'Astrophysique de Marseille, France

Team members:

Steven Beard<sup>1</sup>, Saskia Brierley<sup>1</sup>, Mathieu Cohen<sup>2</sup>, Jean-Gabriel Cuby<sup>3</sup>, Nigel Dipper<sup>4</sup>, Chris Evans<sup>1</sup>, Thierry Fusco<sup>5</sup>, Eric Gendron<sup>6</sup>, Peter Hastings<sup>1</sup>, Pascal Jagourel<sup>2</sup>, Philippe Laporte<sup>2</sup>, David Lee<sup>1</sup>, David Le Mignant<sup>3</sup>, Matt Lehnert<sup>2</sup>, Fabrice Madec<sup>3</sup>, Helen McGregor<sup>1</sup>, Tim Morris<sup>4</sup>, Richard Myers<sup>4</sup>, Phil Parr-Burman<sup>1</sup>, Mathieu Puech<sup>2</sup>, Gerard Rousset<sup>6</sup>, Hermine Schnetler<sup>1</sup>, Brian Stobie<sup>1</sup>, Mark Swinbank<sup>4</sup>, Gordon Talbot<sup>4</sup>, Sebastien Vives<sup>3</sup>, Pascal Vola<sup>3</sup>, Martyn Wells<sup>1</sup>

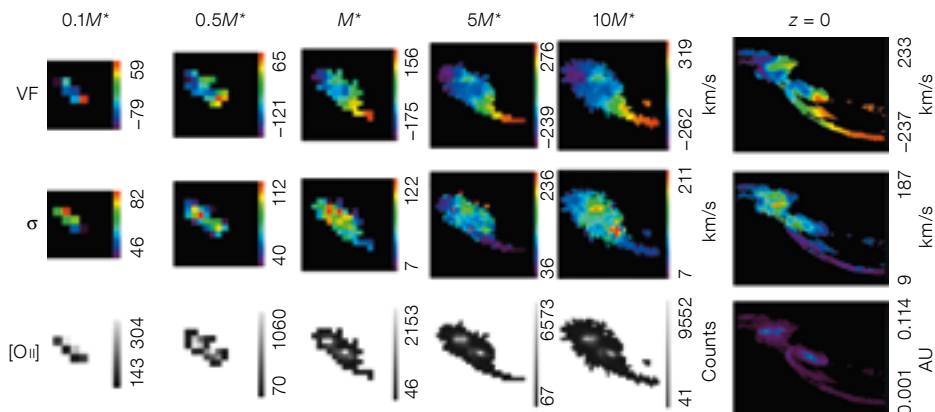
<sup>1</sup> UK ATC, <sup>2</sup> GEPI, Obs. de Paris, <sup>3</sup> LAM, <sup>4</sup> Durham Univ., <sup>5</sup> ONERA, <sup>6</sup> LESIA, Obs. de Paris

EAGLE will provide spatially-resolved (3D) spectroscopy in the near-infrared of  $\geq 20$  science targets (e.g., faint galaxies) simultaneously. It will sense and correct distortions from the atmosphere using multi-object adaptive optics, giving it an unrivalled survey efficiency even in the JWST era.

## Science drivers

A multi-Integral Field Unit (IFU) spectroscopic capability accessing a wide field, fed by high-order adaptive optics, and operating at near-infrared (NIR) wavelengths, has been a common aspiration of all ELT projects from the outset. Such an instrument is required to answer many of the most exciting and vexing questions in contemporary astrophysics. EAGLE is a general facility instrument that will serve a broad community of users. It uses the E-ELT at its best, over a wide field of view and with AO-corrected images.

One of the dominant scientific motivations for the E-ELT is the study of galaxy evolution. This encompasses a huge range of phenomena and scales — from studies of resolved stars in nearby galaxies, right out to our attempts to understand the properties of the most distant galaxies near the dawn of time. From consideration of these cases, and the broader astrophysical landscape, a set of science requirements were compiled for a NIR spectrograph with multiple, deployable IFUs. The three principal science cases used to optimise the EAGLE design were (in decreasing redshift order):



- First light: galaxies at the highest redshifts. Current estimates of surface densities at  $z > 7$  are well-matched to the EAGLE-designed surface densities, even after correction for the fraction that will not be suitable as they have features at wavelengths blocked by sky emission. By combining JWST imaging and low dispersion slit spectroscopy with EAGLE's ability to deliver spatially resolved  $R = 4000$  spectroscopy, even for objects of the sizes predicted at  $z > 7$ , the physics of the first light objects will be determined.
- The physics of high-redshift galaxies. See Figure 1 and Puech et al. (2010) for detailed modelling and discussion of this science case.
- Resolved stellar populations in the local volume. See Evans et al. (2010a) for an extended discussion of this science case. The EAGLE multiplex, combined with the ability to obtain spectra from multiple stars with each IFU field, and its wavelength coverage below the Ca triplet in the rest frame, make it ideal for this stellar archaeology case.

Detailed science simulations were undertaken to quantify the requirements, employing the tools developed by Puech et al. (2010) to generate simulated IFU datacubes for each of the principal cases (see Figure 1 for an example drawn from the Design Reference Mission galaxy formation science case).

The resulting instrument requirements (Table 1) have been used to develop the EAGLE concept, which combines superb image quality (via AO correction) with a wide field of view.

## Instrument design concept

EAGLE is located at the Gravity Invariant Focal Station (GIFS) of the E-ELT (see Cuby et al., 2009 and Figure 2). It consists of 20 IFU

Figure 1. Simulated EAGLE observations of a major merger at  $z = 4$  (Puech et al., 2010), with the input template ( $z = 0$ ) shown on the right-hand side. The simulations are shown as a function of the characteristic galaxy mass ( $M^*$ ); upper panels: recovered velocity field; central panels: recovered velocity dispersion; lower panels: recovered emission-line map.

spectrographs deployable (via pick-off mirrors) over a patrol field of 38.5 arcminutes<sup>2</sup>. Each IFU has an individual field of view of  $\sim 1.65 \times 1.65$  arcseconds. Pairs of IFUs are integrated into a single spectrograph and illuminate a  $4k \times 4k$  detector. Each IFU spectrograph is housed in a small cryostat ( $\sim 1500$  mm long and 600 mm diameter). One of the  $I$ -,  $Y$ -,  $H$ - or  $K$ -bands can be observed at a time resulting in a spectral resolution of  $\sim 4000$ . A high resolution mode of 10 000–13 000 is offered for stellar work. Each channel is equipped with its own deformable mirror (DM) for AO correction. There are wavefront sensors for six laser guide stars and five natural guide stars. There is a high level of duplication and redundancy in the instrument, providing robustness against single-point failures and easing maintenance. EAGLE is, in essence, a single-mode instrument.

EAGLE, in its default mode, uses Multi-Object Adaptive Optics (MOAO, see Figure 3 and Rousset et al., 2010). MOAO is just one more flavour of wide-field AO, as are LTAO, GLAO or MCAO. It is conceptually simple: once the atmospheric turbulent volume above the telescope is measured with tomographic techniques, the correction needed at a given position in the field of view is derived by a simple projection and is performed by a local DM. MOAO has now been demonstrated in the laboratory and there are several programmes underway to further characterise it on sky, in Europe as part of the EAGLE technology development plan (CANARY at the WHT) and in the US and Canada. EAGLE provides an



Table 1. Instrument requirements for EAGLE.

Patrol field	$\geq 5$ arcminute diameter
Science (IFU) field	$\geq 1.5 \times 1.5$ arcseconds
Multiplex (no. science fields)	$\geq 20$
Spatial pixel scale	37.5 milliarcseconds
Spatial resolution	Encircled energy $\geq 30\%$ into $2 \times 2$ spatial pixels
Spectral resolving power	4000 and $\geq 10\,000$
Wavelength coverage	<i>I</i> -, <i>Y</i> -, <i>H</i> -, <i>K</i> -bands (0.8–2.45 $\mu$ m)
Clustering/tiling	Distributed and clustered targets + ability to map contiguous regions

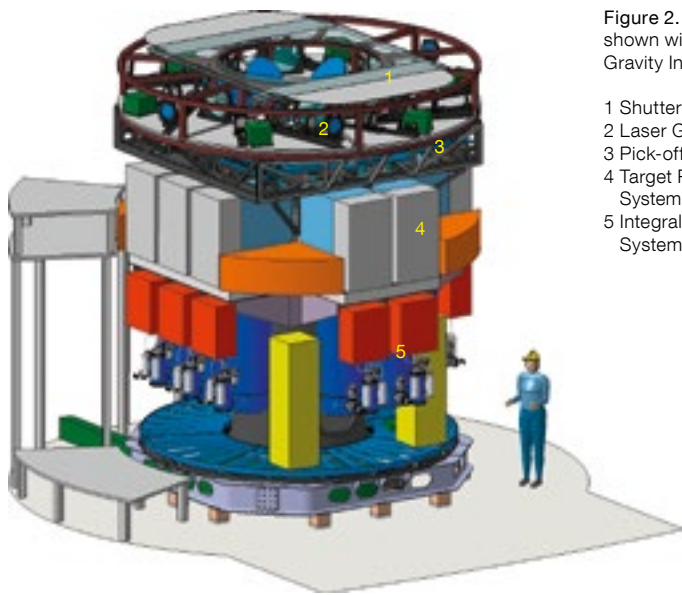


Figure 2. EAGLE mechanical design, shown within the footprint of the E-ELT Gravity Invariant Focal Station.

- 1 Shutter
- 2 Laser Guide Star Sensing System
- 3 Pick-off System (Focal Plane)
- 4 Target Reimaging and Magnification System (including Deformable Mirror)
- 5 Integral Field Unit and Spectrograph System

sensing functions (laser and natural guide stars) at the GIFS in a manner that will be transparent to the rest of the E-ELT systems. Because of this flexibility EAGLE could be used soon after first light for the E-ELT. To support this possibility, EAGLE has been designed using a coordinated systems engineering approach, with a carefully thought-out development plan. We have already had a number of interactions with possible industrial partners, and have an assembly, integration and test plan that includes pre-production of a single channel, to ensure that costs and risks for the whole instrument are minimised.

### Performance

Performance estimates of EAGLE suggest that it will achieve a signal to noise ratio (SNR) of  $\sim 5$  per spectral resolution element in 30 hours on a point-like (or slightly resolved object) of AB magnitude 27 in the *J*- or *H*-bands. This is  $\sim 2$  magnitudes fainter than that which JWST will achieve. For detailed spectroscopic investigations of the most distant galaxies discovered by JWST and for robust 3D studies of high-redshift galaxies, no other facility will be able to compete efficiently with EAGLE on the E-ELT which, in combination with ALMA, will provide us with unprecedented insight into the physical processes that drive galaxy formation and evolution. EAGLE will capitalise on the expertise in highly parallel 3D spectroscopic instruments developed by the MUSE and KMOS projects (which are often presented as E-ELT instrument precursors). Roughly speaking, EAGLE is the E-ELT counterpart of KMOS, with the added AO functionality and with an immensely superior scientific capability. When used in synergy with ALMA and JWST, the E-ELT, if equipped with EAGLE, will allow us to see the first objects to collapse to form stars in the Universe and understand how the majority of galaxies on the Universe are assembled, tracing their evolution from redshifts of more than eight to the present day.

A more extended and less technical description of the EAGLE science case and technical properties is given in Evans et al. (2010b).

### References

- Cuby, J.-G. et al. 2009, SPIE, 7439, 13  
 Evans, C. et al. 2010a, Proc. 1st AO4ELT conference, eds. Y. Clénet et al., EDP Sciences  
 Evans, C. et al. 2010b, Astronomy and Geophysics, 51, 2.17  
 Puech, M. et al. 2010, MNRAS, 402, 903  
 Rousset, G. et al. 2010, Proc. 1st AO4ELT conference, eds. Y. Clénet et al., EDP Sciences

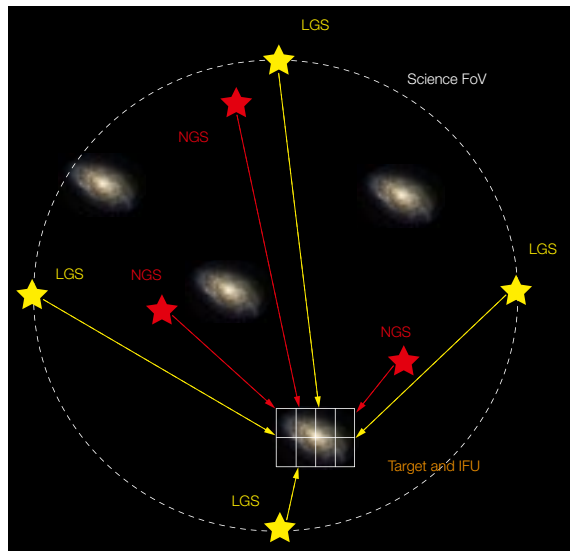


Figure 3. EAGLE will use a wide-field, multi-object adaptive optics system to correct the wavefront errors for each integral field unit (only one shown), using a combination of laser and natural guide stars to map the atmospheric turbulence.

image sampling of the order of 50–100 milliarcseconds, which is a robust trade-off between AO performance, sensitivity, scientific requirement and cost.

By construction (with DMs flat), EAGLE can also operate in GLAO or LTAO modes as the telescope AO is gradually deployed. EAGLE will reproduce several telescope wavefront

# EPICS: An Exoplanet Imaging Camera and Spectrograph for the E-ELT

Markus Kasper<sup>1</sup>  
Jean-Luc Beuzit<sup>2</sup>

<sup>1</sup> ESO

<sup>2</sup> Laboratoire d'Astrophysique de l'Observatoire de Grenoble (LAOG), France

Team members:

Lyu Abe<sup>1</sup>, Emmanuel Aller-Carpentier<sup>2</sup>, Jacopo Antichi<sup>3</sup>, Pierre Baudoz<sup>4</sup>, Anthony Boccaletti<sup>4</sup>, Mariangela Bonavita<sup>5</sup>, Kjetil Dohlen<sup>6</sup>, Enrico Fedrigo<sup>2</sup>, Raffaele Gratton<sup>5</sup>, Hiddo Hanenburg<sup>7</sup>, Norbert Hubin<sup>2</sup>, Rieks Jager<sup>7</sup>, Christoph Keller<sup>8</sup>, Florian Kerber<sup>2</sup>, Visa Korkiakoski<sup>3</sup>, Patrice Martinez<sup>2</sup>, Dino Mesa<sup>5</sup>, Olivier Preis<sup>3</sup>, Patrick Rabou<sup>3</sup>, Ronald Roelfsema<sup>7</sup>, Graeme Salter<sup>9</sup>, Hans Martin Schmid<sup>10</sup>, Mattias Tecza<sup>9</sup>, Niranjana Thatte<sup>9</sup>, Lars Venema<sup>7</sup>, Christophe Verinaud<sup>3</sup>, Natalia Yatskova<sup>2</sup>

<sup>1</sup> FIZEAU, <sup>2</sup> ESO, <sup>3</sup> LAOG, <sup>4</sup> LESIA, <sup>5</sup> Padova Obs.,

<sup>6</sup> LAM, <sup>7</sup> ASTRON, <sup>8</sup> NOVA, <sup>9</sup> Univ. Oxford, <sup>10</sup> ETHZ

EPICS is an instrument project for the direct imaging and characterisation of exoplanets with the E-ELT. The instrument is optimised for observations in the visible and the near-infrared and has photometric, spectroscopic and polarimetric capabilities.

## Science drivers

By about 2015, radial velocity surveys and the Kepler satellite will have provided a very good statistical answer to the crucial question of how frequent exoplanets in close orbits are around main sequence stars. These data will be complemented by the VLT SPHERE and Gemini GPI planet-finding instruments for self-luminous giant planets in outer orbits around young stars. Spectroscopic data are being obtained for transiting planets and additional data will be obtained for self-luminous giant planets. However, with the current and planned space instrumentation, the capability to study the physical properties of exoplanets comprehensively, and in particular their chemical composition, remains limited. The contribution of EPICS will be unique and transformational in various areas of exoplanet research:

- Detection of low-mass and wide-orbit planets to explore the mass–orbit function. Detections of exoplanets at angular separations larger than several AU with other techniques (e.g., transits with Kepler and Plato; radial velocities with CODEX) are inefficient.
- Characterisation of exoplanets down to the size of rocky planets by direct imaging, spectroscopy and polarimetry. Almost all nearby exoplanets detected by radial

velocity or astrometric techniques can only be characterised in larger numbers by direct imaging, since the probability for transits for larger orbital separations is low. In addition transit spectroscopy needs a fairly low exoplanet/star contrast of the order  $10^{-5}$ , limiting the method to rather tight orbits.

- Detection of very young planets (age  $\sim 10^7$  yr or less) close to the ice-line in order to test planet formation and evolution models and to understand the processes driving planet formation. Only EPICS will provide access to the small angular separations ( $\sim 30$ – $50$  milliarcseconds) required to observe giant exoplanets forming at the ice-line around pre-main sequence stars in the closest star-forming regions and young associations. Other techniques have limitations: space telescopes have too low an angular resolution; radial velocity studies suffer from stellar noise of the active young stars; long time frames are needed to follow a 3–5-AU orbit at the ice-line; the probability of catching a transit event of an object orbiting at the ice-line is virtually zero.

In addition, EPICS will make optimal use of the unique light-collecting power and angular resolution provided by the E-ELT. Its spectroscopic and polarimetric capabilities, as well as the AO performance providing diffraction-limited images even at optical wavelengths with angular resolutions down to 5 milliarcseconds (mas), will have a substantial impact on a large variety of astrophysical fields from studies of the Solar System and circumstellar discs to stellar astronomy and physics. Differential polarimetry at optical wavelengths will allow circumstellar debris discs to be imaged several orders of magnitudes fainter than the ones around  $\beta$  Pic or HR 4796 and at 10 mas resolution, to study the dynamic interaction of the disc with the embedded exoplanets.

In order to deliver these science goals, EPICS fulfills the following main requirements:

- The systematic intensity contrast between the exoplanet and the host star is better than  $10^{-8}$  at 30 mas and  $10^{-9}$  beyond 100 mas angular separation.
- Spectroscopic and polarimetric imaging, as well as medium resolution spectroscopy ( $R \sim 3000$ ) for the spectral characterisation of exoplanet chemistry is provided.
- The spectral range covers the optical to the NIR between 600 and 1650 nm.

## Instrument design concept

The key to achieving the highest imaging contrast and sensitivity from the ground is a superb correction of the dynamic and quasi-static

wavefront aberrations introduced by Earth's atmosphere and the telescope/instrument, respectively. In order to correct for dynamic aberrations and to suppress the atmospheric turbulence residual halo to about  $10^{-5}$  at small angular separations and to better than  $10^{-6}$  close to the adaptive optics correction radius, EPICS implements a high-order (or extreme) AO (called XAO) system using a roof-pyramid wavefront sensor.

All optics moving or rotating during an observation, such as atmospheric dispersion compensators or optical de-rotators, will be seen by XAO and the instrument elements, i.e., they will be placed in the common path (see Figure 1). Hence, EPICS will have excellent temporal stability of instrumental aberrations. Non-common path optical aberrations will be calibrated by focal plane wavefront sensing techniques and off-loaded to the XAO system. The diffraction pattern will be suppressed by apodisers and coronagraphs. As a result EPICS will achieve a high quasi-static point spread function (PSF) contrast of better than  $10^{-6}$ .

XAO and quasi-static PSF residuals are further calibrated and removed through instrumental and data analysis techniques such as spectral deconvolution with the NIR IFS (integral field spectrograph) and differential polarimetry with the optical polarimeter EPOL. These techniques will provide the required systematic contrast of the order  $10^{-8}$  at 30 mas to better than  $10^{-9}$  at larger angular separations. This last step of PSF residual calibration will be made possible through an optimisation of the instrument optics (Figure 1) for maximum efficiency of the speckle calibration techniques: i) a small and well-known speckle chromaticity is provided by a design that minimises amplitude aberrations introduced by the Fresnel propagation of optical errors; and ii) a small instrumental polarisation is provided by design, by avoiding large angle reflections and with a careful choice of coatings.

The IFS will provide a field of view of  $0.8 \times 0.8$  arcseconds sampled by 2.33 mas spaxels at the diffraction limit at 950 nm. The spectral range is 950–1650 nm, and the 2-pixel spectral resolution is 125 in the main observing mode. In addition, the IFS offers two higher spectral resolution modes with  $R \sim 1400$  and  $R \sim 20\,000$  with a smaller slit-like FoV of  $0.8 \times 0.014$  arcseconds. EPOL provides a FoV of  $2 \times 2$  arcseconds sampled by 1.5-mas spaxels at the diffraction limit at 600 nm for differential or classical imaging and polarimetry through various astronomical filters in the optical.

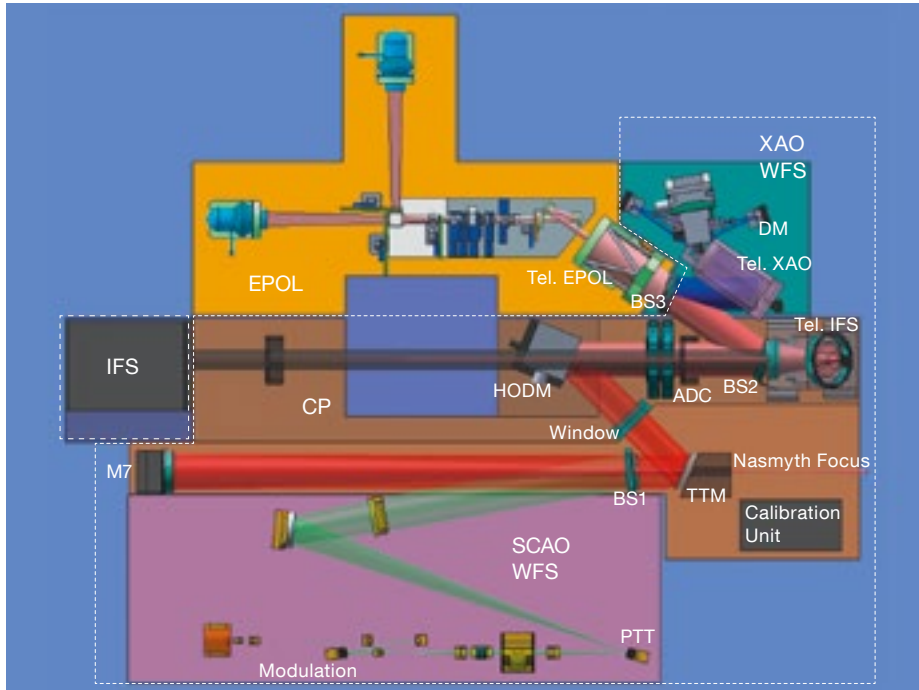


Figure 1. Top view of the optomechanical concept for EPICS.

Figure 2. Cuts along the  $x$ - and  $y$ - directions (full and dashed lines respectively), with distance in arcseconds, of the 2D contrast maps for an  $I = 2.3$  mag. G2 star (10-hour exposure with field rotation) are shown for the EPICS modes IFS (left) and EPOL (right).

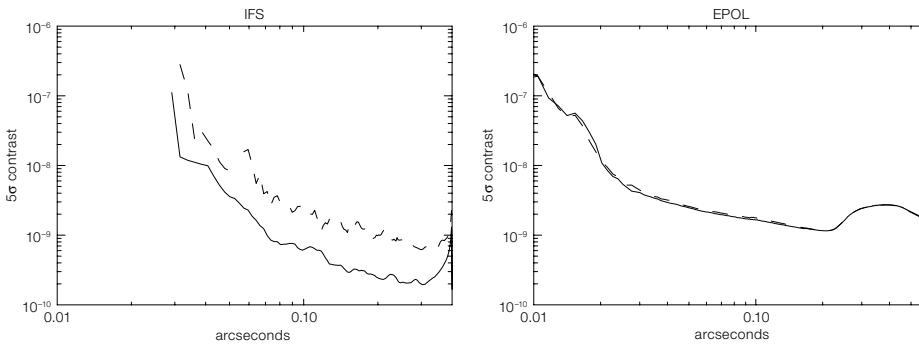
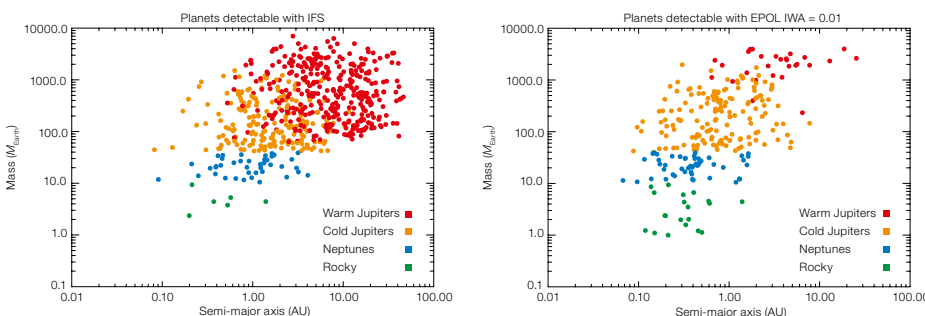


Figure 3. EPICS detections predicted by MESS for the IFS (left) and EPOL (right).



## Performance

In order to design EPICS and evaluate its performance, considering as many real-life error sources as possible, the following tools were developed: i) an end-to-end model of the instrument called PESCA (Parallel EPICS Simulation Codes and Applications); and ii) a Monte Carlo code called MESS to estimate the scientific output.

Combining the XAO residuals with assumptions on object brightness, E-ELT wavefront and amplitude errors and pupil geometry as well as instrument aberrations, throughput, diffraction suppression systems and data analysis, PESCA provides final contrast curves such as the ones shown in Figure 2. These contrasts demonstrate that EPICS is pushing the systematic limits below the photon noise level for virtually all possible targets with the IFS and EPOL. It therefore achieves photon-noise-limited contrast levels of the order  $10^{-9}$  at separations around 0.1 arcsecond required to observe exoplanets in reflected light. The lower number of photons available for EPOL when compared to the IFS (taking planet polarisation  $< 30\%$  and for a smaller spectral bandwidth) and the higher AO residuals at optical wavelengths, make EPOL less sensitive than the IFS at larger angular separations. The use at shorter wavelengths and the efficient apodised Lyot coronagraph, however, allow EPOL to achieve high contrast at the smallest angular separations down to 10 milli-arcseconds.

The PESCA contrast curves are then used to analyse the discovery space of EPICS with MESS, comparing expected properties of a population of exoplanets with the detection limits. MESS models stellar parameters (mass, distance, age, etc.) from samples of real stars, and models planet populations using theoretical models and observational results.

Figure 3 shows the EPICS detection rates predicted by MESS applied to a large sample of nearby or young stars. While the IFS generally achieves a better photon-noise-limited contrast and has higher detection rates on Neptune-like and giant planets, the very small inner working angle of EPOL allows it to detect several rocky planets that cannot be accessed by the IFS. Besides the detection capabilities of IFS and EPOL, the two instruments are also highly complementary in their characterisation capabilities and offer a variety of secondary science cases, e.g., the observation of circumstellar debris discs with EPOL at the highest angular resolutions.



# HARMONI: A Single Field, Visible and Near-infrared Integral Field Spectrograph for the E-ELT

Niranjan Thatte<sup>1</sup>

<sup>1</sup> Department of Physics, University of Oxford, United Kingdom

Team members:

Santiago Arribas<sup>1</sup>, Roland Bacon<sup>2</sup>, Giuseppina Battaglia<sup>3</sup>, Naidu Bezawada<sup>4</sup>, Neil Bowles<sup>5</sup>, Fraser Clarke<sup>5</sup>, Luis Colina<sup>1</sup>, Roger L. Davies<sup>5</sup>, Eric Emsellem<sup>3</sup>, Pierre Ferruit<sup>2</sup>, Ana Frago<sup>6</sup>, David Freeman<sup>7</sup>, Javier Fuentes<sup>6</sup>, Thierry Fusco<sup>8</sup>, Fernando Gago<sup>3</sup>, Angus Gallie<sup>4</sup>, Adolfo Garcia<sup>9</sup>, Ana Garcia-Perez<sup>10</sup>, Szymon Gladysz<sup>3</sup>, Timothy Goodall<sup>11</sup>, Felix Gracia<sup>6</sup>, Isobel Hook<sup>3</sup>, Patrick Irwin<sup>5</sup>, Matt Jarvis<sup>10</sup>, Aurelien Jarno<sup>2</sup>, Robert Kennicutt<sup>12</sup>, Johan Kosmowski<sup>2</sup>, Andrew Levan<sup>13</sup>, Andy Longmore<sup>4</sup>, David Lunney<sup>4</sup>, James Lynn<sup>5</sup>, John Magorrian<sup>5</sup>, Evencio Mediavilla<sup>6</sup>, Mark McCaughrean<sup>14</sup>, Stewart McLay<sup>4</sup>, David Montgomery<sup>4</sup>, Livia Origlia<sup>15</sup>, Arlette Pecontal<sup>5</sup>, Rafael Rebolo<sup>6</sup>, Alban Remillieux<sup>2</sup>, Dimitra Rigopoulou<sup>5</sup>, Sean Ryan<sup>10</sup>, Hermine Schnettler<sup>4</sup>, Harry Smith<sup>5</sup>, Dario Sosa<sup>6</sup>, Mark Swinbank<sup>16</sup>, Nial Tanvir<sup>17</sup>, Matthias Tecza<sup>5</sup>, Eline Tolstoy<sup>18</sup>, Aprajita Verma<sup>5</sup>

<sup>1</sup> CSIC, <sup>2</sup> CRAL, <sup>3</sup> ESO, <sup>4</sup> UK ATC, <sup>5</sup> Univ. Oxford, <sup>6</sup> IAC, <sup>7</sup> Kidger Optics, <sup>8</sup> ONERA, <sup>9</sup> SENER, <sup>10</sup> Univ. Hertfordshire, <sup>11</sup> JPL, <sup>12</sup> IoA, Cambridge, <sup>13</sup> Univ. Warwick, <sup>14</sup> ESA, <sup>15</sup> Bologna Obs., <sup>16</sup> Univ. Durham, <sup>17</sup> Univ. Leicester, <sup>18</sup> Kapteyn Inst.

**HARMONI provides a powerful E-ELT spectroscopic capability, in the visible and near-infrared (0.47–2.45  $\mu\text{m}$ ), at resolving powers ~ 4000, 10 000 and 20 000. Its integral field delivers ~ 32 000 simultaneous spectra, at scales ranging from seeing-limited to diffraction-limited.**

HARMONI is conceived as a workhorse instrument, addressing many of the key E-ELT science cases, to exploit the scientific niche resulting from its unique combination of collecting area and spatial resolution. At scales close to the diffraction limit, it will capitalise on the  $D^4$  sensitivity gain of the E-ELT to transform the landscape in visible and NIR astronomy. Even in seeing-limited conditions (or at wavelengths where AO cannot provide high Strehl ratios), HARMONI provides impressive gains with respect to the current generation of VLT instruments, e.g., a gain of ~ 25 in speed relative to MUSE at the ESO-VLT. HARMONI will provide complementarity and synergy with ALMA and JWST, with similar angular resolution to the former, and higher spectral and spatial resolution than the latter at very competitive sensitivities.

## Science drivers

The detailed science cases for HARMONI address many of the major questions of

astrophysics, such as distant supernovae as key diagnostics of dark energy, the nature of other planetary systems, the role of black holes and AGN in limiting the growth of massive galaxies, the properties of the highest redshift objects and the epoch and mechanism of reionisation. We summarise two cases, part of the E-ELT core science case, selected to illustrate the versatility of the instrument.

## Resolved stellar populations

The chemical and dynamical evolution of galaxies is imprinted in their resolved stellar populations, which provide the archaeological record of their star formation history and dynamical assembly. One of the principal goals of the E-ELT is to study the resolved stellar populations of massive galaxies spanning the full range of morphologies (including, for the first time, giant ellipticals), going beyond the Local Group to reach the Virgo cluster. The galaxy groups Centaurus (3.5 Mpc) and Leo (10 Mpc) are well within reach (including two ellipticals: Centaurus A and NGC 3379), as are spiral systems in Sculptor, starburst galaxies and compact dwarf elliptical galaxies.

Direct measurements of the chemo-dynamical properties of resolved stars require accurate velocity measurements combined with metallicity indicators for significant numbers of stars in each sub-component (e.g., thin disc, thick disc, halo, bulge). Key chemical elements are released by stars with different mass progenitors (e.g.,  $\alpha$ -elements from Type II SNe compared to iron peak, C, N and s-process elements from Type I a SNe), and on different time scales (~ 10 Myr vs. ~ 1 Gyr). The  $[\alpha/\text{Fe}]$  abundance ratio is thus a powerful tracer of the relative enrichment by Type II and I a SN at any given time in the star formation history (SFH) of a galaxy. Homogenous spectroscopic surveys enable an accurate study of the current dynamical state and thus dark matter masses and distributions in these systems as well as their chemical evolution (Battaglia et al., 2006).

Simulations around the Ca II triplet (~ 850 nm) at a resolution of 10 000 and 20 000 show that HARMONI can provide the accurate measurements of velocity and metallicity (Rutledge et al., 1997) to the required precision (velocities  $\pm 5 \text{ km s}^{-1}$  for dwarf galaxy types and  $\pm 20 \text{ km s}^{-1}$  for large galaxies and  $[\text{Fe}/\text{H}] \pm 0.3 \text{ dex}$ ) for main sequence stars in globular clusters and the field throughout the halo of the Milky Way (thus augmenting the picture of halo assembly built by Gaia), Magellanic Cloud globular clusters (multiple main sequences and possibly enhanced He abundances) and massive elliptical galaxies.

HARMONI can make precision measurements of velocity and metallicity for 1000 stars below the tip of the red giant branch (RGB) in Centaurus A, sampling three different radii, in 90 hours.

## The physics of high-redshift galaxies

The global properties of high-redshift galaxies (luminosity functions, stellar and total masses, sizes, spectral energy distributions [SEDs]) and their evolution with redshift is being revealed through deep, large area, multi-wavelength galaxy surveys. These studies have helped us to develop and constrain the theory of galaxy assembly; however, we have little (c.f. Swinbank et al., 2009) or no data to test the physical mechanisms at work, as we cannot yet probe the internal structure of high-redshift galaxies. Detailed studies with HARMONI of the internal kinematics, stellar population gradients, dust distribution, ionisation structure, nuclear properties, and interaction with the intergalactic medium (IGM) will show how the different physical processes are interrelated, and how they give rise to the integrated physical properties (see Figure 1).

Ultraluminous infrared galaxies (ULIRGs) are rare in the local Universe, but are much more common at high redshift (Le Floc'h et al., 2005). Intense star formation (and AGN activity), driven by large reservoirs of gas and dust, powers these dust-enshrouded objects, which are the likely progenitors of the most massive galaxies. In many cases ULIRGs show clear signs of an ongoing merging process. The merger may trigger star formation through gas transport, and also feed the central AGN, whose energetic outflows may provide the feedback that limits the growth of massive galaxies (Sanders & Mirabel, 1996). HARMONI can probe the properties of these objects over a wide range of spatial scales. In particular we can detect nuclear discs or rings, non-rotational flows such as starburst-induced superwinds, tidally induced motions, or nuclear gas inflows (Figure 2), measure rotation curves and infer the possible subsequent evolution of ULIRGs into normal ellipticals by measuring their fundamental plane parameters.

The combination of high spatial and spectral resolution provided by HARMONI+LTAO will allow the processes occurring within galaxies to be probed on scales of individual H II regions. Such observations promise to yield the distribution of star formation, gas dynamics, metallicity and outflow properties of high-z galaxies in unprecedented detail, testing the route by which primitive systems form their bulges, distribute their metals and how efficiently

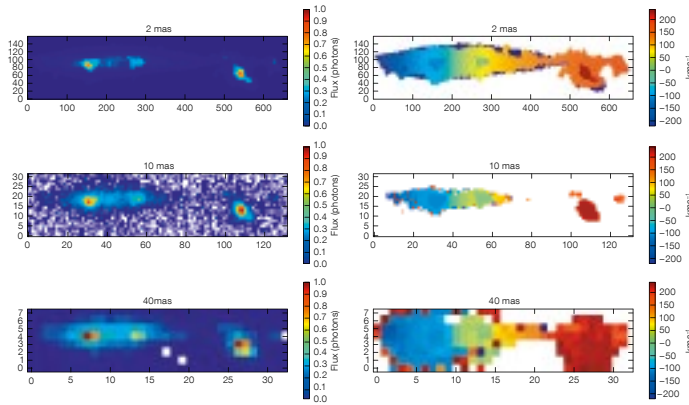


**Figure 1.** Emission line maps and velocity fields of an edge-on Lyman-break galaxy at  $z \sim 3$ , observed with HARMONI at various spaxel scales. The top panel shows the input to the simulations. The complementarity between sensitivity to extended structure and spatial resolution is clearly seen.

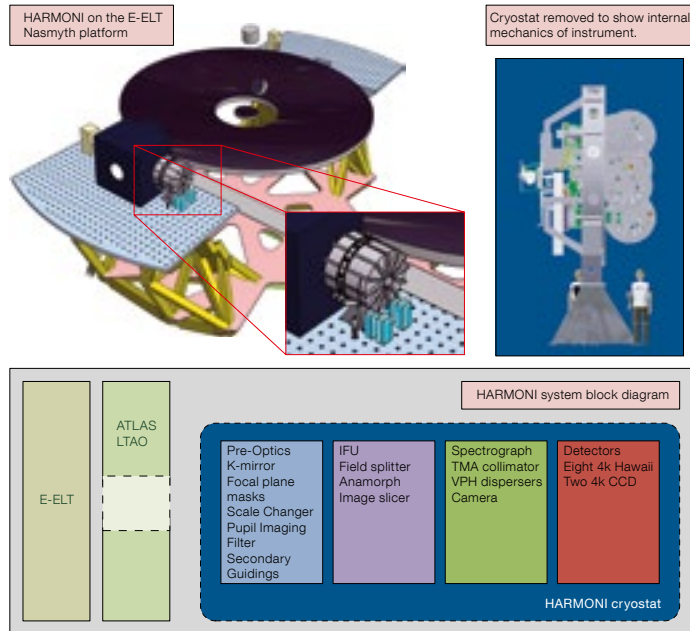


**Figure 3.** HARMONI deployed at the E-ELT Nasmyth focus (top left). A CAD rendering of the inside of the cryostat (top right) shows all the optomechanical components organised into four subassemblies, as shown in the block diagram below. The ATLAS LTAO module (ring geometry) introduces no optical surfaces within the HARMONI FoV.

baryons are ejected from the galaxy potential and into the IGM.

### Instrument design concept

HARMONI provides a range of spaxel scales (0.04, 0.02, 0.01 and 0.004 arcseconds) to match a wide range of science programmes. The coarsest scale provides a  $5 \times 10$  arcsecond FoV, well suited to seeing-limited observations. The FoV scales with spaxel size for other scales. The rectangular FoV allows nodding-on-IFU, providing accurate sky subtraction with no sky overheads. With its large range of spaxel scales, HARMONI can easily adapt to any flavour of adaptive optics — GLAO, LTAO and SCAO, or even with no AO at all!

HARMONI is conceptually simple, and will be easy to calibrate and operate, providing the

E-ELT with a “point and shoot” spectroscopic capability. It is based on a proven concept, and requires no significant R&D before it can be built.

The instrument concept (Figure 3) employs an optical de-rotator (“K-mirror”) at the input, allowing for a fixed cryogenic instrument with a constant gravity vector, and eliminating flexure-induced variations. Secondary (on-instrument) guiding, using faint stars/compact galaxies, ensures absolute focal plane stability of the de-rotated field. Scale-changing pre-optics provides four spaxel scales, selectable “on-the-fly”, and also accommodates the filter wheel, shutter, and pupil imaging mechanism. The “heart” of the instrument is the integral field unit, comprising a four-way field splitter feeding image slicers. The back-end spectrographs disperse the pseudo-slits on to eight  $4k \times 4k$  NIR detectors, with grating wheels providing the different

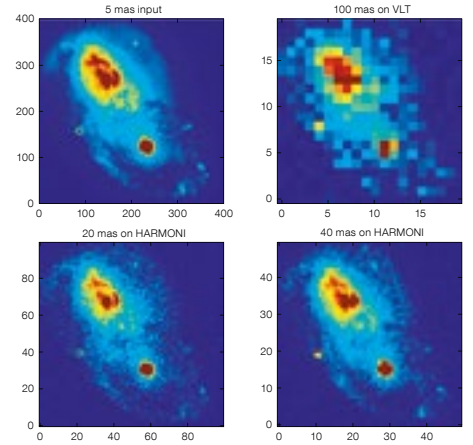


**Figure 2.** Simulations showing a ULIRG at  $z \sim 2$ , imaged in the  $K$ -band (rest frame  $H\alpha$ ) using HARMONI with SCAO or LTAO at two different spaxel scales (20 and 40 mas, bottom panels). The corresponding VLT view is shown at top right, and the simulation input at top left.

dispersions and wavelength ranges. The design is entirely reflective up to the dispersers, allowing two additional disperser-camera units to be easily accommodated, providing visible wavelength (0.47–0.8  $\mu\text{m}$ ) coverage.

### Performance

With its very high throughput ( $> 35\%$ , including detector), and superb image quality (FWHM  $< 1$  detector pixel, both spatially and spectrally), HARMONI provides excellent performance. A signal-to-noise ratio of 5 per spectral pixel (in-between the OH lines) for point sources (20-mas spaxel sampling) is achieved in 5 hours (900 s exposures, 0.8-arc-second seeing, LTAO correction) for  $R_{AB} = 25.4$  and  $H_{AB} = 27.4$ , at  $R \sim 4000$ . For extended sources, SNR of 5 per spectral and spatial (40 mas) spaxel is achieved for  $R_{AB} = 22.7$  arcsecond $^{-2}$  and  $H_{AB} = 21.1$  arcsecond $^{-2}$ . HARMONI will be more sensitive than JWST in the NIR for medium/high resolution spectroscopic work, where the angular resolution gain over JWST will be a factor of seven.

### References

Battaglia, G. et al. 2006, A&A, 459, 423  
 Rutledge, G. A. et al. 1997, PASP, 109, 883  
 Swinbank, M. et al. 2009, MNRAS, 400, 1121  
 Le Floch, E. et al. 2005, ApJ, 632, 169  
 Sanders, D. B. & Mirabel, I. F. 1996, ARAA, 34, 749

# MAORY: A Multi-conjugate Adaptive Optics Relay for the E-ELT

Emiliano Diolaiti<sup>1</sup>

<sup>1</sup> INAF–Osservatorio Astronomico di Bologna, Italy

Team members:

Andrea Baruffolo<sup>1</sup>, Michele Bellazzini<sup>2</sup>, Valdemaro Biliotti<sup>3</sup>, Giovanni Bregoli<sup>2</sup>, Chris Butler<sup>4</sup>, Paolo Cilieggi<sup>2</sup>, Jean-Marc Conan<sup>5</sup>, Giuseppe Cosentino<sup>6</sup>, Sandro D’Odorico<sup>7</sup>, Bernard Delabre<sup>7</sup>, Italo Foppiani<sup>2</sup>, Thierry Fusco<sup>5</sup>, Norbert Hubin<sup>7</sup>, Matteo Lombini<sup>2,6</sup>, Enrico Marchetti<sup>7</sup>, Serge Meimon<sup>5</sup>, Cyril Petit<sup>5</sup>, Clélia Robert<sup>5</sup>, Pierfrancesco Rossetti<sup>8</sup>, Laura Schreiber<sup>6</sup>, Raffaele Tomelleri<sup>8</sup>

<sup>1</sup> INAF–OAPd, <sup>2</sup> INAF–OABo, <sup>3</sup> INAF–OAA, <sup>4</sup> INAF–IASFBo, <sup>5</sup> ONERA, <sup>6</sup> Univ. Bologna, <sup>7</sup> ESO, <sup>8</sup> Tomelleri s.r.l.

MAORY provides atmospheric turbulence compensation for the E-ELT over a 2-arc-minute field of view in the near-infrared. Correction performance and sky coverage are achieved by three deformable mirrors, driven by a wavefront sensing system based on laser and natural guide stars.

## Science drivers

MAORY is an MCAO module designed for the E-ELT devoted to the compensation of the effects of the atmospheric turbulence in the wavelength range 0.8–2.4  $\mu\text{m}$  over a field of view of up to 2 arcminutes diameter. Among the candidate science instruments fed by MAORY, the high angular resolution camera MICADO requires a correction of high quality and uniformity over a medium-sized field of approximately 1 arcminute. High accuracy photometry and astrometry are key science drivers of MICADO: the achievement of these goals relies on a stable adaptive optics correction and on suitable calibration methods. MICADO also requires a gravity invariant output port. MAORY is also requested to provide a second output port designed to feed another instrument located on the side of the module on the Nasmyth platform. Candidate science instruments that might be served by MAORY are either a single field near-infrared spectrograph, such as SIMPLE, for which the on-axis point spread function energy concentration delivered by the adaptive optics module is a key science requirement, or a multi-object spectrograph, requiring a good level of PSF energy concentration over the full field corrected by MAORY. Other instrument concepts, such as a wide-field imaging camera with reduced angular resolution, might be considered. Sky coverage, defined as the

fraction of sky where adaptive optics provides a useful correction, is a key requirement, common to all science instruments. The sky coverage of MAORY has also to be high at the Galactic pole, where the star density is low.

## Instrument design concept

The expected location of MAORY is the E-ELT Nasmyth platform, on one of the bent foci (see Figure 1). From the optical design point of view, it is a finite conjugate relay formed by two pairs of aspheric off-axis mirrors (see Figure 2). Three flat mirrors fold the relay to fit the reserved area on the Nasmyth platform; two of these flat mirrors are deformable and compensate for the atmospheric turbulence. The optical relay produces an image of the telescope focal plane with unit magnification. A dichroic reflects the science channel light (wavelengths longer than 0.6  $\mu\text{m}$ ) and transmits the laser guide star light (0.589  $\mu\text{m}$ ), that is focused by a refractive objective. The module feeds two focal stations: the gravity invariant port underneath the optical bench, providing mechanical derotation for a light instrument such as MICADO, and the lateral port on one side of the bench to feed an instrument standing on the Nasmyth platform, detached from the module. Using optical coatings similar to those foreseen for the telescope, the thermal background of MAORY is expected to have little impact on MICADO even at ambient temperatures. The post-focal relay has an expected optical throughput larger than 82 % at all wavelengths longer than 0.8  $\mu\text{m}$  and larger than 91 % at all wavelengths longer than 2.0  $\mu\text{m}$ .

MAORY is based on the MCAO concept, first introduced by Beckers (1989). Three levels of wavefront correction are implemented: the telescope adaptive mirror M4, optically conjugated to a few hundred metres above the telescope pupil; and two post-focal deformable mirrors, conjugated at 4 km and 12.7 km from the telescope pupil, in order to correct the high altitude turbulence effectively (see Figure 2). The correction of the tip-tilt, due to the atmosphere and the telescope windshake, is mainly performed by the telescope mirror M5.

The measurement of the high-order wavefront distortions is performed by means of six sodium laser guide stars, arranged on a circle of 2 arcminutes diameter. This angular separation was found to be a good compromise between errors related to the LGS cone effect, pushing towards larger launching angles, and isoplanatic effects. The LGS are assumed to be projected from the telescope edge: this choice translates into a slightly higher measurement error than central projection, due to the larger perspective spot elongation, however it can eliminate the so-called fratricide effect among different guide stars, related to the Rayleigh and Mie scattering in the atmosphere. The guide stars feed six Shack–Hartmann wavefront sensors (WFS). The LGS constellation is kept fixed with respect to the telescope pupil, so that it rotates with the elevation axis as seen from the Nasmyth platform. This choice minimises the requirements on the derotation, either optomechanical or software, of the LGS WFS probes and of the LGS footprints on the post-focal deformable mirrors.

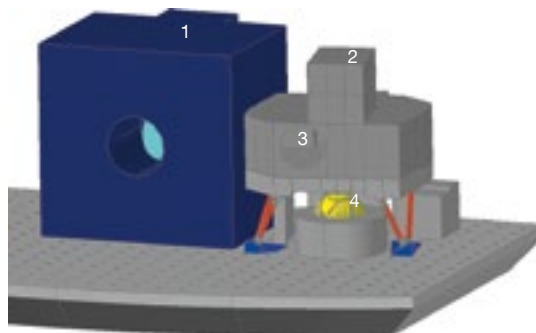


Figure 1. MAORY on the E-ELT Nasmyth platform; MICADO is on the gravity invariant port underneath the optical bench.

- 1 Pre-focal station
- 2 MAORY
- 3 Lateral port
- 4 MICADO

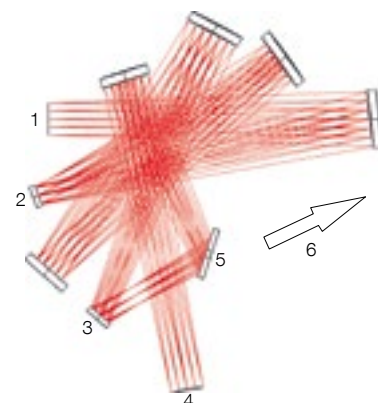
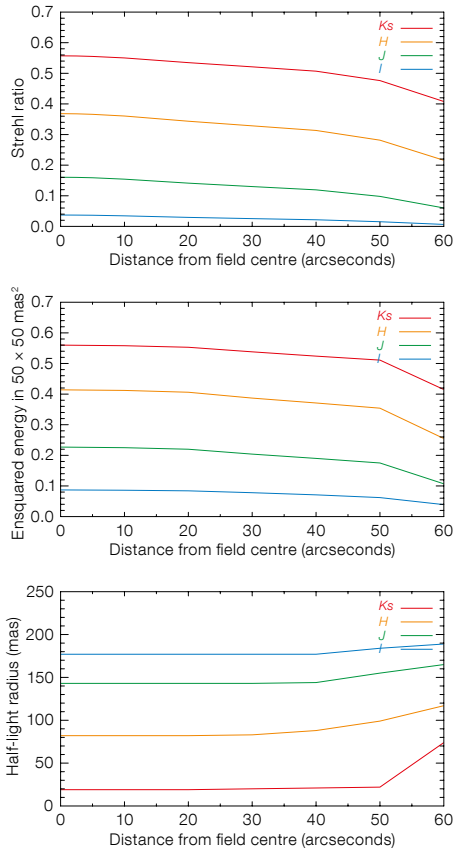


Figure 2. The post-focal relay optical layout of MAORY; the two post-focal deformable mirrors are shown (2 and 3).

- 1 E-ELT focus
- 2 DM 4 km
- 3 DM 12.7 km
- 4 MAORY output focus (lateral port)
- 5 Dichroic
- 6 LGS channel





**Figure 3.** MCAO correction performance vs. radial distance from centre of field of view. Different colours correspond to different wavelengths. Upper: Strehl ratio. Middle: PSF energy enclosed in a  $50 \times 50$  mas aperture. Lower: Radius of circular aperture enclosing 50% of the PSF energy (half-light radius). All simulations for median seeing.

To solve the LGS tip-tilt indetermination problem, three natural guide stars are required (Ellerbroek & Rigaut, 2001): as a baseline two of them are used to measure tip-tilt only, while the third, positioned on the brightest star found on the search field, is used to measure tip-tilt and focus in order to provide a reference for the rapidly varying focus term in the LGS signals due to the sodium layer instability. The three NGS are searched over a wide field of 2.6-arcminute diameter; they are observed in the near infrared ( $H$ -band, 1.5–1.8  $\mu\text{m}$ ), to take advantage of the spot-shrinking resulting from the high-order correction driven by the LGS WFS, thus allowing the use of faint NGS that translates into a high sky coverage. In each of the three NGS probes, light of wavelength 0.6–0.9  $\mu\text{m}$  is split from the infrared light used for tip-tilt and focus measurement. This light feeds a reference WFS, operating at frequencies in the range 0.1–1 Hz and used to monitor the LGS non-common

**Table 1.** Expected performance and corresponding sky coverage at the Galactic pole. The performance is expressed in terms of Strehl ratio averaged over the MICADO field of view ( $53 \times 53$  arcsecond) for median seeing.

Minimum field-averaged Strehl ratio (field $53 \times 53$ arcsecond)				Sky coverage
$Ks$	$H$	$J$	$I$	
0.53	0.34	0.14	0.03	39%
0.51	0.32	0.13	0.02	50%
0.41	0.22	0.06	< 0.01	80%

path aberrations related to the sodium layer profile variability (Pfrommer et al., 2009). During normal operations, the reference WFS has a pupil sampling of approximately  $10 \times 10$  subapertures. An engineering mode with up to  $84 \times 84$  subapertures is foreseen as well. This mode would allow a high-order MCAO correction based on three NGS, in a configuration similar to MAD (Marchetti et al., 2007), to be performed.

### Performance

The MCAO performance was evaluated by an analytic code, allowing the power spectral density of the residual turbulence to be estimated. All the error sources that could not be directly included in the code were accounted for in the global error budget, which amounts to a wavefront error of  $\sim 300$  nm root-mean squared (rms). PSFs were computed over a grid of directions in the field and for different wavelengths ( $Ks$ : 2.16  $\mu\text{m}$ ,  $H$ : 1.65  $\mu\text{m}$ ,  $J$ : 1.215  $\mu\text{m}$ ,  $I$ : 0.9  $\mu\text{m}$ ). The performance is shown in Figure 3 for median seeing conditions (FWHM = 0.8 arcseconds at 0.5  $\mu\text{m}$  wavelength,  $\tau_0 = 2.5$  ms,  $\theta_0 = 2.08$  arcseconds,  $L_0 = 25$  m). The top panel shows the Strehl ratio, i.e. the ratio of the central value of the MCAO PSF to the central value of the ideal PSF. The middle panel shows the PSF enclosed energy in a square aperture of  $50 \times 50$  mas. The enclosed energy in the rectangular slit of SIMPLE ( $28 \times 54$  mas) is only slightly lower than this: in  $Ks$ -band it decreases from 0.56 to 0.50, in  $I$ -band from 0.09 to 0.08. The lower panel shows the half light radius of the PSF. The sky coverage, estimated by means of Monte Carlo simulations of random asterisms with star densities derived from the TRILEGAL code (Girardi et al., 2005), is shown in Table 1 for the Galactic pole. The first line in this table refers to the nominal performance: in this case the limited NGS brightness translates into an image jitter within 2 mas rms. To draw a few conclusions on the estimated performance: MAORY provides the science instruments with a field of 2 arcminutes diameter (up to 2.6 arcminutes, considering the whole field available for NGS search), corrected with good quality (average Strehl ratio  $\sim 0.5$  in  $Ks$ -band

over 2 arcminutes under median seeing) and with an exceptional correction uniformity (rms variation of Strehl ratio lower than 0.05 over the full field). A notable feature is the high sky coverage that is obtained by a robust closed loop correction over the whole NGS search field.

On the basis of a study on simulated images, accounting for PSF shape, field variation and seeing dependency, it was shown that the relative photometric accuracy (0.03 mag rms) and the relative astrometric accuracy (0.05–0.1 mas) required by MICADO are both achievable. A more detailed analysis of these errors, including atmospheric effects, will be pursued further in the future, using PSFs obtained by end-to-end simulations.

Additional information on the performance and PSF datasets may be found on the project web page<sup>1</sup>.

### References

- Beckers, J. 1989, SPIE, 1114, 215
- Ellerbroek, B. & Rigaut, F. 2001, J. Opt. Soc. Am. A, 18, 2539
- Girardi, L. et al. 2005, A&A, 463, 895
- Marchetti, E. et al. 2007, The Messenger, 129, 8
- Pfrommer, T. et al. 2009, Geophysical Research Letters, 36, L15831

### Links

<sup>1</sup> <http://www.bo.astro.it/~maory>

# METIS: A Mid-infrared E-ELT Imager and Spectrograph

Bernhard Brandl<sup>1</sup>  
 Joris Blommaert<sup>2</sup>  
 Alistair Glasse<sup>3</sup>  
 Rainer Lenzen<sup>4</sup>  
 Eric Pantin<sup>5</sup>

<sup>1</sup> Leiden Observatory, the Netherlands  
<sup>2</sup> Katholieke Universiteit Leuven, Belgium  
<sup>3</sup> United Kingdom Astronomy Technology Centre, Edinburgh, United Kingdom  
<sup>4</sup> Max-Planck-Institut für Astronomie, Heidelberg, Germany  
<sup>5</sup> CEA Saclay, Gif-sur-Yvette, France

**Team members:**

Maarten Baes<sup>1</sup>, Richard Bennett<sup>2</sup>, Hermann Boehnhardt<sup>3</sup>, Wolfgang Brandner<sup>4</sup>, Christoph Cara<sup>5</sup>, Celine Cavarroc<sup>5</sup>, Gilles Durand<sup>5</sup>, Stefan Hippler<sup>4</sup>, Pascal Gallais<sup>5</sup>, Thomas Henning<sup>4</sup>, Rik ter Horst<sup>6</sup>, James Hough<sup>7</sup>, Laurent Jollissaint<sup>8,9</sup>, Hans Ulrich Kaeuffi<sup>10</sup>, Sarah Kendrew<sup>9</sup>, Jan Kragt<sup>6</sup>, Gabby Kroes<sup>6</sup>, Pierre-Olivier Lagage<sup>5</sup>, David Lee<sup>2</sup>, Frank Molster<sup>11</sup>, Toby Moore<sup>12</sup>, Vincent Moreau<sup>5</sup>, Ramon Navarro<sup>6</sup>, Ad Oudenhuyzen<sup>6</sup>, Phil Parr-Burman<sup>2</sup>, Wim Pessemier<sup>13</sup>, Johan Pragt<sup>6</sup>, Gert Raskin<sup>13</sup>, Ronald Roelfsema<sup>6</sup>, Ralf-Rainer Rohloff<sup>4</sup>, Samuel Ronayette<sup>5</sup>, Remko Stuik<sup>9</sup>, Stephen Todd<sup>2</sup>, Stefan Uttenthaler<sup>13</sup>, Bart Vandenbussche<sup>13</sup>, Paul van der Werf<sup>9</sup>, Ewine van Dishoeck<sup>8,14</sup>, Lars Venema<sup>9</sup>, Christoffel Waelkens<sup>13</sup>

<sup>1</sup> Univ. Gent, <sup>2</sup> UK ATC, <sup>3</sup> MPS, <sup>4</sup> MPIA, <sup>5</sup> CEA Saclay, <sup>6</sup> NOVA-ASTRON, <sup>7</sup> Univ. Hertfordshire, <sup>8</sup> Leiden Obs., <sup>9</sup> aquilAOptics, <sup>10</sup> ESO, <sup>11</sup> NOVA, Leiden, <sup>12</sup> John Moores Univ., <sup>13</sup> KU Leuven, <sup>14</sup> MPE

METIS is the only instrument concept for the E-ELT that covers the thermal infrared wavelengths from 2.9–14  $\mu\text{m}$ . METIS contains a diffraction-limited imager and an integral field unit high resolution spectrograph. The science case for METIS includes exoplanets, circumstellar discs, Solar System objects, supermassive black holes and high-redshift galaxies.

**Science drivers**

Generally, mid-infrared astronomy focuses mainly on objects that are very dusty or dust-obscured, intrinsically cool or significantly redshifted by the cosmic expansion. Furthermore, the mid-infrared (MIR) wavelength range is extremely rich in spectral diagnostics, such as emission and absorption lines of virtually all molecules, numerous atoms and ions, and solid-state features — most of which are unique or complementary to diagnostics found at other wavelengths.

The five main science drivers, for which METIS is expected to produce breakthrough science, are:

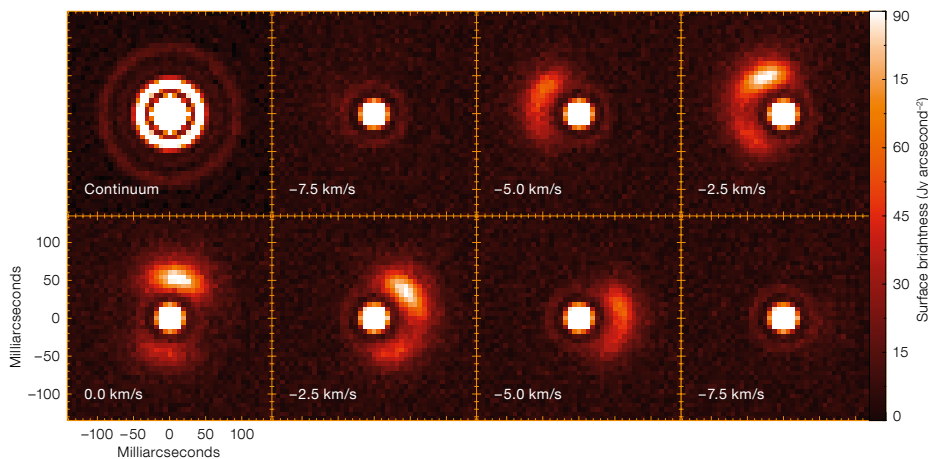
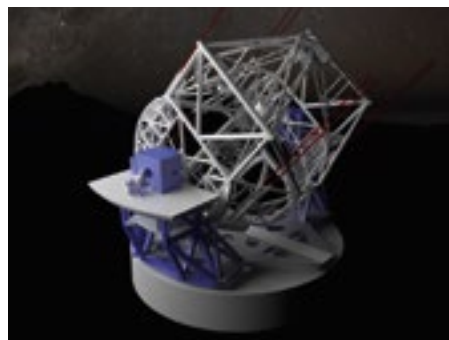


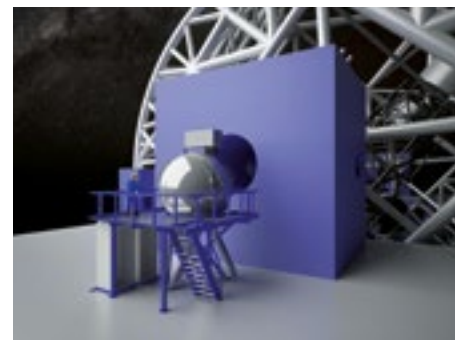
**Figure 1.** Simulation of a METIS IFU image cube of the CO P(8) line from SR 21 for an assumed distance of 125 pc (Pontoppidan et al., 2009). The disc has an inner gap in the gas at 6.5 AU (similar to the orbit of Jupiter) and is oriented at 20 degrees inclination, with the far side of the disc toward the top of the image.

- Protoplanetary discs and formation of planets: METIS will allow us to spatially resolve protoplanetary discs in the MIR to search for the footprints of protoplanets as well as to perform spectral line imaging (see Figure 1) and spectro-astrometry. METIS may be able to directly detect the signatures of hot, accreting protoplanets and the dynamical structure of the accretion flow onto the planet. METIS will reveal the dominant mechanisms for gas dissipation and the chemical content of the planet-forming regions, and clarify the role of water and organic molecules of astrobiological interest. Probing the warmer molecular gas, these studies will complement the work of ALMA.
- Physical and chemical properties of exoplanets: METIS will allow us to investigate the basic physical and chemical properties of exoplanets such as their orbital parameters

**Figure 2.** Left: The E-ELT with METIS on its Nasmyth platform A. Right: Zoom-in to show details of the cryostat, the detached service platform, and the location of the electronics racks.



- and internal structures, temperature profiles, composition of their atmospheres, weather and seasons. METIS has the greatest detection potential in younger planetary systems, and will be able to study exo-Neptunes with a few tens of Earth masses. METIS will be rather unique in its ability for photometric and spectroscopic characterisation of a large number of young exoplanets.
- The formation history of the Solar System: METIS will enable the determination of the composition and temperature gradients in the planetary formation disc, as well as the D/H isotope ratios in cometary volatiles and how they relate to that of terrestrial H<sub>2</sub>O. Furthermore, METIS will substantially extend the study of surface ices and organics in Kuiper Belt objects (currently, only Pluto is detectable), and measure the thermal inertia of asteroidal bodies and cometary nuclei to constrain their internal constitution.
- The growth of supermassive black holes (SMBHs): METIS provides a unique opportunity to investigate the nuclei in local AGN and ultra-luminous IR galaxies by mapping gas flows and measuring dynamic black hole masses. The unique combination of high angular resolution, high sensitivity and dust-penetrating wavelengths, will allow METIS to determine the masses of SMBHs, especially in heavily obscured nuclei. Detailed imaging



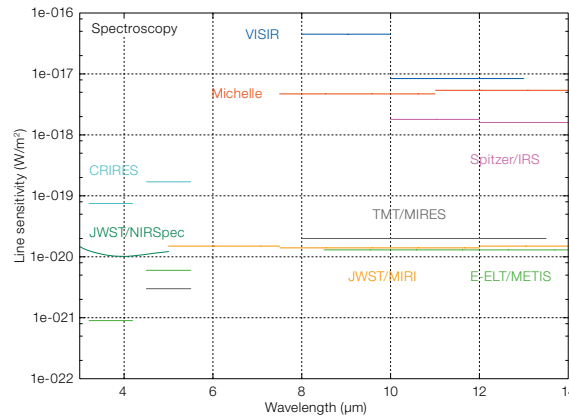
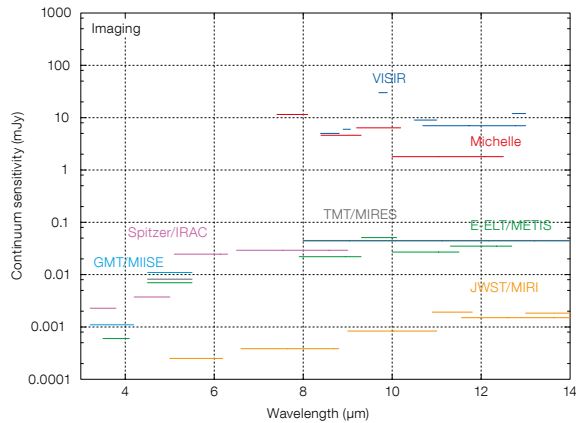


**Figure 3.** Point source/unresolved line sensitivities,  $10\sigma$ , 1-hour exposure for METIS and its competitors. Note that the instruments shown under “Spectroscopy” have different spectral resolutions:  $R = 100\,000$  (CRIRES),  $R = 25\,000$  (VISIR),  $R = 30\,000$  (Michelle),  $R = 600$  (IRS),  $R = 3000$  (MIRI),  $R = 2700$  (NIRSpec).

and spectroscopy will help to analyse the size, geometry and dynamics of the circum-nuclear tori and to investigate the interplay between star formation and nuclear feedback.

- Morphologies and dynamics of high- $z$  galaxies: METIS can ideally be used to study the structures and dynamics of high-redshift galaxies and the validity of scaling laws and the concept of a fundamental plane. Observationally, the ideal probe of stellar dynamics is provided by the calcium triplet, which is redshifted to the METIS wavelength range. It will take the resolution provided by a 42-metre telescope to provide an accurate measurement of stellar dynamical masses of high-redshift galaxies. ALMA in its widest configuration can only measure the gas kinematics from the CO line, but not the stellar velocities.

Other typical objects to be studied with METIS are the Martian atmosphere, low-mass brown dwarfs, the Galactic Centre, evolved stars and their environments, the birthplaces of massive stars and ultra-compact H II regions and the initial mass function (IMF) in massive stellar clusters.

#### Instrument design concept

The science case for METIS, as sketched above, requires two main instrument modes:

1. A diffraction-limited imager at  $LM$ -bands, and  $N$ -band with an approximately  $18 \times 18$  arcsecond wide FoV. The imager includes the following observing modes: coronagraphy at  $L$ - and  $N$ -band, low resolution ( $900 \leq R \leq 5000$ ) long-slit spectroscopy at  $LM$ - and  $N$ -bands, and polarimetry at  $N$ -band.
2. An integral field unit (IFU) feeding a high resolution ( $R \sim 100\,000$ ) spectrograph at  $LM$ -bands ( $2.9\text{--}5.3\ \mu\text{m}$ ) with a FoV of about  $0.4 \times 1.5$  arcseconds.

All of these observing modes require AO correction, unless the atmospheric conditions are very favourable (METIS will be able to achieve quasi-diffraction-limited images at  $10\ \mu\text{m}$  without AO when the outer scale of turbulence becomes significantly smaller than the telescope aperture). METIS will achieve diffraction-limited performance with the E-ELT’s M4/M5 and does not require additional adaptive mirrors. METIS AO will follow a two-step approach: first, an internal wavefront sensor, which is optimised for the highest Strehl ratios for on-axis, self-referencing targets, will be used; then a couple of years after commissioning, an LGS with an LTAO system will be needed to provide full sky coverage.

The optical system of METIS uses all-reflective optics (with the exception of the spectral filters and dichroic beam splitters) to simplify testing and integration and to minimise chromatic aberrations. The optical system provides superb diffraction-limited performance. The main optical modules of METIS are:

- The wavefront sensor module, which hosts the internal wavefront sensor, an atmospheric dispersion corrector, field selector and derotator.
- The warm and cold calibration units, which provide a set of important calibration sources, including an integrating sphere as flux reference.
- The common fore-optics, which is the central part of the optical system. It directs the science beam to the AO/calibration modules, and it includes two essential optical components: (i) the cold pupil stop, which can also provide fast, two-dimensional chopping ( $\pm 5$  arcseconds) and residual tip/tilt beam stabilisation; (ii) the image derotator to provide a stable focal plane in both science modules.
- The  $LMN$ -band imager consists of two very similar, parallel channels for  $LM$ -band and  $N$ -band. They include a reimaging system with slit, filter and grism wheels, as well as pupil imaging optics. Coronagraphy can be

performed by inserting a four quadrant phase mask (4QPM) into the entrance focal plane with a matched pupil mask.

- The  $LM$ -band high-resolution IFU spectrograph cuts the image in 24 slices, rearranges the slices and sends the light to an echelle grating spectrometer. Tilt of the grating allows selecting the spectral range within the pre-selected diffraction order.

The modules are mounted to a common “backbone” structure, which acts as a mechanical and thermal interface. The cold system is surrounded by a spherical cryostat, with a diameter of approximately 2.5 m, made of stainless steel. Figure 2 shows METIS at the A1–Nasmyth port of the E-ELT.

#### Performance

The combination of high angular resolution for imaging and the photon-collecting power for high resolution spectroscopy makes METIS an extremely powerful instrument. METIS is highly complementary to JWST, with the former being superior in angular resolution and unique in high resolution spectroscopy, while the latter provides unsurpassed imaging sensitivity, in particular to low surface brightness objects. Having overlapping scientific goals with ALMA, but probing different physical conditions, there is also an excellent synergy between METIS and ALMA.

The sensitivity of METIS on the 42-metre E-ELT for a Paranal-like site, in comparison with other major facilities, is shown in Figure 3. All sensitivities have been normalised to one hour,  $10\sigma$  point source/unresolved line sensitivities.

#### References

Pontoppidan, K. M. et al. 2009, ApJ, 704, 1482



# MICADO: The Multi-adaptive Optics Imaging Camera for Deep Observations

Richard Davies<sup>1</sup>  
Reinhard Genzel<sup>1</sup>

<sup>1</sup> Max-Planck-Institut für extraterrestrische Physik, Garching, Germany

Team Members:

Nancy Ageorges<sup>1</sup>, Lothar Barl<sup>1</sup>, Luigi Bedin<sup>2,3</sup>, Ralf Bender<sup>4</sup>, Pernelle Bernardi<sup>5</sup>, Frédéric Chapron<sup>5</sup>, Yann Clenet<sup>5</sup>, Atul Deep<sup>6,7</sup>, Erik Deul<sup>6,7</sup>, Marco Drost<sup>8</sup>, Frank Eisenhauer<sup>1</sup>, Renato Falomo<sup>2</sup>, Giuliana Fiorentino<sup>6,8</sup>, Natascha M. Förster Schreiber<sup>1</sup>, Eric Gendron<sup>5</sup>, Damien Gratadour<sup>5</sup>, Laura Greggio<sup>2</sup>, Frank Grupp<sup>4</sup>, Enrico Held<sup>2</sup>, Tom Herbst<sup>9</sup>, Hans-Joachim Hess<sup>4</sup>, Zoltan Hubert<sup>5</sup>, Knud Jahnke<sup>9</sup>, Konrad Kuijken<sup>6,7</sup>, Dieter Lutz<sup>1</sup>, Demetrio Magrin<sup>2</sup>, Bernard Muschiolk<sup>4</sup>, Ramon Navarro<sup>6</sup>, Eva Noyola<sup>1</sup>, Thibaut Paumard<sup>5</sup>, Giampaolo Piotto<sup>2</sup>, Roberto Ragazzoni<sup>2</sup>, Alvio Renzini<sup>2</sup>, Hans-Walter Rix<sup>9</sup>, Gerard Rousset<sup>5</sup>, Roberto Saglia<sup>1</sup>, Linda Tacconi<sup>1</sup>, Markus Thiel<sup>1</sup>, Eline Tolstoy<sup>6,8</sup>, Sascha Trippe<sup>1,10</sup>, Niels Tromp<sup>6</sup>, Edwin Valentijn<sup>6,8</sup>, Gijs Verdoes Kleijn<sup>6,8</sup>, Michael Wegner<sup>4</sup>

<sup>1</sup> MPE, <sup>2</sup> OAPD, <sup>3</sup> STScI, <sup>4</sup> USM, <sup>5</sup> LESIA, <sup>6</sup> NOVA, <sup>7</sup> Univ. Leiden, <sup>8</sup> Univ. of Groningen, <sup>9</sup> MPIA, <sup>10</sup> IRAM

MICADO will image a ~ 1 arcminute field of view at the diffraction limit of the E-ELT. Its simple and robust design is optimised to yield unprecedented sensitivity and resolution across this field and to bring high precision astrometry into the mainstream. Its auxiliary arm provides the flexibility to include spectroscopy and other capabilities.

### Science drivers

MICADO will address a large number of science topics that span key elements of modern astrophysics combining wide field, high resolution, and remarkable sensitivity. In what follows, we look at how MICADO's characteristics enable it to address these science cases.

MICADO will fully sample the 6–10-mas FWHM in the *J–K*-bands with the E-ELT. With a throughput exceeding 60%, its sensitivity at 1–2  $\mu\text{m}$  will be comparable to, or surpass, JWST for isolated point sources. A project currently underway to develop OH-suppressing filters could significantly improve the sensitivity. MICADO will thus realise the full power and unique features of a 42-metre AO telescope. MICADO's resolution means that it will be clearly superior to JWST in crowded regions and its field of view of nearly 1 arcminute is much larger than for other cameras planned for ELTs. Together, these characteristics make MICADO a powerful tool for many science cases. Continuum and emission line mapping

of high-redshift galaxies (see Figure 1) will enable us to address questions concerning their assembly, and subsequent evolution in terms of mergers, internal secular instabilities and bulge growth. The resolution of better than 100 pc at  $z \sim 2$ , equivalent to 1 arcsecond at the distance of the Virgo Cluster, will resolve the individual star-forming complexes and clusters, which is the key to understanding the processes that drive their evolution. Alternatively, one can probe a galaxy's evolution through colour–magnitude diagrams that trace the fossil record of its star formation. Spatially resolving the stellar populations in this way is a crucial ability, since integrated luminosities are dominated by only the youngest and brightest populations. MICADO will extend the sample volume from the Local Group out to the Virgo Cluster and push the analysis of stellar populations deeper into the centres of these galaxies.

With only fixed mirrors in its primary imaging field, gravity invariant rotation and HAWAII-4RG detectors (developed for space astrometry missions), MICADO is an ideal instrument for astrometry. A robust pipeline will bring precision astrometry into the mainstream. An analysis of the statistical and systematic effects by Trippe et al. (2010) shows that an accuracy of 40  $\mu\text{as}$  in a single epoch of observations is achievable; and after only 3–4 years it will be possible to measure proper motions of 10  $\mu\text{as}/\text{yr}$ , equivalent to 5 km/s at 100 kpc. At this level, many astronomical objects are no longer static, but become dynamic, leading to dramatic new insights into the three-dimensional

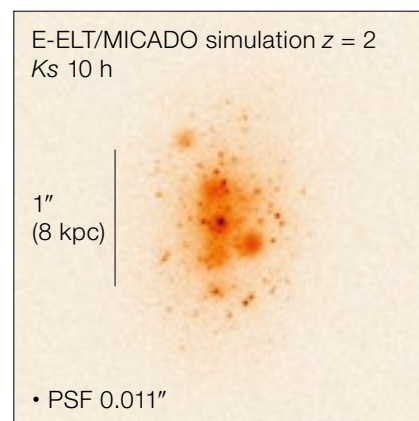
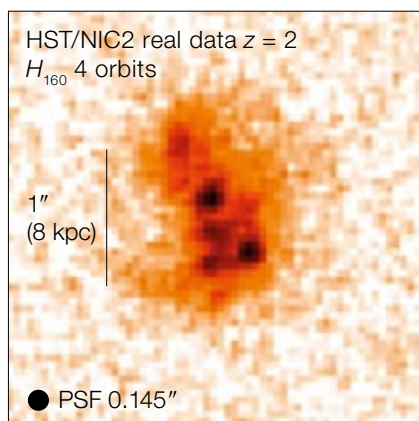
structure and evolution of many phenomena. Proper motions of faint stars within light-hours of the Galactic Centre (Figure 2) will measure the gravitational potential in the relativistic regime very close to the central black hole, and may also reveal the theoretically predicted extended mass distribution from stellar black holes that should dominate the inner region. The internal kinematics and proper motions of globular clusters will yield insights on intermediate mass black holes as well as the formation and evolution of the Galaxy. Similar analyses of dwarf spheroidal galaxies will reveal the amount and distribution of dark matter in these objects, and hence test models of hierarchical structure formation.

Spectroscopy is an obvious and powerful complement to pure imaging, and is implemented as a simple slit spectrometer with a high throughput that is ideal for obtaining spectra of compact objects. The resolution of  $R \sim 3000$  is sufficient to probe between the near-infrared OH lines. This simple addition will enhance many science cases, for example: deriving stellar types and 3D orbits in the Galactic Centre; using velocities of stars in nearby galaxies to probe central black hole masses and extended mass distributions; measuring absorption lines in galaxies at  $z = 2\text{--}3$  and emission lines in galaxies at  $z = 4\text{--}6$  to derive their ages, metallicities and star-forming histories; and obtaining spectra of supernovae at  $z = 1\text{--}6$ .

### Instrument design concept

The instrument design has been optimised for the MCAO module MAORY. But the MICADO study included its own simple and robust single-conjugate natural guide star AO system, with which it can operate before the full multi-conjugate system MAORY is available. In this way the camera can exploit and promote the E-ELT scientifically, at the earliest opportunity. The optical relay and support structure for

Figure 1. Two views of a high-redshift galaxy. Left: HST/NICMOS image of a  $z \sim 2$  galaxy, showing several bright clumps. Right: Simulation of how such a galaxy might appear when imaged with MICADO. Numerous faint clumps were included in the simulation, to show what structures might be observable. Observations with MICADO will be able to confirm the number, size, luminosity, and distribution of the star-forming complexes in such galaxies.



single conjugate AO provide the same interface as MAORY, and in principle enable MICADO to be used with other AO systems such as ATLAS. This phased approach means that MICADO will be able to make use of increasingly sophisticated AO systems as they become available.

The instrument is compact and is supported underneath the AO systems, rotating in a gravity invariant orientation to minimise flexure (Figure 3). A tunable atmospheric dispersion corrector ensures that the images are always sharp. The collimator is at the centre of the instrument, with a mechanism to switch between the two arms, each of which has space for 20 broad- and narrowband filters mounted in a large wheel. These, and also the focal plane mask, are driven at their rim to lessen torque on the motors. The primary arm is a high-throughput camera that images a 53-arcsecond field with a fixed 3-mas pixel scale on a  $4 \times 4$  array of detectors. This arm is designed with fixed monolithic mirrors for superior stability, optimising astrometric precision. In addition, MICADO will have an auxiliary arm with one detector to provide an increased degree of flexibility. In the current design, a mechanism in this arm switches between (i) imaging a smaller field at a finer 1.5-mas pixel scale, and (ii) a 4-mas pixel scale for spectroscopy. However, in principle the auxiliary arm also opens the door to many other options, including a “dual imager” based on a Fabry–Perot etalon to image separate emission line and continuum wavelengths simultaneously, or a high time resolution detector.

The mechanical design minimises torques and maintains optical alignment during cool-down. The electronics racks are mounted on a co-rotating platform on the Nasmyth floor, which minimises cable lengths, limits the mass mounted on the derotator, and houses the cable-wrap for external supplies. Servicing the key elements of the instrument, while mounted, is possible through two large doors in the cryostat, which is rotated by  $25^\circ$  with respect to the core structure to maximise access. MICADO will be cooled by liquid nitrogen to avoid vibrations that could otherwise have an adverse effect on the AO performance.

### Performance

The broadband imaging performance for the MICADO primary field has been calculated for isolated point sources using PSFs provided by the MAORY consortium and for standard broadband filters similar to those in HAWK-I. It shows that the  $5\sigma$  sensitivity will be better than a few nano-Jy (30 mag AB) in one hour for the *J*- and *H*-bands, and in two hours for the

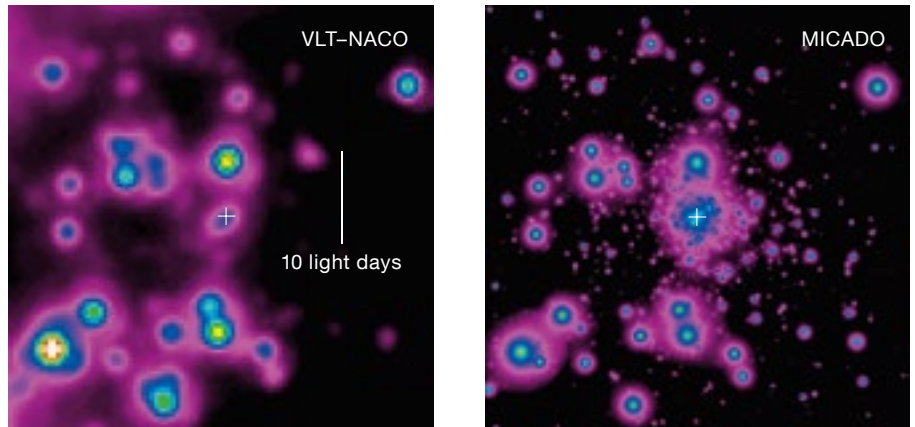


Figure 2. The innermost arcsecond of the Galactic Centre. Left: NACO image at the VLT diffraction limit, showing S-stars and the location of the black hole Sgr A\* (cross). Right: A simulated image with MICADO, extrapolating from the measured luminosity function and density profile. Proper motions of hundreds of stars will be measurable, providing detailed constraints on the black hole mass and extended mass distribution.

*I*-band. The *K*-band performance depends strongly on the thermal background and hence the ambient temperature, but is likely to be about 1 mag less. Advanced filters — high throughput broadband filters and OH suppressing filters — will have a very significant impact on MICADO sensitivity. The prototype *J*-band filters increase the sensitivity by 0.3 mag. More advanced design optimisation techniques could lead to a 0.5-mag sensitivity gain in this band, and comparable gains may be expected for the *I*-band and *H*-band.

The spectroscopic performance has been calculated for isolated point sources that are nodded back and forth along a slit that is

8 arcseconds long and 12 milliarcsseconds wide. Because of the unusually extreme core + halo shape of the adaptive optics PSF, this width maximises the signal-to-noise reached for point sources in the *J*- and *H*-bands. In the *K*-band, additional diffraction losses at the slit reduce the throughput slightly. The sensitivity calculation takes account of all effects (including the Strehl ratios predicted by MAORY, the limited coupling efficiency due to the PSF shape, diffraction losses at the slit, and the thermal background). The resulting  $5\sigma$  sensitivities are  $J_{AB} = H_{AB} = 27.2$  mag between the OH lines in a five-hour integration; and similarly  $K_{AB} = 25.7$  mag (brighter limit again primarily due to the thermal background).

### References

Trippe, S. et al. 2010, MNRAS, 402, 1126

### Links

<http://www.mpe.mpg.de/ir/instruments/micado/micado.php>

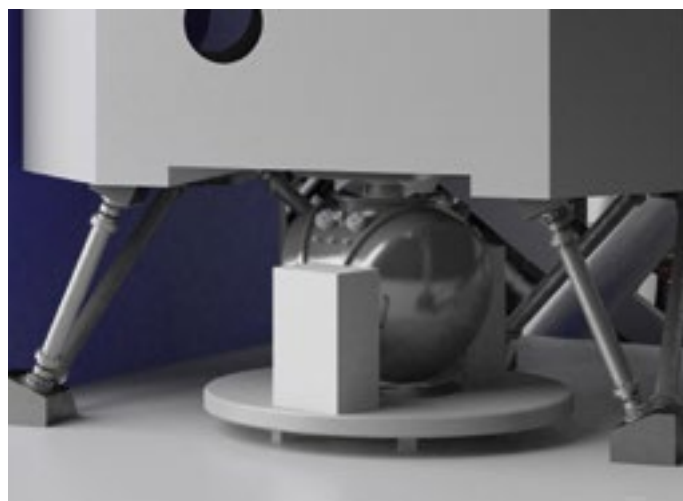


Figure 3. CAD view of MICADO mounted in the 2.5 m space underneath the multi-conjugate adaptive optics system MAORY. The feed-throughs in the cryostat, and the large access doors for on-site maintenance, are visible. The electronics are mounted on a co-rotating platform that also houses the cable-wrap.

# OPTIMOS–DIORAMAS: A Wide-field Imaging and Multi-slit Spectrograph for the E-ELT

Olivier Le Fèvre<sup>1</sup>  
 Lucien Hill<sup>1</sup>  
 David Le Mignant<sup>1</sup>  
 Dario Maccagni<sup>2</sup>  
 Laurence Tresse<sup>1</sup>  
 Stéphane Paltani<sup>3</sup>

<sup>1</sup> Laboratoire d'Astrophysique de Marseille, CNRS – Université de Provence, Marseille, France

<sup>2</sup> INAF–IASF, Milano, Italy

<sup>3</sup> Observatoire de Genève, Université de Genève, Switzerland

Team members:

Jarle Brinchmann<sup>1</sup>, Stéphane Charlot<sup>2</sup>, Benedetta Ciardi<sup>3</sup>, Vincenzo de Caprio<sup>4</sup>, Adriano Fontana<sup>5</sup>, Jesus Gallego<sup>6</sup>, Bianca Garilli<sup>4</sup>, Ludovic Genolet<sup>7</sup>, Olivier Ilbert<sup>8</sup>, Marc Jaquet<sup>8</sup>, Francisco Garzon Lopez<sup>9</sup>, Dario Maccagni<sup>4</sup>, Laurent Martin<sup>8</sup>, Baptiste Meneux<sup>10</sup>, Omar Almaini<sup>11</sup>, Florence Roman<sup>8</sup>, Gérard Rousset<sup>8</sup>

<sup>1</sup> Univ. Leiden, <sup>2</sup> IAP, <sup>3</sup> MPA, <sup>4</sup> INAF–IASF, Milano, <sup>5</sup> Obs. Roma, <sup>6</sup> Univ. Complutense–Madrid, <sup>7</sup> Obs. Genève, <sup>8</sup> LAM, <sup>9</sup> IAC, <sup>10</sup> MPE, <sup>11</sup> Univ. Nottingham

We present the science, design and performance of OPTIMOS–DIORAMAS, an imager and multi-slit spectrograph for the E-ELT. It covers a wide  $6.8 \times 6.8$  arcminute field, a large wavelength range of 0.37 to 1.6  $\mu\text{m}$ , with up to  $\sim 500$  slits observed simultaneously.

## Science drivers

The study of first light in the Universe, the seeds of galaxies, as well as the main phases of galaxy evolution are some of the main science goals of the E-ELT, as identified in the Design Reference Mission. The sheer collecting power of the E-ELT will enable very faint objects to be observed, with a gain in performance far superior to that when the 8–10-metre class telescopes surpassed the 4-metre class. On a point source, with similar seeing, one can expect a 1.8 magnitude gain with the E-ELT compared to the VLT, or a factor of about 27 in exposure time, a considerable advantage.

However, the gain in performance is not only related to the telescope light-gathering power, but also, for many science investigations, to the capability to assemble large, statistically representative samples of stars, galaxies, AGN, or any other (rare) categories of objects in the Universe. If one is able to observe more than one object at once, the performance

gain is proportional to the number of objects observed simultaneously, and a key instrument driver is the size of the field of view adapted to the science. Large wide-field imagers have been very powerful even on smaller telescopes (e.g., CFHT, VISTA, PanStarrs, soon the VST, leading to LSST), where the etendue,  $A\Omega$ , combining the aperture of the telescope ( $A$ ) and the FoV ( $\Omega$ ) is high. In spectroscopy the situation is similar, as the etendue plays an important role, but is also coupled to the multiplex, or the ability to place a high number of apertures on sky objects and collect their spectra simultaneously. In addition, the instantaneous wavelength coverage of a spectrograph also drives the performance when it is necessary to observe many spectral features or to find the redshift of a previously unknown source.

The technique of multi-object spectroscopy has matured since the 1990s, and has led to remarkable progress in our understanding of many fields of astrophysics, including galaxy and large-scale structure evolution, the dynamics of our Galaxy, clusters of galaxies, and identifying the most distant galaxies (see e.g., Lilly et al., 1995, Steidel et al., 1996, Le Fèvre et al., 2005). Multi-slit spectrographs have been the instruments of choice to push the limits of very large samples to the greatest depths. The versatile observing modes of imaging multi-slit spectrographs have become the workhorses of many observatories, like FORS1 and FORS2 and VIMOS on the VLT (Le Fèvre et al., 2003), LRIS–Keck, DEIMOS–Keck, GMOS–Gemini, IMACS–Magellan, Subaru–FOCAS, etc.

With this in mind, we have conducted a Phase A study of a wide-field multi-slit imaging spectrograph for the E-ELT (originally called OPTIMOS), which we named DIORAMAS (a diorama is a 3D scene). DIORAMAS has been designed based on the requirements of ESO for a wide-field multi-slit spectrograph in the context of the OPTIMOS study. DIORAMAS is intended to be a general purpose facility instrument, offering both deep imaging and deep multi-slit spectroscopy, over a wide field of  $6.8 \times 6.8$  arcminutes, and a large wavelength domain from 0.37 to 1.6  $\mu\text{m}$ .

We have defined test science cases to drive the requirements for a wide-field imaging spectrograph to the limits. As a first approach we have concentrated on extragalactic, high-redshift, deep observations. This is by no means limiting, as an imaging and multi-slit spectrograph of this scope is a general purpose facility with the ability to study astronomical objects from very nearby in the Solar System, Galactic programmes or ones dealing

with resolved stellar population studies in nearby galaxies, up to the most distant galaxies and large surveys. One only needs to look at the programmes executed by FORS or VIMOS on the VLT to grasp the wide range of science that such instruments are capable of tackling.

Some of the main science drivers for the instrument design have been:

- extremely deep imaging in a wide field, e.g., as a means of identifying galaxy populations at all redshifts;
- the detection and study of “first light” galaxies or AGN at  $z > 6$ , from identifying the candidates in imaging to the secure spectroscopic redshift measurement, and to physical diagnostics enabled by spectrophotometric analysis;
- the history of galaxy mass assembly and star formation at  $1 < z < 6$ ;
- the detection and study of the oldest galaxies at increasingly early cosmic times;
- the co-evolution of galaxies and AGN;
- the tomography of the high-redshift Universe to understand the role played by the interplay between galaxies and the intergalactic medium in galaxy formation and evolution processes; and
- the early development of large-scale structures and clustering at  $z > 2$ .

Even with a relatively small field of view, the E-ELT will be capable of obtaining extremely deep images in a short time, and we believe that the E-ELT should have a wide-field visible-to-NIR imager at first light. Another important element will be that the E-ELT must be autonomous in the definition of targets to be observed. It must be possible to carry out

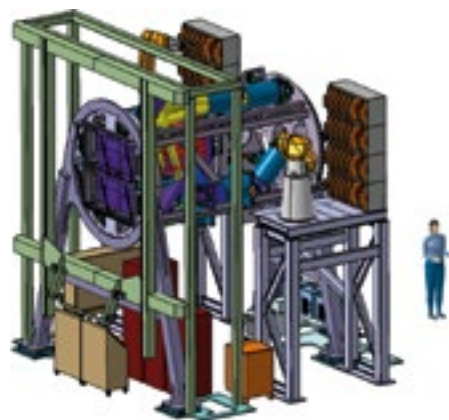
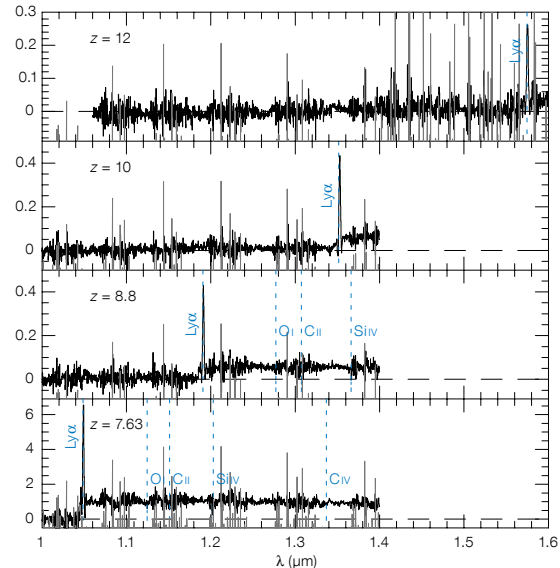


Figure 1. DIORAMAS instrument layout. The beam from the E-ELT enters the instrument from the left with slit masks (for MOS) or without (for imaging), and is then split into four channels, each with its own optical train, filters and gratings with their exchange robots, flexure compensation, detector array and dewar.





**Figure 2.** Left: Simulated  $g'J$  composite image ( $AB \sim 30$  mag) covering 1/15th of the total 44 arcminutes<sup>2</sup> FoV of DIORAMAS, as expected to be observed after 1-hour integration per filter with a 0.05 arcsecond pixel scale under 0.50 arcsecond seeing. There are about 45 000 sources in one  $6.8 \times 6.8$  arcminute field of view. Courtesy E. Bertin. Right: Simulated spectra of young galaxies with Lyman- $\alpha$  emission observed from  $z \sim 8$  to  $z \sim 12$  with DIORAMAS in 4–10-hour integrations (ordinate is relative flux in  $F_0$ ).

science programmes in a self-consistent manner, ie. without the necessity of relying on other facilities. Of course, the E-ELT must be capable of observing targets identified using data from other telescopes; DIORAMAS allows both, as the deep imaging capability enables the production of exhaustive source lists in photometric catalogues.

### Instrument design concept

Visible and NIR coverage has become an essential element in the observation of faint sources, as the large wavelength baseline enables many important spectral features in the spectral energy distribution to be measured, and therefore DIORAMAS offers a large instantaneous wavelength range. The instrument layout is organised around four channels, each with its own optical train, slit-masks, filters, gratings, flexure compensation, detector array and dewar, and associated hardware (Figure 1). Two channels are optimised for the visible from 0.37 to 1  $\mu\text{m}$ , the two other channels are optimised for the NIR from 0.6 to 1.6  $\mu\text{m}$ , cutting off before the thermal background becomes dominant. The optics provide excellent image quality and a high total instrument throughput of about 72 % excluding detector arrays. Together with a fine pixel sampling of 0.05 arcsecond/pixel, this will enable DIORAMAS to make use of the best images delivered by the telescope, particularly if the GLAO system in the telescope delivers improved images over the wide field of the instrument. Flexure is actively compensated along each of the channels using a tip-tilt actuation based on the second folding mirror in each channel. The camera of each channel

focuses on a  $4\text{k} \times 12\text{k}$  pixel array of 15  $\mu\text{m}$  pixels, with CCDs for the visible channels and HgCdTe arrays for the NIR. Slits are cut in metal sheets with a laser machine, with exceptional slit roughness accuracy. Masks, filters and gratings are installed/removed on the optical path using robust industrial robots. In addition, high spatial and spectral resolution integral field spectroscopy in a field of  $\sim 10$  arcsecond<sup>2</sup> could be easily added as the instrument is conceived in such a way that it can host a slicer-based integral field unit. DIORAMAS makes use of mature and proven technology, minimising the development risk, and could therefore start being built now, and certainly could be ready by the EELT first light.

### Performance

DIORAMAS offers exceptional performance. It aims at using the field of view available at the E-ELT, with a field of view of  $6.8 \times 6.8$  arc-

minute<sup>2</sup>. It can perform extremely deep imaging to magnitude  $AB \sim 28.75$  (4 h,  $3\sigma$ , in 1.2-arcsecond aperture) over the full FOV with a high density of sources (Figure 2, left), as well as multi-slit spectroscopy of about 480 objects at once down to  $AB \sim 26.5$  (4 h,  $3\sigma$ ,  $R \sim 300$ , point source), or 160 objects at  $R \sim 3000$ . This will allow the detection of very high redshift “first light” objects (Figure 2, right). This performance can be reached without the use of GLAO, and is comparable to that of JWST NIRCAM and NIRSPEC at 1  $\mu\text{m}$ , and the best currently planned for ELTs. Using the GLAO-corrected images delivered by the telescope, DIORAMAS allows an even deeper exploration of the Universe.

### References

- Le Fèvre, O. et al. 2003, SPIE, 4841, 1670
- Le Fèvre, O. et al. 2005, A&A, 439, 845
- Lilly, S. et al. 1996, ApJ, 460, 1
- Steidel, C. C. et al. 1996, ApJ, 462, 17

**Table 1.** Essential instrument parameters for DIORAMAS.

Item	Design status
Spectral range	0.37 $\mu\text{m}$ to 1.6 $\mu\text{m}$
Field of view	$6.78 \times 6.78$ arcminutes <sup>2</sup>
Slit size	Any width: mean 0.5 arcseconds, min.: 0.1 arcseconds
Pixel scale and sampling	0.05 arcseconds per pixel
MOS multiplex	480 slits of 5 arcseconds length at $R \sim 300$ 160 slits of 5 arcseconds length at $R \sim 2000\text{--}3000$
Spatial image quality	> 80 % encircled energy within 150 mas over 90 % FOV
Spectral image quality	> 80 % encircled energy within 200 mas over 90 % FOV
Imaging throughput	42 % averaged over (0.37 $\mu\text{m}$ , 0.43 $\mu\text{m}$ ); > 48 % for (0.43 $\mu\text{m}$ , 0.84 $\mu\text{m}$ ); > 63 % for (0.86 $\mu\text{m}$ , 1.60 $\mu\text{m}$ )
Spectroscopic throughput	> 28 % over (0.37 $\mu\text{m}$ , 0.43 $\mu\text{m}$ ); > 30 % for (0.43 $\mu\text{m}$ , 0.86 $\mu\text{m}$ ); > 45 % for (0.86 $\mu\text{m}$ , 1.6 $\mu\text{m}$ )
Spectral resolution	$R \sim 300$ to 2700 for visible; $R \sim 400$ to 3000 for NIR

# OPTIMOS–EVE: A Fibre-fed Optical–Near-infrared Multi-object Spectrograph for the E-ELT

François Hammer<sup>1</sup>  
Lex Kaper<sup>2</sup>  
Gavin Dalton<sup>3</sup>

<sup>1</sup> GEPI, Observatoire de Paris, France

<sup>2</sup> NOVA, University of Amsterdam, the Netherlands

<sup>3</sup> Science and Technology Facilities Council, Rutherford Appleton Laboratory, Didcot, United Kingdom

Team members:

Michael Andersen<sup>1</sup>, Giuseppina Battaglia<sup>2</sup>, Piercarlo Bonifacio<sup>3</sup>, Bart Buijs<sup>4</sup>, Andrew Bunker<sup>5</sup>, Fanny Chemla<sup>3</sup>, Paolo di Marcantonio<sup>6</sup>, Hector Flores<sup>3</sup>, Isabelle Guinouard<sup>3</sup>, Paul Groot<sup>7,4</sup>, Eike Günther<sup>3</sup>, Hans-Günter Ludwig<sup>3</sup>, Christophe Martayan<sup>2</sup>, Ramon Navarro<sup>7,9</sup>, Patrick Petitjean<sup>10</sup>, Mathieu Puech<sup>3</sup>, Johan Pragt<sup>7,9</sup>, Per Kjaergaard Rasmussen<sup>1</sup>, Myriam Rodrigues<sup>3</sup>, Emmanuel Rollinde<sup>10</sup>, Eric Sawyer<sup>11</sup>, Luca Sbordone<sup>3</sup>, Daniel Schaerer<sup>12</sup>, Paolo Spanò<sup>13</sup>, Ian Tosh<sup>11</sup>

<sup>1</sup> NBI Copenhagen, <sup>2</sup> ESO, <sup>3</sup> GEPI, Obs. Paris, <sup>4</sup> Univ. Nijmegen, <sup>5</sup> Univ. Oxford, <sup>6</sup> INAF–OAT, <sup>7</sup> NOVA, <sup>8</sup> TLS Tautenburg, <sup>9</sup> ASTRON, <sup>10</sup> IAP, <sup>11</sup> STFC–RAL, <sup>12</sup> Obs. de Genève, <sup>13</sup> INAF–OAB

OPTIMOS–EVE is a fibre-fed, optical-to-infrared multi-object spectrograph designed to explore the largest field of view provided by the E-ELT at seeing or GLAO-limited conditions. OPTIMOS–EVE can detect planets in nearby galaxies, explore stellar populations beyond the Local Group, and probe the physical conditions of galaxies including the most distant ones accessible with the E-ELT.

One of the major challenges in spectrograph design for the E-ELT is to build an instrument addressing some of the key, but versatile science cases of present day astrophysics. The solution is to design an instrument that samples the largest discovery space in terms of wavelength range, spectral and spatial resolutions and multiplex. OPTIMOS–EVE is unique in covering a very large space in the spectral resolution ( $R = 5\,000\text{--}30\,000$ ) versus multiplex

Table 1. Key capabilities for OPTIMOS–EVE.

Patrol field of view	7' diameter (unvignetted), 10' full field
Wavelength range	370–1700 nm
Spectral resolving power	6000 18000 30000
Number of targets	240 70 40
Apertures on sky	Single objects (0.9"); 30 medium IFUs (1.8 × 2.9"); single large IFU (7.8 × 13.5")
Wavelength coverage	$\lambda/3\text{--}\lambda/6$ (VIS); $\lambda/10\text{--}\lambda/20$ (NIR)

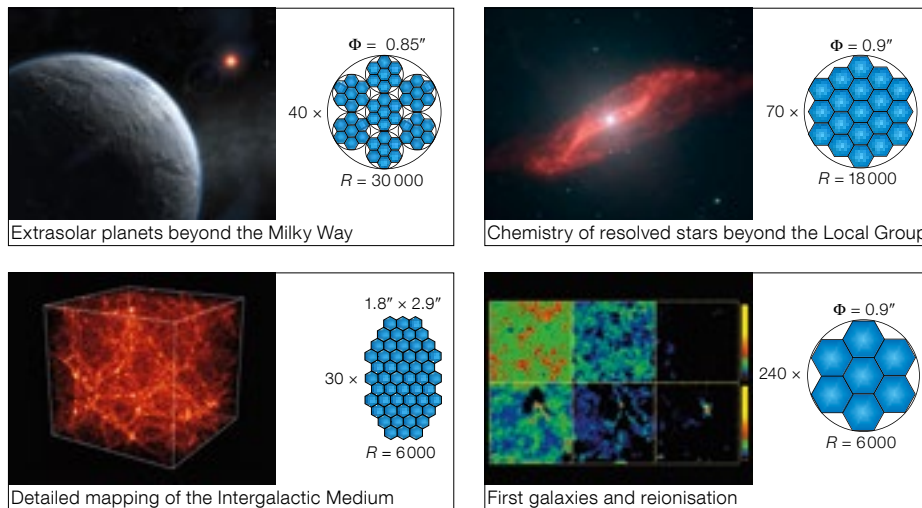


Figure 1. Four of the five science cases of OPTIMOS–EVE with, on the right of each panel, the aperture ( $\Phi$ ), multiplex and the spectral resolution that will be offered to study them. The 30 medium, deployable IFUs (bottom left) can provide the best sky removal and can be used for all extragalactic cases. The fifth mode of OPTIMOS–EVE is the large IFU with  $13.5 \times 7.8$  arc-second area for extended objects, including the 100 kpc haloes of galaxies up to  $z = 3.5$ .

(40–240) plane, with a large wavelength range (370–1700 nm). It also offers a unique range of apertures, including integral field units, which can be adapted to a large variety of science cases (see Figure 1). OPTIMOS–EVE aims at best exploiting the photon collection capability offered by the E-ELT. It is well suited for use in the early operational phase of the E-ELT and beyond, without a need for full adaptive optics corrections.

## Science drivers

Spectroscopy over the wavelength region accessible from the ground, from the UV to the non-thermal infrared, has been, and will remain, a key technique to investigate virtually all types of astrophysical targets. At  $z = 0$  most of the spectral lines, fundamental for deriving astrophysical information, are found in the UV–optical range. At higher redshifts important spectral diagnostics shift into the near-infrared (NIR), and Lyman- $\alpha$  becomes accessible in the optical wavelength range. Due to the unique combination of wavelength coverage, multiplex and spectral resolution, most of the science that will be explored by OPTIMOS–EVE can neither be addressed by any other instrument concept under study for the E-ELT, nor by JWST instruments. OPTIMOS–EVE responds to several of the key science goals put forward by the E-ELT Science Working Group and will explore the visible to

NIR wavelength region, for sources both nearby and at cosmological distances.

The OPTIMOS–EVE Phase A study Science Team explored five key science cases (see Figure 1) from which the scientific and technical requirements (see Table 1) have been derived.

*Planets in the Galactic Bulge and stellar clusters, also in external dwarf galaxies.* Although over 400 extrasolar planets are known, these are mostly hosted around stars in the solar vicinity. For the few distant planets, besides those around radio pulsars, the orbits and masses are unknown. On theoretical grounds, environment is expected to play a significant role in the process of planet formation. Therefore, it is important to detect and characterise planets in environments different from the solar vicinity, such as the Galactic Bulge and Local Group galaxies. With a radial velocity precision of 10 m/s for giant stars down to magnitude 20, OPTIMOS–EVE will make such a study possible and allow to be monitored up to 40 stars in each observed field.

*Resolved stellar populations in nearby galaxies.* With the VLT, a detailed study of the stellar populations of the Local Group galaxies has been possible. However, many galaxy types are not represented in the Local Group. In order to make further progress in our understanding of galaxy formation and evolution we need to study in detail many different types of galaxies, e.g., in the groups of Sculptor and Centaurus A. With the high efficiency, low-resolution mode of OPTIMOS–EVE and its high multiplex, the E-ELT will open up the possibility of studying the stars down to the turn-off and addressing cosmologically relevant problems, such as the lithium abundance. The medium-resolution mode, with its multiplex of 70, is well adapted for this purpose.

Tracking the first galaxies and cosmic reionisation from redshift 5 to 13. From polarisation measurements of the cosmic microwave background it appears that at  $z = 10$  the Universe was already largely reionised, but little is known of the objects that powered this reionisation. The search for those “first sources” can be carried out with OPTIMOS–EVE to trace Lyman- $\alpha$  up to  $z = 13$ . The ionised gas of very distant galaxies can be far more extended than the compact distribution of stellar light. With its 240 apertures, OPTIMOS–EVE will be an ideal instrument with which to catch most of the Ly- $\alpha$  photons that can be diffused over relatively large areas (median 1.4 arcsecond at  $z \sim 3$ , see Rauch et al., 2008). Moreover the 30 medium IFUs are optimised to achieve excellent sky subtraction by sampling the sky around the target, and are thus very well suited for the first studies of the kinematics and chemistry of such primordial objects.

Mapping the ionised gas motions at large scales in distant galactic haloes. Observations of the local and distant Universe have shown that galaxies are surrounded by extended haloes of ionised gas that are the interfaces to the IGM and its enrichment with metals. The study of these haloes unravels the history of galaxy–galaxy interactions that leave recognisable signatures on the halo kinematics. OPTIMOS–EVE will be able to study galaxy haloes over the last 12 Gyr (up to  $z = 3.5$ ).

3D reconstruction of the IGM. The space between galaxies and galaxy clusters is not empty, but is filled with a very low density warm medium that is detectable as Lyman- $\alpha$  absorption in the spectra of distant quasars. Although this provides a “cut-through” of the structure of the IGM along the line of sight, nothing is known about its transverse structure. Cosmological simulations suggest that the IGM has a filamentary structure, where filament crossings correspond to the locations of galaxy clusters. OPTIMOS–EVE will provide sufficient resolution and sensitivity to use Lyman-break galaxies of magnitude 25 as background sources. These galaxies have a sufficient spatial density to allow a real 3D reconstruction (tomography) of the IGM, which may be directly compared to cosmological simulations.

The OPTIMOS–EVE targets will be selected from imaging observations obtained with other telescopes, and many OPTIMOS–EVE studies will significantly benefit from complementary observations with JWST, ALMA and Gaia.

### Instrument design concept

OPTIMOS–EVE has been designed for the E-ELT Nasmyth focus. The fibre-positioner pro-

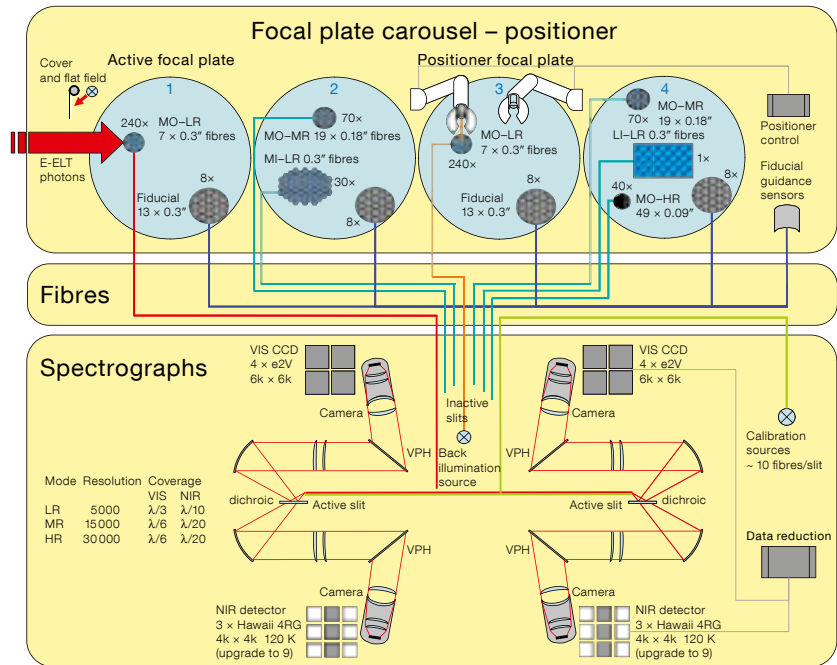


Figure 2. Schematic overview of OPTIMOS–EVE. The three main subsystems of the instrument are clearly indicated: the focal plate carousel-positioner, containing four focal plates with various single object fibre inputs and IFUs as well as a robot positioner; the fibres, to transport the collected light to the spectrograph, guidance sensors and from the calibration source; the spectrographs, consisting of a visible arm and a NIR arm, separated by a dichroic. The dispersing elements are VPH gratings.

vides the opportunity to observe up to 240 single targets within the  $\geq 7$  arcminute FoV, or to combine the fibres into medium- or large-sized IFUs. Astrophysical sources have many different apparent sizes on the sky, ranging from unresolved stars to  $\geq 10$  arcsecond extended sources, even at high redshift. For point sources the aperture has been optimised to 0.9 arcseconds; the IFUs are matched to the size of  $z \geq 1$  galaxies. The fibre/positioner approach provides the advantage of avoiding flexure issues when invoking such a large physical field of view ( $> 2$  m diameter). A spectral resolving power  $> 5000$  is mandatory in the NIR to provide enough spectral regions that are not affected by strong OH skylines. The wavelength coverage of an individual spectrum ( $\geq \lambda/3$  to  $\geq \lambda/6$  in the visible and  $\geq \lambda/10$  to  $\geq \lambda/20$  in NIR) is a trade-off between spectral resolution, multiplex and detector cost. Sky correction is a crucial issue, especially for the detection of faint sources that are in reach of the E-ELT. It is often believed that fibre-fed spectrographs have difficulties performing robust sky corrections. However a large number of sky-fibres will be used to sample the temporal variations over the whole field of view,

and other possible effects can be overcome by calibrating the fibre throughput and using beam-switching.

The instrument design (Figure 2) includes a focal plate carousel and fibre positioner feeding two dual-beam VIS/NIR optimised spectrographs. The spectrographs employ VPH gratings in first order for optimal performance. The concept and operability are based on FLAMES/GIRAFFE and X-shooter; it is a robust instrument, which can be developed, manufactured and integrated using existing technologies.

### Performance

A few examples of instrument performance among the science drivers are presented. For diffuse Ly- $\alpha$  sources, the use of fibres on the sky to map temporal sky variations, allows the detection with  $S/N = 8$  for fluxes of  $10^{-19}$  erg  $s^{-1}$   $cm^{-2}$  in 40 hours. Galaxy halo kinematics to  $z = 3.5$  can be studied in 10 hours per galaxy. Observation of multiple Ly- $\alpha$  emitters with the IFUs at  $R = 6000$  from IGM studies enables a continuum  $S/N$  from 30 to 50 to be reached in 10 hours exposure.

### References

Rauch, M. et al. 2008, ApJ, 681, 856

### Links

<http://www.OPTIMOS-EVE.eu>



# SIMPLE: A High Resolution Near-infrared Spectrograph for the E-ELT

Livia Origlia<sup>1</sup>  
 Ernesto Oliva<sup>2</sup>  
 Roberto Maiolino<sup>3</sup>

<sup>1</sup> INAF–Bologna Observatory, Italy  
<sup>2</sup> INAF–Arcetri Observatory, Firenze, Italy  
<sup>3</sup> INAF–Roma Observatory, Monteporzio  
 Catone, Italy

Team members:

Eike Guenther<sup>1</sup>, Bengt Gustafsson<sup>2</sup>, Artie Hatzes<sup>1</sup>,  
 Oleg Kochuckov<sup>2</sup>, Dante Minniti<sup>3</sup>, Nikolai Piskunov<sup>2</sup>,  
 Leonardo Vanzani<sup>3</sup>, Manuela Zoccali<sup>3</sup>

<sup>1</sup> TLS Tautenburg, <sup>2</sup> Uppsala Obs., <sup>3</sup> PUC

SIMPLE is an optimised near-infrared spectrograph designed to deliver a complete 0.84–2.5  $\mu\text{m}$  spectrum with resolution up to  $R = 130\,000$  and limiting magnitudes to  $JHK \sim 20$ . Its most prominent science cases include the study of the intergalactic medium in the early Universe (at  $z > 6$ ) and of the atmospheres of exoplanets transiting nearby low-mass stars.

## Science drivers

High resolution infrared spectroscopy is one of the youngest branches of astronomical research with a huge scientific potential. It is opening new windows in our understanding of several hot topics of modern stellar and extragalactic astrophysics, and it will have a major impact in the JWST and ALMA era and beyond.

Quantitative spectroscopy of key absorption lines in intrinsically red (cool stars and planets), reddened (protoplanetary discs, stellar populations in the inner Galaxy) or red-shifted (high- $z$  Universe) targets requires a spectral resolution  $R \sim 100\,000$  over the 0.84–2.5  $\mu\text{m}$  spectral range. However, high spectral resolution of faint objects at optical and NIR wavelengths can only be performed using large telescopes. At a resolution of  $R \sim 100\,000$  the sky and thermal backgrounds are quite low, even in most of the  $K$ -band. Since the targets (either compact sources or sub-structures) are typically smaller than the spectrometer entrance aperture (which is about diffraction-limited) regardless of the telescope size, the limiting flux observable with a given signal-to-noise (S/N) scales with the square of the telescope aperture. This implies a limiting magnitude about 3.5 magnitudes fainter than any other current or planned NIR high resolution spectrometer at 8–10-metre telescopes.

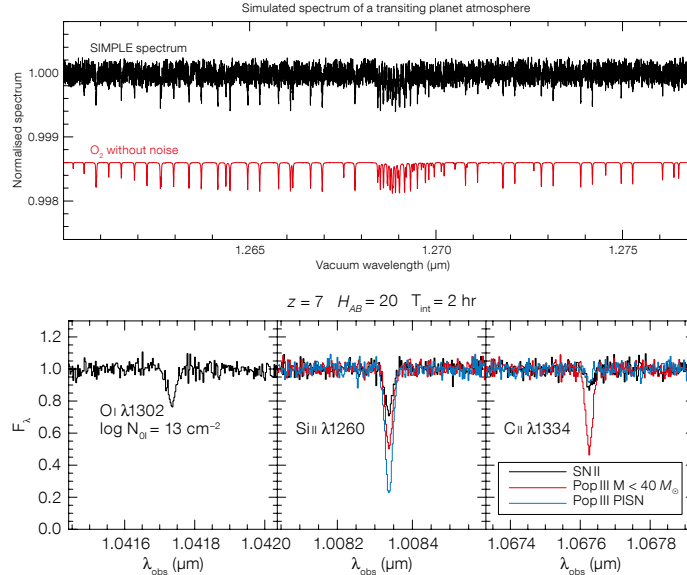


Figure 1. Top panel: expected  $J$ -band spectrum at  $R \sim 100\,000$  of the  $\text{O}_2$  lines, for a transiting planet with an atmosphere cross-section of  $6 \times 10^{-4}$ . Bottom panel: SIMPLE 2-hour simulation of absorption systems at  $z = 7$  in the foreground of a quasar with  $H_{AB} = 20$ , for different abundance patterns of the intervening proto-galaxy. The black line is for abundances typical of SN II; the red line is for abundances expected from Population III stars with masses  $M < 40 M_\odot$ , while the blue line is for abundances from Population III Pair Instability SNe.

This huge jump in sensitivity will place a NIR high resolution spectrometer at the E-ELT at the forefront in the astronomical context of the next two decades. SIMPLE has two major aims:

1. To characterise the atmospheres of exoplanets and detect signatures of life. High spectral resolution studies can be performed on planetary systems with cross-sections exceeding  $3 \times 10^{-4}$  (see Figure 1), i.e. on planets with extended atmospheres ( $> 100$  km) down to the Earth-size, or on massive planets (super-Earths, Neptunes) with less expanded ( $< 50$  km) atmospheres. Small planets with more normal atmospheres (such as ocean planets or Earth/Venus planets) are most challenging, but the chemical composition of their atmospheres can still be investigated by applying an adaptive rebinning of the individual molecular lines in their high resolution spectra. A number of surveys are specifically dedicated to the search for transiting exoplanets and strong synergies are also expected with, e.g., Kepler, EPICS and CODEX for planet search and classification, and with METIS, which can provide complementary information from mid-IR spectra. A potential competitor is JWST, but according to simulations, SIMPLE outperforms JWST because of the much larger telescope aperture of the E-ELT and of the higher spectral resolution for measuring the intrinsically narrow lines.
2. To detect the signature of the “first light” sources in the early Universe i.e. Population III stars (see, e.g., Figure 1). SIMPLE will provide high S/N, high resolution absorption spectra of QSOs and GRBs at, or beyond, the reionisation epoch, thus tracing the early chemical enrichment and dust content of proto-galaxies along their line of sight.

Targets (mostly QSOs at  $z > 6.5$ ) will be provided by ongoing and planned NIR surveys (VISTA, PanSTARRS, Euclid/SNAP). While SIMPLE will be unique in detecting the chemical fingerprint of the first light galaxies in absorption, JWST and other ELT instruments (HARMONI and EAGLE) will provide complementary information by searching for Population III signatures in emission.

The high spectral and angular resolution, and high S/N delivered by SIMPLE will also be crucial to obtain: a) detailed chemical abundances of the key metals, and their isotopes, and kinematics with accuracy better than 1 km/s for cool stars and stellar clusters; b) accurate radial velocities down to 1m/s to search and characterise exoplanets (and in particular rocky planets) around low mass stars; c) spectro-astrometry of the inner structure of protoplanetary discs tracing the early phases of planet formation; d) magnetic fields and astro-seismology; e) molecular tracers of stratification in the atmospheres of Solar System moons. The much-reduced extinction in the IR also allows SIMPLE to pierce the dust embedding several Galactic and extragalactic objects, which are heavily obscured in the optical, and, for example, to characterise the stellar populations of the Galactic Centre, including the study of relativistic effects in the stars orbiting the supermassive black hole.

The scientific requirements of SIMPLE yielded an instrument concept that includes and optimises two distinct observing modes, namely:

1. Single-object. This mode must deliver the full 0.84–2.5  $\mu\text{m}$  spectrum in a single exposure, providing the highest possible sensitivity, spectral quality and stability;

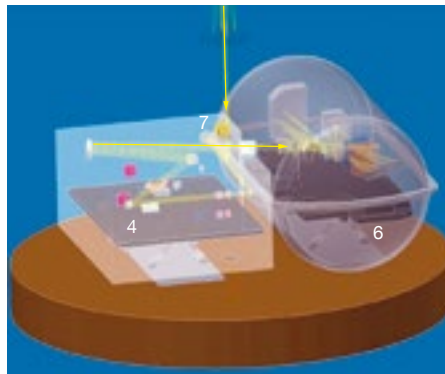
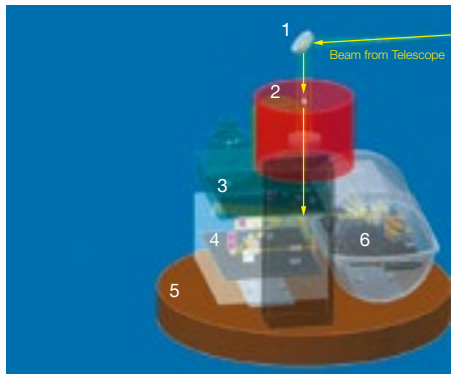


**Figure 2.** 3D views of SIMPLE identifying the subsystems, the optical path and the sub-modules of the pre-slit and spectrometer.

- 1 Fold mirror fixed relative to Nasmyth platform
- 2 Re-imager and guider module
- 3 SCAO-WFS module
- 4 Pre-slit module
- 5 Derotator
- 6 Cryogenic spectrometer
- 7 Calibration unit

2. Long-slit. This mode does not require full spectral coverage, but must provide optimised image quality along the slit with a spatial sampling of 9 mas/pixel or smaller.

While truly unique in terms of performance, capabilities and scientific expectations, the concept we propose is a relatively simple instrument (hence the name) exploiting known technologies, which translate into a relatively low risk facility, suitable for early operation at the E-ELT and capable of delivering major scientific results from the early operation phase onwards.

### Instrument design concept

SIMPLE consists of a canonical cross-dispersed echelle spectrometer whose slit width is a few times the diffraction limit at the longer wavelengths (*K*-band), i.e. its design is independent of the telescope diameter (Oliva & Origlia, 2008). It is a single channel system with fixed, all-mirror optics. The collimated beam has a diameter of 180 mm and the disperser is a commercial R2 echelle grating. Therefore, the required resolving power of  $R = 130\,000$  is achieved with a slit width of 27 mas, equivalent to  $2.5 \times \lambda/D$  in the *K*-band. The spectrometer can cover the whole 0.84–2.5  $\mu\text{m}$  range in one exposure because it employs prisms as cross-dispersers. It delivers a complete cross-dispersed spectrum on a mosaic of three  $4\text{k} \times 4\text{k}$  array detectors. The slit length in this mode is limited to 0.45 arcseconds, to avoid order overlap. The long-slit (4-arcsecond)

mode requires a dedicated order-sorter device included in the pre-slit system. Four slits of different widths are available: 27 mas ( $R = 130\,000$ ); 36 mas ( $R = 100\,000$ ); 54 mas ( $R = 67\,000$ ); and 72 mas ( $R = 50\,000$ ). The slits are at a fixed position inside the spectrometer and are selected by sliding a dekker/mask, which is also used to switch between the long-slit and full-spectrum modes. The dekker unit is the only moving part at cryogenic temperatures.

The spectrometer requires a good level of AO correction to concentrate the light into the slit and maximise throughput. To properly quantify this requirement, we define the slit efficiency parameter (SLE), which measures the fraction of light falling within the  $27 \times 54$  mas aperture used to extract the spectrum in the baseline observing mode with  $R = 130\,000$ . SIMPLE on the E-ELT with a poor AO correction ( $\text{SLE} < 0.03$ ) would achieve similar limiting magnitudes as the same spectrometer mounted on the VLT. Therefore, to take proper advantage of the telescope area, the minimum requirement is  $\text{SLE} > 0.1$  over most of the wavelength range. LTAO/MCAO matches the requirements, while GLAO is unable to concentrate enough light, even when using an image-slicer. On-axis SCAO correction with  $42 \times 42$  sub-apertures provides performance very similar to LTAO/MCAO down to *JH*-band limiting magnitude  $\sim 12$ .

The instrument design consists of subsystems (see Figure 2) that are well separated both from the logical and physical point of view:

- the spectrometer, which includes the slit and the optical elements necessary to collimate, disperse and re-focus the light onto the detector. It operates in a vacuum-cryogenic environment cooled by liquid nitrogen. It can be divided into two main modules, namely the cryostat and the optical bench carrying the spectrometer optics;
- the pre-slit, which is refrigerated to  $-30\text{ }^\circ\text{C}$  and includes a pupil stop, an acquisition camera and slit viewer and selectable sub-

- modules for the different observing modes, i.e. an ADC, a fibre scrambler and a polarimeter;
- an infrared (0.9–2.1  $\mu\text{m}$ ) SCAO WFS that uses the light from bright (*JH*-band  $< 12$ ) targets and includes a pupil-steering mirror, a viewing/tracking camera at an intermediate focus, a fast (up to 1 kHz) modulation mirror, and two selectable cameras to switch between the  $42 \times 42$  and  $84 \times 84$  sub-aperture modes. The splitting between scientific-light (transmitted) and WFS-light (reflected) is made by means of selectable beam splitters with parameters optimised for the different scientific cases;
- a calibration unit; and
- a re-imager and guider module, including a small (360 mm diameter) telescope, which creates an intermediate F/36 focal image 1 metre below its primary mirror.

The instrument is mechanically separated from the LTAO/MCAO module and collects the light far ( $\sim 3\text{ m}$ ) beyond the F/17.7 focus. The instrument can be positioned on the Nasmyth platform at any focal station. Should no LTAO/MCAO module be available at the beginning of E-ELT observations, SIMPLE can be mounted at a “naked-focus” and operate as a first-light instrument for all those observations that can be performed with SCAO-WFS correction. Notably, these include the scientifically prominent programme aimed at the detection of molecules in the atmospheres of planets transiting in front of their parent star (see Figure 1).

### Performance

The total instrument efficiencies are remarkably high, ranging between 20% (*I*-band) and 40% (*K*-band), because the instrument optics is mostly composed of mirrors whose high throughput is guaranteed by protected Ag coating. A dedicated exposure time calculator for the instrument was developed and made publicly available on the SIMPLE web page<sup>1</sup>. Limiting *JHK*-band Vega-magnitudes of  $\sim 20$ – $21$  ( $\text{S/N} \sim 10$ ) and  $17$ – $18$  ( $\text{S/N} \sim 100$ ) can be obtained with an on-source integration time of two hours at the maximum resolving power of 130 000.

### References

Oliva, E. & Origlia, L. 2008, SPIE, 7014, 701410

### Links

<sup>1</sup> <http://simple.bo.astro.it>



The grand design spiral galaxy Messier 83 (NGC 5236) is shown in a HAWK-I colour composite formed from *J*-, *H*- and *K*-band images. The effects of dust extinction are mitigated by the near-infrared imagery, cooler stars are preferentially detected and the H<sub>II</sub> regions appear red from Brackett-gamma emission. See release eso1020 for details.



# The CRIRES Search for Planets at the Bottom of the Main Sequence

Jacob Bean<sup>1</sup>  
 Andreas Seifahrt<sup>1,5</sup>  
 Henrik Hartman<sup>2</sup>  
 Hampus Nilsson<sup>2</sup>  
 Günter Wiedemann<sup>3</sup>  
 Ansgar Reiners<sup>1</sup>  
 Stefan Dreizler<sup>1</sup>  
 Todd Henry<sup>4</sup>

<sup>1</sup> Institut für Astrophysik Göttingen, Germany

<sup>2</sup> Lund Observatory, Sweden

<sup>3</sup> Hamburger Sternwarte, Germany

<sup>4</sup> Georgia State University, Atlanta, USA

<sup>5</sup> University of California at Davis, USA

We present the first results obtained from our ongoing search for planets around very low-mass stars and brown dwarfs using radial velocities measured with the CRIRES spectrograph on the VLT. High-precision radial velocity measurements for a large sample of these previously neglected stars are enabled by observing at near-infrared wavelengths and using a new type of gas cell that we have developed. Unprecedented long-term near-infrared radial velocity precisions of  $\sim 5 \text{ ms}^{-1}$  have been demonstrated using CRIRES with the cell. As a first scientific result, data obtained for the very low-mass star VB 10 have been used to refute a claimed planet detection based on astrometry. These results demonstrate the unique sensitivity of our methodology, and confirm its power to detect planets, including potentially habitable ones, around the most numerous stars in the Galaxy.

The vast majority of known exoplanets have been detected around solar-type stars with spectral types F, G or K. However, the vast majority of stars in the Solar Neighbourhood, and likely our entire Galaxy, are M or later type dwarfs. Indeed, current estimates suggest that at least 75 % of stars within 10 pc of our Solar System are M dwarfs. Furthermore, the very lowest-mass stars, those with  $M < 0.2 M_{\odot}$ , make up more than 50 % of the M dwarf population. Therefore, objects at the bottom of the main sequence constitute a very significant fraction of potential planet hosts, and it is imperative

that we characterise the nature of the planetary systems around them in order to constrain the Galactic planet census.

The paucity of detections of planets around M type and later dwarfs is due to two factors. The first reason is that these stars are intrinsically very faint at the wavelengths typically used for planet searches due to their low masses. For example, a Sun-like star at 10 pc will have a visual magnitude of 4.8, while M3, M6, and M9 dwarfs would have visual magnitudes of 11.1, 16.5, and 19.5 respectively. As a consequence of this, many fewer late-type stars have been included in planet search programmes than brighter solar-type stars, and only stars with spectral types down to M3 have been included in planet searches in any substantial number to date. For example, the sample of 40 stars in a long-term radial velocity planet search programme specifically targeting low-mass stars that utilised UVES at the VLT only included two objects with masses below  $0.2 M_{\odot}$ , and only three with masses below  $0.35 M_{\odot}$  (Kürster et al., 2009).

Another reason why many planets have not been found around late-type stars is that giant planets seem to be rare around the few such objects that have been targeted by planet searches. This result is consistent with the predictions of the so-called “core accretion” model of planet formation, which posits that a critical part of the formation of gas giants is the build up of a rock and ice core about ten times the mass of the Earth before the gas in the protostellar disc is dispersed by the central star’s wind. It is thought that it is less likely that such cores can form fast enough around low-mass stars mainly because they host correspondingly low-mass circumstellar discs. Ultimately, what this means is that the easiest planets to detect with current methods (i.e., primarily the radial velocity method) are rare around late-type stars due to their low mass.

A directly testable prediction of the core accretion model is that giant planets should be vanishingly rare around the very lowest-mass stars. By contrast, the competing model for giant planet formation, the so-called “gravitational instability” mechanism, predicts that gas

giants should be just as common around very low-mass stars as solar-type stars. Therefore, low-mass stars offer the potential for definitively establishing the efficiency of the two competing theories of giant planet formation. Furthermore, the search for planets around low-mass stars can offer further insight into planet formation and evolution processes. Comparing the overall mass function of planets around low-mass stars and higher-mass stars can yield constraints on the time-scales of planet growth, planet migration, and protoplanetary disc depletion.

Low-mass stars are also interesting potential hosts for habitable exoplanets that could be detected and studied in the near future, despite their currently neglected status. Low-mass stars of course have correspondingly lower luminosities, and this suggests that their habitable zones are closer in than for their higher-mass counterparts. Therefore, low-mass planets in the habitable zones of low-mass stars will yield much larger signals in radial velocities and also have a much higher probability of transiting. These factors taken together with the overwhelming ubiquity of low-mass stars suggest that the nearby low-mass stars have the best potential for finding a transiting habitable planet, and studying the atmosphere using the technique of transmission spectroscopy using future facilities like the James Webb Space Telescope.

Given the unique opportunities that very low-mass stars offer for advancing our understanding of exoplanets, we were recently motivated to initiate the first comprehensive search for planets around these kinds of stars. This survey is being carried out in Periods 82–85 as a Large Programme with 33 nights of visitor mode time on the VLT. Our methodology is to use high-precision radial velocities measured for the first time in the near-infrared (NIR) spectral regime. The advantages of the NIR for radial velocity measurements are that it is possible to obtain high-resolution and high-signal-to-noise spectra of very low-mass stars at these wavelengths, and also that the effect of activity-induced “jitter” is reduced relative to the visible. This later advantage is particularly important because low-mass stars are generally much more active than solar-type stars and this can hinder the detec-

tion of planets with the radial velocity method. For this work we are taking advantage of the one-of-a-kind instrument CRIRES, which is mounted on the VLT's Unit Telescope 1 (UT1). Of all available NIR spectrographs in the world, only CRIRES has the resolution, throughput and large spectral format necessary to obtain spectra of very low mass stars suitable for high-precision radial velocity measurements.

### The planet search sample

We have selected 36 of the nearest very low-mass stars and brown dwarfs for our CRIRES planet search. See Figure 1 for a summary of their physical properties. We are concentrating primarily on stars with masses less than  $0.2 M_{\odot}$ , and that are too faint and/or display too much activity-related jitter for efficient high-precision radial velocity measurements in the visible using existing instruments. A few higher-mass stars that are known to be extremely active were included in this first survey to characterise the reduction in jitter seen when going from the visible to the NIR. We are obtaining contemporaneous visible wavelength radial velocity measurements of some of these stars using the Hobby Eberly Telescope for this aspect of the project.

### A new gas cell

The potential of the NIR for high-precision radial velocity studies of low-mass stars had previously been discussed extensively before this project began. However, no previous work had achieved a long-term NIR radial velocity precision on a star other than the Sun within an order of magnitude of the precision that is routinely obtained in the visible. The main reason for this up until recently was the lack of high-resolution NIR spectrographs on large telescopes that could deliver sufficient spectral coverage in a single shot. Indeed, the possibility of high-precision NIR radial velocities was one of the motivations for CRIRES during the later part of its design phase. The commissioning of this instrument in 2006 opened the door for high-precision radial velocity measurements of very low-mass stars.

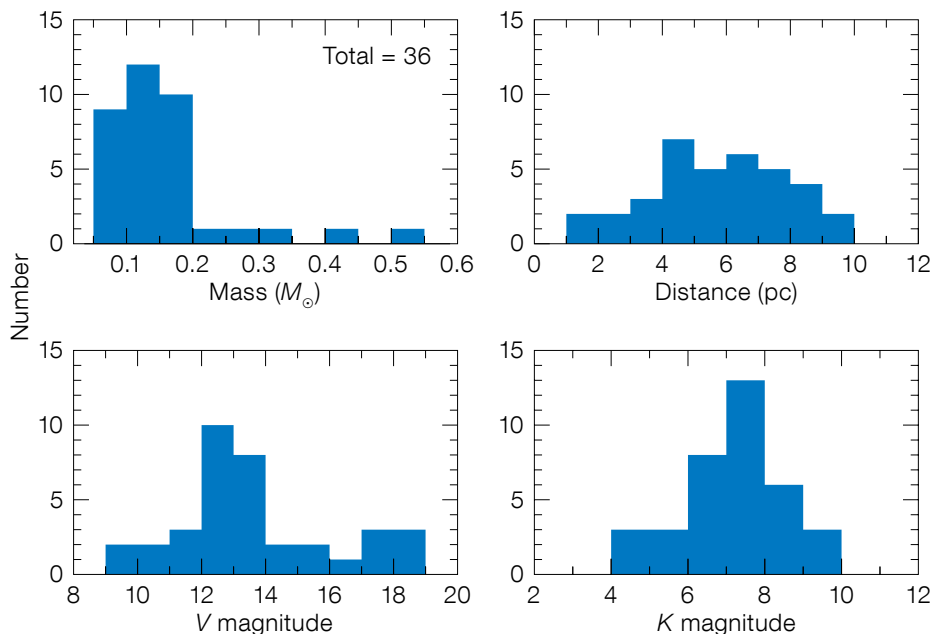


Figure 1. Summary of the physical properties of our planet search targets among low-mass stars.

The final missing ingredient for measuring high-precision NIR radial velocities was the lack of a suitable calibration method. Useful lines from available emission sources, like thorium–argon (ThAr) lamps, are infrequent in the NIR relative to the visible and there are many CRIRES settings where no lamp lines exist. Furthermore, as a long slit spectrograph, CRIRES experiences significant variations in illumination on a variety of timescales. So, although CRIRES could, in principle, be fed with light from an emission lamp, no appropriate lamps exist currently and anyway such a calibration technique would not track all the necessary effects for high-precision radial velocity measurements.

The success of the “iodine cell” in the visible suggested that a gas cell could be a useful way to calibrate CRIRES, and the instrument was designed to use this calibration method. However, at the time of the CRIRES commissioning the questions of which gas or combination of gases to use, and which specific wavelength region in the NIR to observe, were still unsolved. The main constraint for the gas cell method is that the gas or gases in question should exhibit numerous sharp and deep lines in a wavelength interval

where the stars targeted for radial velocity measurements have lines as well. Ideally, this region would also be free of atmospheric lines. However, this is a particularly challenging requirement in the NIR due to the prevalence of strong atmospheric lines even in the traditional windows between water absorption bands. A significant bonus would be if the cell did not present a safety hazard to people or other equipment if it broke during the course of its use. For CRIRES specifically, there was also no room to include a temperature heating or stabilisation apparatus such as is needed for iodine cells, which are typically heated to 50–70 °C and held to within 0.01 °C of a fixed temperature. So any potential cell would have to work at the temperatures normally seen in the telescope dome (~ 10 °C) and be immune to modest variations in the temperature.

With our interest in carrying out a high-precision radial velocity planet search of very low-mass stars in the NIR, we were motivated to work on the problem of building a useful gas cell. After combing line lists and performing simulations we came to the conclusion that simple ammonia ( $^{14}\text{NH}_3$ ) could provide the desired calibration. Ammonia is in its gas-

eous state at room temperature and exhibits a rich molecular spectrum in the NIR even with the relatively low column densities possible in a cell to be used at an astronomical observatory. Simulations using calculated synthetic spectra suggested that the expected temperature variations the cell would see in CRIRES ( $\pm 10^\circ\text{C}$  maximal) would only result in a systematic radial velocity shift of  $\sim 1\text{ ms}^{-1}$ , which is a sufficient level of stability for our purpose.

Although ammonia exhibits lines in different regions of the NIR, even CRIRES yields only relatively small wavelength coverage in a single exposure. Therefore, a careful consideration of the region for observations was necessary in parallel with the choice of a gas for the calibration cell. We chose to make observations in a window in the *K*-band for several reasons: very low-mass stars exhibit numerous sharp and deep lines in this wavelength region suitable for radial velocity measurements; ammonia exhibits a number of lines useful for calibration in this wavelength range. Unfortunately, the window in which we are observing also contains a significant number of absorption lines arising from telluric methane and water. This was already known before we began our work. High-precision radial velocity measurements are usually made by avoiding regions containing telluric lines due to the expectation that these lines will exhibit variability on the order of a few to tens of  $\text{ms}^{-1}$ , or that they are at least difficult to model properly. However, the lack of another obvious method for achieving the desired calibration meant that a more flexible approach was called for. We decided that using an ammonia cell in the *K*-band and including direct modeling of the telluric contamination was a good option considering all the competing issues.

The ammonia cell that we ultimately built and are using for our CRIRES planet search is a glass tube with chemically fused windows that has a length of 17 cm, and diameter of 5 cm. The pressure of the ammonia gas in the cell is 50 mb at  $15^\circ\text{C}$ . In principle, the bonds holding the windows on to the body of the cell should remain sealed for more than ten years. A picture of the cell in the laboratory is shown in Figure 2.

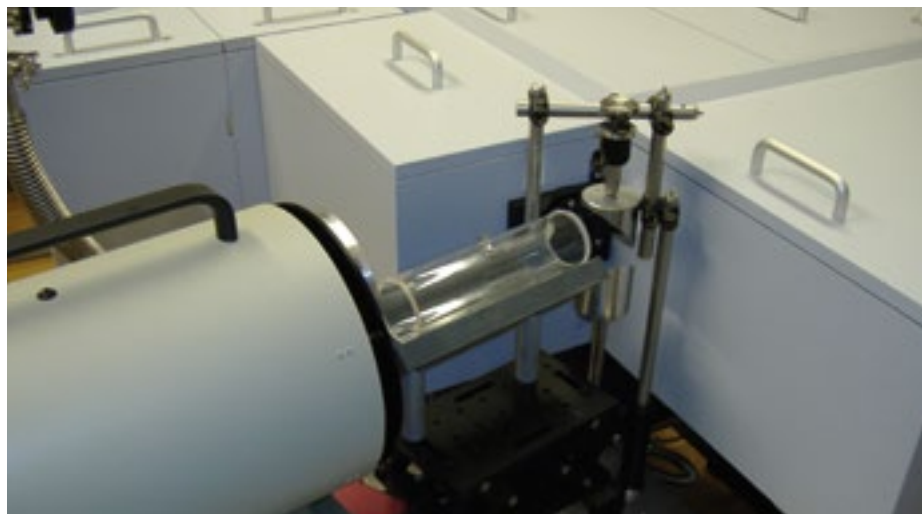


Figure 2. Picture of the ammonia cell being measured with a laboratory Fourier Transform Spectrometer (FTS) at Lund Observatory. The cell is being illuminated with light from a  $1200.0^\circ\text{C}$  blackbody source (grey cylinder on the left). The FTS is in the vacuum box at the upper right.

### Using the gas cell with CRIRES

Our ammonia cell was commissioned by ESO staff as a visiting instrument in CRIRES during the early part of P82, and it has been in routine use since February 2009. The cell is mounted inside the CRIRES warm optics box in an aluminium housing on a carriage that moves the cell in and out of the telescope beam. The carriage has room for two gas cells at one time and CRIRES is normally equipped with cells filled with  $\text{N}_2\text{O}$  and  $\text{CO}$ . These cells are part of the normal calibration plan, but are not useful for high-precision radial velocity work because they do not yield lines in regions where stars also have useful lines. One of the standard cells has to be removed so that our ammonia cell can be inserted. All observations to date with our cell have been performed in visitor mode so as not to impede the necessary calibrations for service mode programmes and regular instrument monitoring.

The gas cells in CRIRES sit just in front of the Nasmyth focus de-rotator in the converging  $f/15$  beam from the telescope. At this location, they are in front of all the spectrograph optics, as well as the instrument's integrated AO system. Our observations of a star for radial veloc-

ity measurements are obtained with the ammonia cell in the beam, which causes the absorption lines of the cell to be imprinted on the stellar spectrum. The cell lines, whose position and shapes are well known, serve as a fiducial to precisely establish the wavelength scale and point spread function of the instrument at the time of the observation independently for each of the obtained spectra during analysis of the data.

We have performed laboratory measurements of our ammonia cell using the Lund Observatory Bruker IFS125 HR Fourier Transform Spectrometer (FTS) to obtain the characteristic spectrum that is needed for the radial velocity measurements during analysis of the data (see Figure 2). The obtained FTS spectrum has a resolution  $R = 620\,000$  and measured  $S/N > 700$  in the continuum at  $2.3\ \mu\text{m}$ . A plot of this spectrum in the wavelength region at which we are observing is shown in Figure 3.

The primary FTS measurement was obtained with the cell cooled to  $13^\circ\text{C}$ . This temperature is close enough to the temperatures the cell experiences in CRIRES given the stability of ammonia. In addition to this spectrum, we also obtained measurements of the cell at  $24^\circ\text{C}$



on two separate occasions 13 months apart — once right before the cell was originally handed over to ESO in August 2008 and again after our programme had started in September 2009. Comparison of these data reveals no change in the cell's spectrum, which supports our assumption of the cell's stability.

### Tests of radial velocity precision

In addition to the very low-mass stars we are monitoring as part of our ongoing planet search, we have also frequently observed Proxima Centauri (GJ 551) and Barnard's Star (GJ 699) to characterise the performance of the cell and our radial velocity measurement algorithms. These stars are two of the few very low-mass stars for which it is possible to obtain high-precision radial velocity measurements in the visible wavelength range (due to their being very nearby, and thus bright even at visible wavelengths), and previous work has shown their radial velocity to be constant at the level of  $3 \text{ ms}^{-1}$ .

The radial velocities we have obtained for these stars between February 2009 and February 2010 are shown in Figure 4. These data exhibit a typical root mean square (rms) scatter about a constant value of  $\sim 5 \text{ ms}^{-1}$ . This demonstrates that we have obtained the long-awaited breakthrough in NIR radial velocity precision on very low-mass stars using CRIRES with our ammonia cell. The details of our radial velocity measurement technique and more extensive tests of the obtained precision can be found in Bean et al. (2010b).

### First result: no giant planet for VB 10

The unique capability of CRIRES when used with our ammonia cell to obtain high-precision radial velocities of low-mass stars is demonstrated by the case of VB 10. This object lies right at the boundary between stars and brown dwarfs (estimated mass is  $\sim 0.08 M_{\odot}$ ). It is very faint in the visible ( $V = 17.3$ ) despite being one of the closest examples of its spectral type. However, it is reasonably bright in the NIR ( $K = 8.8$ ) due to its extreme redness. Pravdo & Shaklan

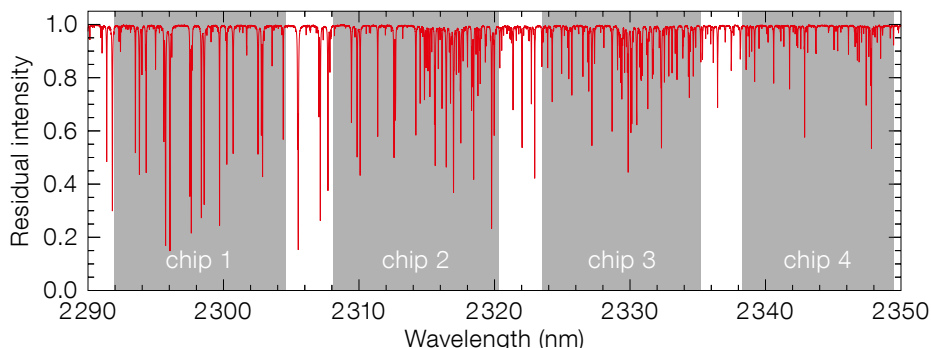
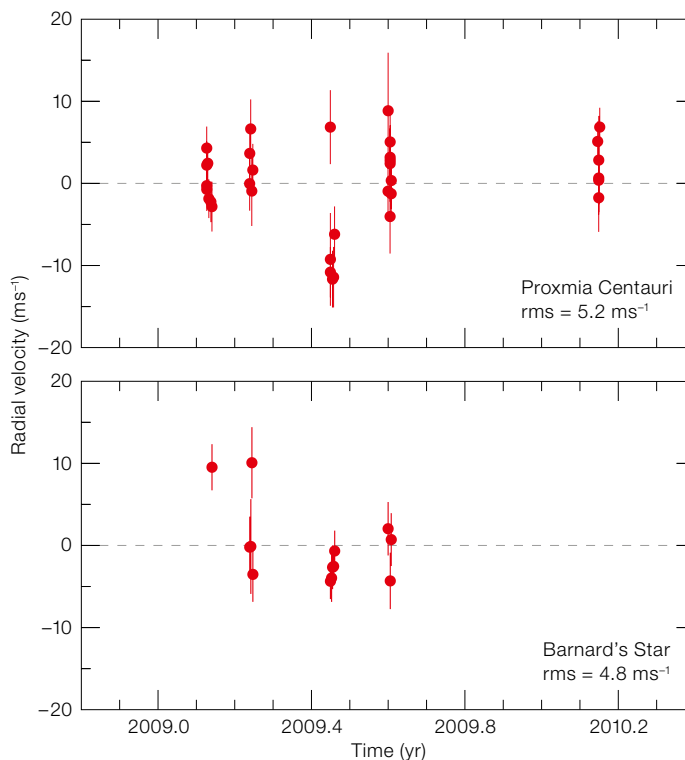


Figure 3 (above). Spectrum of the ammonia cell in the observed wavelength region at  $R = 100\,000$ . The grey boxes indicate the wavelength coverage of the four chips in the CRIRES detector mosaic.

Figure 4 (below). Radial velocities of two stars, with velocities known to be constant from visible range measurements, observed with CRIRES using the ammonia cell.



(2009) reported the detection of a giant planet around this star based on ground-based astrometry. This would have been the first detection of a planet around a nearby very low-mass star, and would also have been the first astrometric discovery of an exoplanet.

We obtained 12 radial velocity measurements of VB 10 over four epochs using CRIRES with our ammonia cell during the first year of our programme. These velocities are shown in Figure 5. Our measured velocities exhibit an rms dispersion of

only  $10 \text{ ms}^{-1}$ , whereas the expected signal from the proposed giant planet is  $\sim 1 \text{ kms}^{-1}$ . We were able to completely rule out the existence of the proposed planet using the observed constancy of the radial velocities (Bean et al., 2010a).

For comparison, other groups have obtained radial velocity measurements of VB 10 in an attempt to detect the planet as well. These measurements have been done in the visible using the Magellan telescope, and in the NIR using Keck. However, even though these other meas-

urements were made with similarly sized telescopes and similar exposure times as our measurements, they only had precisions of  $\sim 300 \text{ ms}^{-1}$ . This clearly demonstrates both the superiority of CRILES among existing NIR spectrographs, and the power of our observational methodology for very low-mass stars.

### Outlook

Our search for planets around very low-mass stars is continuing until at least the end of P85 and we have recently proposed to continue the programme for another two years. One of the goals of the new programme is to continue monitoring the 36 objects surveyed in the previous study in order to confirm planet candidates that we have identified around some of the stars, and to probe for lower-mass and longer-period planets around all the stars. The new measurements should enable us to be sensitive down to even terrestrial-mass planets in the habitable zones around many of the stars we are targeting. We also aim to widen our survey to include 30 new targets that we will search for gas giant companions in a sort of shallow-wide survey.

In addition to our work with CRILES, we are also beginning a similar survey in the northern hemisphere using the NIR spectrograph IRCS on the Subaru telescope with a copy of our ammonia cell. The radial velocity precision obtained with this facility will be significantly less than with the VLT + CRILES due to the IRCS's lower spectral resolving power (20 000) and throughput, but it will still be useful to search low-mass stars for gas giant

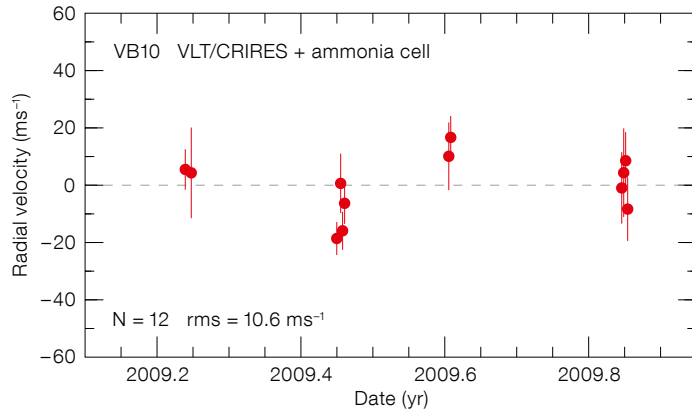


Figure 5. Radial velocities measured for the very low-mass star VB 10 with CRILES using the ammonia cell.

planets. Together, the new CRILES programme and the Subaru programme are volume complete for all known stars with masses  $< 0.2 M_{\odot}$  and spectral type earlier than T0 out to 10 pc. Therefore, we are adding important information to the census of planets around nearby stars.

Technically speaking, our results have shown that obtaining NIR radial velocity precisions comparable to those which are routinely obtained in the visible is possible, and we see no reason why a level of precision of  $1 \text{ ms}^{-1}$  could not be obtained in the future with a new approach or instrument. Our current measurements are limited by the presence of telluric lines in the window in which we are observing, and it is likely we would be doing about a factor of two better if these lines were not present. Therefore, if a new type of gas cell for the NIR was designed that yielded useful calibration lines where interesting stars also have lines and where the Earth's atmosphere does not, then that would probably give a boost in performance. However, our ex-

perience suggests such a breakthrough is unlikely. Instead, it is more likely that improving on our results will require applying the HARPS concept of building a highly stabilised instrument for the NIR. Indeed, such new instruments are currently being considered for the immediate future for telescopes in the 4-metre class range, and in the longer-term for 8–10-metre class telescopes and even ELTs.

### Acknowledgements

We are grateful to the OPC for their generous allocation of observing time for this project. We thank the ESO staff, in particular Alain Smette and Hans Ulrich Käufel, for their assistance with the implementation of the gas cell in CRILES and carrying out our observations.

### References

- Bean, J. et al. 2010a, *ApJ*, 711, L19
- Bean, J. et al. 2010b, *ApJ*, 713, 410
- Kürster, M. et al. 2009, *The Messenger*, 136, 39
- Käufel, H. U. et al. 2006, *The Messenger*, 126, 32
- Pravdo, S. & Shaklan, S. 2009, *ApJ*, 700, 603

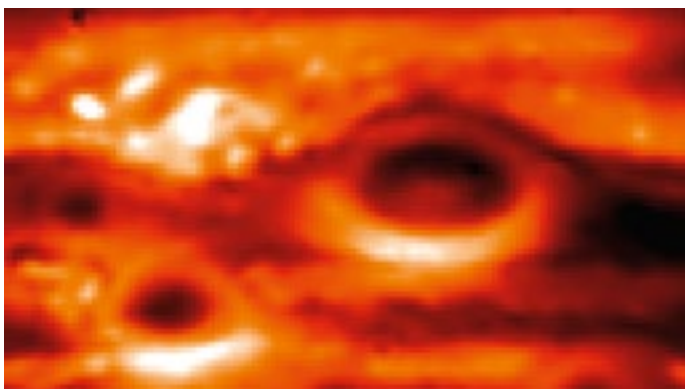


Image of the Great Red Spot on Jupiter taken with the VLT Imager and Spectrometer for mid Infrared (VISIR). The structure of the Great Red Spot in the thermal emission at 8–13 microns is revealed in this image. See release eso1010 for more details.

# Spectropolarimetry of Wolf–Rayet Stars in the Magellanic Clouds: Constraining the Progenitors of Gamma-ray Bursts

Jorick Vink<sup>1</sup>

<sup>1</sup> Armagh Observatory, College Hill, Northern Ireland, United Kingdom

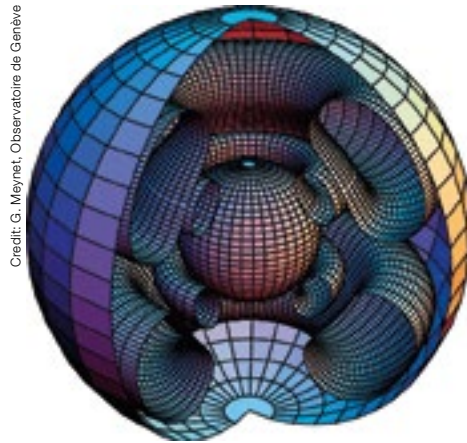
Wolf–Rayet stars have been identified as objects in their final phase of massive star evolution. It has been suggested that Wolf–Rayet stars are the progenitors of long-duration gamma-ray bursts in low-metallicity environments. However, this deduction has yet to be proven. Here we report on our initial results from a VLT/FORS linear spectropolarimetry survey of Wolf–Rayet stars in the Magellanic Clouds, which is intended to constrain the physical criteria — such as weaker stellar winds, rapid rotation, and associated asymmetry — of the collapsar model. Finally, we provide an outlook for polarisation studies with an extremely large telescope.

Stars like the Sun spin slowly, with speeds of only a few  $\text{kms}^{-1}$ . By contrast, massive stars rotate much more rapidly, reaching rotational velocities of over  $400 \text{ kms}^{-1}$ . This rapid rotation is understood to have dramatic consequences for their evolution and ultimate demise, which may involve the production of a long-duration gamma-ray burst (long GRB), the most intense type of cosmic explosion since the Big Bang.

## Rotating massive stars

The evolution of massive stars is thought to be the result of a complex interplay between mass loss, rotation and possibly magnetic fields. Whilst the importance of mass loss was established in the 1970s, following the discovery of mass loss from normal O-type supergiants and radiation-driven wind theory, the role of rotation was only fully appreciated in the 1990s (for example, Langer, 1998; Maeder & Meynet, 2000).

When a star rotates, the pole becomes hotter than the stellar equator (Von Zeipel theorem), which enables a rather complex meridional circulation in the stellar interior (see Figure 1). In this process, nu-



Credit: G. Meynet, Observatoire de Genève

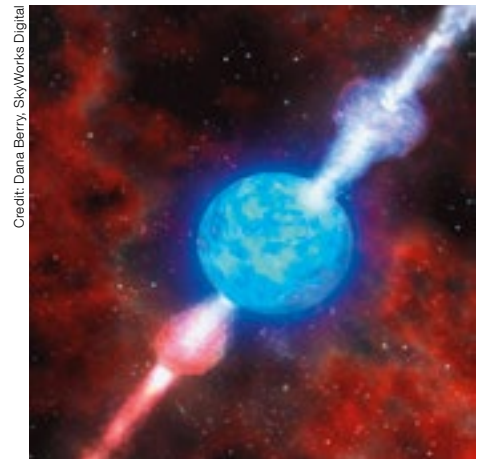
Figure 1. Schematic of the 3-dimensional interior structure of a rotating massive star.

clear processed material is transported from the core to the stellar envelope, thereby enriching the stellar surface with elements such as nitrogen, which is produced during the CNO cycle of hydrogen burning (in contrast to the proton–proton cycle that operates in solar-type stars).

During later evolutionary phases, the combination of mass loss and rotation also leads to the transfer of products of helium burning to the surface, enriching the atmosphere with carbon during the final carbon-rich Wolf–Rayet (WC) phases before the stellar core is expected to collapse, producing a supernova (SN) — in some cases in conjunction with a long GRB.

## The collapsar model for gamma-ray bursts

From the 1960s onwards, GRBs were discovered appearing from all cosmic directions. However, an explanation for their origin was still to be found. A massive breakthrough occurred in 1998 when a European team led by graduate student Titus Galama discovered that the unusual supernova 1998bw fell within the error box of GRB980425, which was subsequently confirmed with the case of SN2003dh/GRB030329. This was convincing evidence that long (those lasting longer than two seconds) GRBs were associated with the deaths of massive stars.



Credit: Dana Berry, SkyWorks Digital

Figure 2. Artist's impression of a long gamma-ray burst.

The most popular explanation for the long GRB phenomenon is that of the collapsar model (Woosley, 1993), where a rapidly rotating massive core collapses, forming an accretion disc around a black hole. In this process, part of the gaseous material is ejected in the form of two relativistic jets, which are aligned with the rotation axis of the dying star (see Figure 2). These jets are thought to involve an opening angle of just a few degrees, and only when these jets happen to be directed towards Earth are we able to detect the event as a gamma-ray burst.

## The gamma-ray burst puzzle

One of the persistent problems with the collapsar model was that it not only required the star to have a high rotation speed initially, but that the star needs to maintain this rapid rotation until the very end of its life. The reason this is such a challenge is that one of the most characteristic features of massive stars, their strong stellar outflows, are expected to remove angular momentum. Most stellar evolution models show that as a result of mass loss, the objects not only remove up to 90 % of their initial mass when reaching their final Wolf–Rayet (WR) phase, but as a result of this wind, the stars are expected to come to an almost complete standstill. This property seems to be supported by the fact that most Galactic WR winds are found to be spherically symmetric (Harries et al., 1998). Because of the observed spheric-



ity, which is thought to be characteristic for their slow rotation, we would not anticipate Galactic WR stars to produce a GRB when they expire.

The question is what do we expect for WR stars in low-metallicity galaxies? Do WR stars in low-metallicity galaxies suffer from similar mass and angular momentum loss? To address these issues we need to explore the underlying physical origin of massive star winds.

### Iron iron iron

Radiation hydrodynamic simulations show that stellar winds from massive O-type stars are driven by the radiation pressure on metal lines, and specifically on iron (Fe), despite the fact that it is such a rare element. In the Milky Way, for each and every Fe atom there are more than 2500 H atoms, and Fe becomes even scarcer in galaxies with lower metal content, such as the nearby Large and Small Magellanic Clouds, at respectively 1/2 and 1/5 of solar metallicity. Owing to the highly complex atomic structure of Fe, it has millions of line transitions, which makes it an extremely efficient absorber of radiation in the inner atmosphere where the mass-loss rate is set (Vink et al., 1999; Puls et al., 2000).

Up to 2005, most stellar modellers assumed that due to the overwhelming presence of carbon in WC star atmospheres, it should also be the element carbon that drives Wolf–Rayet winds, rather than the few Fe atoms, which were basically assumed to constitute a negligible amount. This assumption also implied that WC stars in low-metallicity ( $Z$ ) galaxies would have stellar winds equally as strong as those in the Galaxy, still removing the required angular momentum. It was for this very reason that there was no satisfactory explanation for the long GRB puzzle.

Nevertheless, GRBs were found to arise in low-metallicity galaxies (e.g., Vreeswijk et al., 2004), characteristic of conditions in the early Universe. It is interesting to note that the most distant object in our Universe known today is indeed a GRB, estimated to have resulted from the collapse of a massive star only some 500 mil-

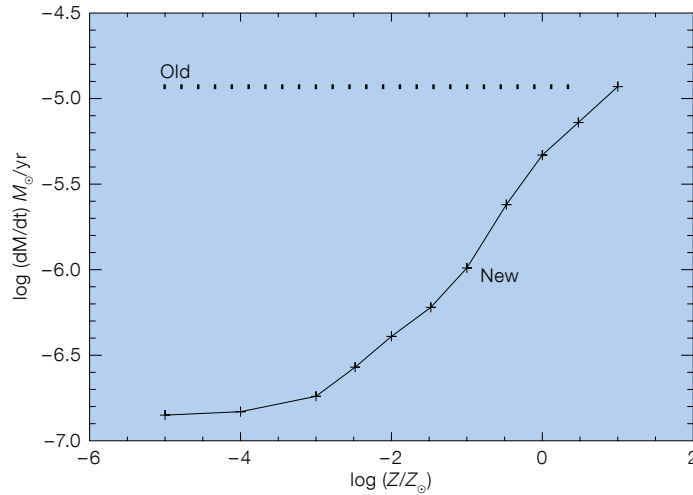


Figure 3. The mass loss versus (host galaxy) metallicity relation for late-type WC stars as found by Vink & de Koter (2005). The earlier concept of metallicity-independent rates is referred to as “old”.

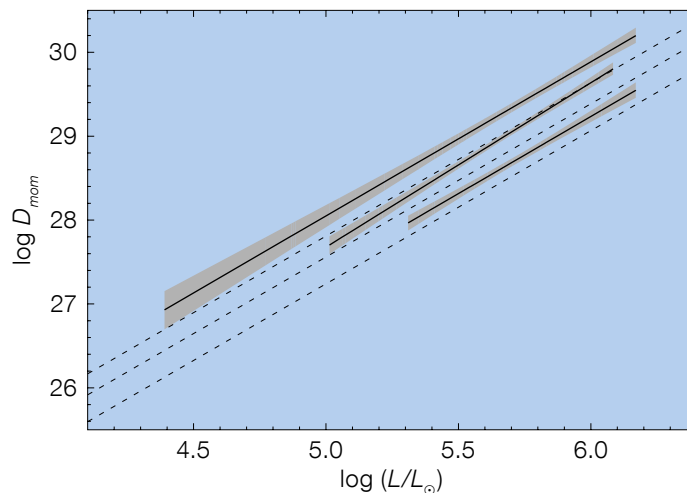


Figure 4. Comparison of the empirical wind–momentum–luminosity relations (solid lines) to theoretical predictions (dashed lines) for the Milky Way, the LMC and SMC respectively (see Mokiem et al. [2007] for details).

lion years after the Big Bang (Tanvir et al., 2009). That GRBs occur in low-metallicity environments may imply that they were common at earlier times in the Universe when the interstellar gas was less enriched.

In 2005 Vink & de Koter performed a pilot study of Wolf–Rayet mass loss as a function of metallicity (see Figure 3) and found that, although C is the most abundant metallic element in the Wolf–Rayet atmosphere, it is the much more complex Fe element that drives the stellar wind. Thus host galaxy metallicity plays a crucial role: objects that are born with fewer Fe atoms will lose less matter by the time they reach the ends of their lives, despite their large CNO-type material content. The striking implication is that objects

formed in the early Universe and in other low-metallicity environments can retain their angular momentum, maintaining their rapid spin towards collapse, enabling a GRB event (see Figure 4). More recent stellar evolution models involving very rapidly spinning stars in which the objects become almost fully mixed, such as those of Yoon & Langer (2005) and Woosley & Heger (2006), but now assuming that the mass loss depends on the original Fe metal content (rather than that of self-enriched CNO elements) indeed shows that massive stars can maintain their rapid rotation until collapse. This finding appears to resolve the collapsar puzzle for long GRBs: the outcome depends on just a very few Fe atoms! The key question is now what happens in nature.

### Observational tests

The key assumptions and predictions of the collapsar model for GRBs that have to be met are that stellar winds should depend on metallicity and that lower metallicity Wolf–Rayet stars should rotate more rapidly than their higher metallicity Galactic counterparts.

The first part of the observational evidence concerns the issue of whether stellar winds are observed to depend on metallicity. For O-type stars this has been suspected for a long time and the most recent results by the FLAMES consortium on massive stars find good agreement between observed and predicted wind momenta versus stellar luminosities (see Figure 4). The situation for Wolf–Rayet stars has been more confused, with controversial results in the early 2000s, although more recently a mass-loss metallicity dependence of  $\dot{M} \propto Z^{0.8}$  was suggested by Crowther (2006), in good agreement with theoretical relations (Vink & de Koter, 2005; Gräfener & Hamann, 2008).

The second observational step would be to show that WR stars at lower metallicity rotate more slowly than those in the Galaxy. For most stellar applications one would simply measure the rotation rate (actually  $v \sin i$ ) from the width of stellar absorption lines, but in WR stars the spectra are dominated by emission lines, and it is not clear whether the line shape arises from rotation or from other dynamical effects associated with the outflow. In other words, the route of stellar spectroscopy is unsuitable for measuring rotation rates directly in WR winds. Fortunately, there is an alternative method available via measurement of the polarisation properties across emission lines, in the form of linear spectropolarimetry.

### The tool of linear spectropolarimetry

Linear polarisation is a very powerful technique to deduce the presence of asymmetric structures, even in cases where the objects under consideration cannot be spatially resolved. The amount of linear polarisation is simply given by the vector sum of the Stokes parameters  $Q$  and  $U$ . In many instances however,

interstellar dust grains produce additional polarisation, and this would normally not occur at exactly the same position angle (see Figure 5). If the interstellar and the observed polarisations can be disentangled, the amount of polarisation from the source can be measured directly, and it is easy to infer whether any given object is spherically symmetric or not. One way to achieve this is by performing spectropolarimetry.

In its simplest form, the technique is based on the expectation that line photons arise over a larger volume than continuum photons. If so, then line photons undergo fewer scatterings from, for example, a flattened wind than continuum photons, and the emission-line flux becomes less polarised, resulting in a polarisation variation across the line (see Figure 7).

The high incidence (~ 60 %) of “line effects” revealed among classical Be stars in the 1970s indicated that all classical Be stars possess discs, with orientation towards the observer ( $\sin i$ ) determining whether any given object is subject to a line effect or not. This serves to show that significantly sized samples are needed for meaningful analysis. Another criterion is high signal-to-noise, as spectropolarimetry is a “photon-hungry” technique, and the tool is thus best served by the largest telescopes, such as ESO’s VLT.

### VLT/FORS spectropolarimetry programme of low-metallicity WR stars

Over the last couple of years, we have utilised the tool of linear spectropolarimetry on WR stars in the Large and Small Magellanic Clouds (LMC & SMC) to test the assumptions of the collapsar model for long GRBs. This has been generously supported in Periods 78, 81 and 85.

If the WR mass-loss metallicity dependence, and the subsequent inhibition of angular momentum removal are the keys to explaining the high occurrence of GRBs at low metallicity, WR stars in the Magellanic Clouds should, on average spin faster than those in the Galaxy. A linear spectropolarimetry survey of LMC WR stars (see examples in Figures 6 and 7) showed that ~ 15 % of LMC WR stars

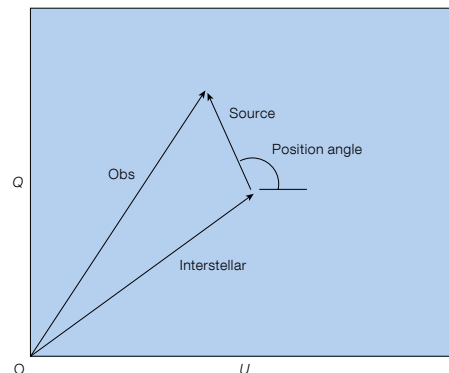


Figure 5. A schematic  $QU$  diagram. The observed linear polarisation is a vector addition of the interstellar plus source polarisation. The length of the vectors represents the degree of polarisation, whilst the angle provides the position angle  $\theta$ .

bear the sign of rapid rotation, as only two out of thirteen of them show a significant amount of linear polarisation (Vink, 2007). The incidence rate is equal to that of the Galactic WR survey by Harries et al. (1998). The LMC sample, however, was necessarily biased towards the brightest objects (with  $V$  magnitude  $< 12$ , mostly containing very late type nitrogen-rich WR stars and/or binaries), and for an unbiased assessment we have been allocated time to study a larger sample.

The data obtained thus far may suggest that the metal content of the LMC is high enough for WR winds to remove the necessary angular momentum, and single star progenitors may be constrained to an upper metallicity of that of the LMC at 1/2 solar. Alternatively, rapid rotation of WR-type objects may only be achievable for objects that are the products of binary evolution. Meaningful correlations between binarity and large amounts of linear polarisation have yet to be performed, which is one of the main tasks of our ongoing VLT/FORS programme.

### Future testing with the E-ELT?

Looking further ahead, with linear spectropolarimetry on a 42-metre European Extremely Large Telescope (E-ELT), one could properly probe WR wind geometries for very faint objects such as those in the very low metallicity SMC (at 1/5 solar), and beyond. The aim is to constrain GRB progenitor models in the criti-

cal metallicity range between 1/5 and 1/2 solar, which is anticipated to have crucial implications for understanding the production of GRBs at low metallicity in the early Universe.

Future Extremely Large Telescope (ELT) work could also involve a complete census of all evolved massive supernova progenitors (Wolf–Rayet stars, B[e] supergiants, and Luminous Blue Variables) in both the LMC and SMC, in order to map the links between mass loss and rotation in the most massive stars.

If the spectral resolution of a potential E-ELT spectropolarimeter were ultra-high, one could also perform complementary circular spectropolarimetry to measure magnetic fields in these low-metallicity massive stars, and study the intricate interplay between mass loss, rotation and magnetic fields, in order to constrain massive star models as a function of  $Z$ , with unique constraints on models of GRBs and Pair–Instability SNe in the early Universe.

Massive stars play a vital role in the Universe as providers of ionising radiation, kinetic energy, and heavy elements. Their evolution towards collapse is driven by mass loss and rotation. As the favoured progenitors of long GRBs, massive stars may also be our best signpost of individual objects in the early Universe, but we do not know why certain massive stars collapse to produce GRBs while others do not. Studies of wind asymmetries in massive stars are vital for understanding massive star evolution, and thereby GRB production and related phenomena.

#### References

- Crowther, P. A. 2006, *ASPC*, 353, 157  
 Galama, T. J. et al. 1998, *Nature*, 395, 670  
 Gräfener, G. & Hamann, W.-R. 2008, *A&A*, 482, 945  
 Harries, T. J. et al. 1998, *MNRAS*, 296, 1072  
 Langer, N. 1998, *A&A*, 329, 551  
 Maeder, A. & Meynet, G. 2000, *ARAA*, 38, 143  
 Mokiem, M. R. et al. 2007, *A&A*, 473, 603  
 Puls, J. et al. 2000, *A&AS*, 141, 23  
 Tanvir, N. et al. 2009, *Nature*, 461, 1254  
 Vink, J. S. 2007, *A&A*, 469, 707  
 Vink, J. S. & de Koter, A. 2005, *A&A*, 442, 587  
 Vink, J. S. et al. 1999, *A&A*, 345, 109  
 Vreeswijk, P. M. et al. 2004, *A&A*, 419, 927  
 Woosley, S. E. & Heger, A. 2006, *ApJ*, 637, 914  
 Woosley, S. E. 1993, *ApJ*, 405, 273  
 Yoon, S.-C. & Langer, N. 2005, *A&A*, 443, 643

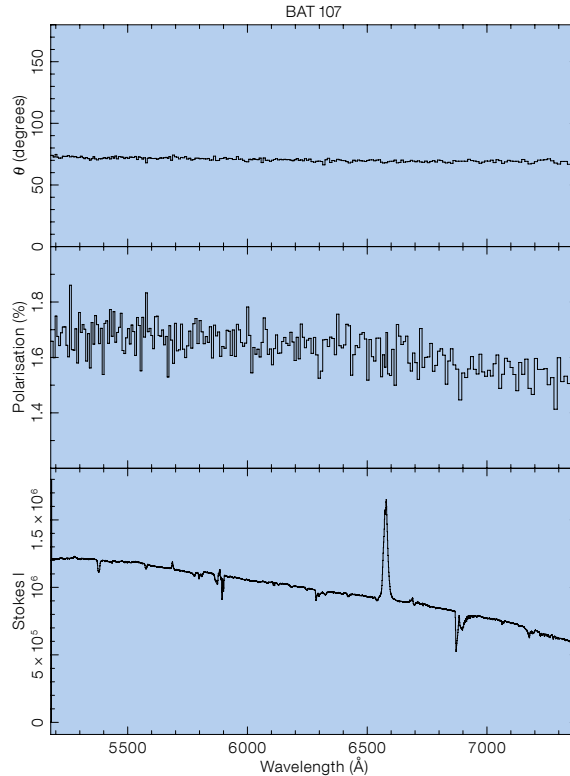


Figure 6. Linear polarisation triplot for the LMC Wolf–Rayet star BAT 107. The upper panel shows the polarisation position angle, the middle panel the degree of polarisation, and the lower panel the normal Stokes I spectroscopy. BAT 107 does not show any “line effects” (*viz.* polarisation signature across the lines) and thus no evidence for intrinsic polarisation, nor asphericity (Vink, 2007).

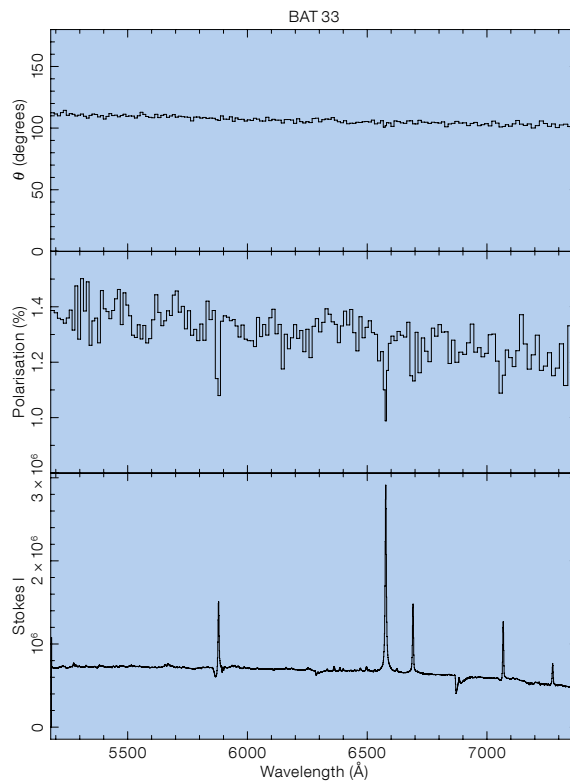


Figure 7. Linear polarisation triplot for the LMC Wolf–Rayet star BAT 33, layout as Figure 4. BAT 33 clearly shows some “line effects” and thus clear-cut evidence for intrinsic polarisation and asymmetry (Vink, 2007).



# ESO–GOODS: Closing the Book, Opening New Chapters

Piero Rosati<sup>1</sup>  
The ESO–GOODS Team\*

<sup>1</sup> ESO

The Great Observatories Origins Deep Survey (GOODS) was the first public multi-wavelength survey with an extensive coordination between space- and ground-based observations. ESO–GOODS, a public Large Programme carried out with ESO facilities, has provided essential complementary data to this project that have allowed the full scientific exploitation of a very rich multi-observatory dataset in the Chandra Deep Field South. The public release of all advanced data products from ESO–GOODS, completed in December 2009, is summarised here.

The GOODS survey originally covered two 150 square arcminute fields, centred around the Hubble Deep Field North and the Chandra Deep Field South (CDFS). It was the first coordinated effort to combine the deepest survey data over the widest wavelength range (from X-ray through radio) from space- and ground-based observatories, setting the stage for many other multi-wavelength surveys that have been carried out over the last decade. Observations were designed to promote major advances in our understanding of the mass assembly history of galaxies over a broad range of cosmic time, to obtain a census of energetic output from star formation and supermassive black holes, and to trace the star formation history out to  $z \sim 7$ . The same dataset and synergy between the Hubble Space Telescope (HST) and the largest ground-based telescopes were also utilised to discover many Type Ia super-

novae with crucial implications for understanding the cosmic expansion.

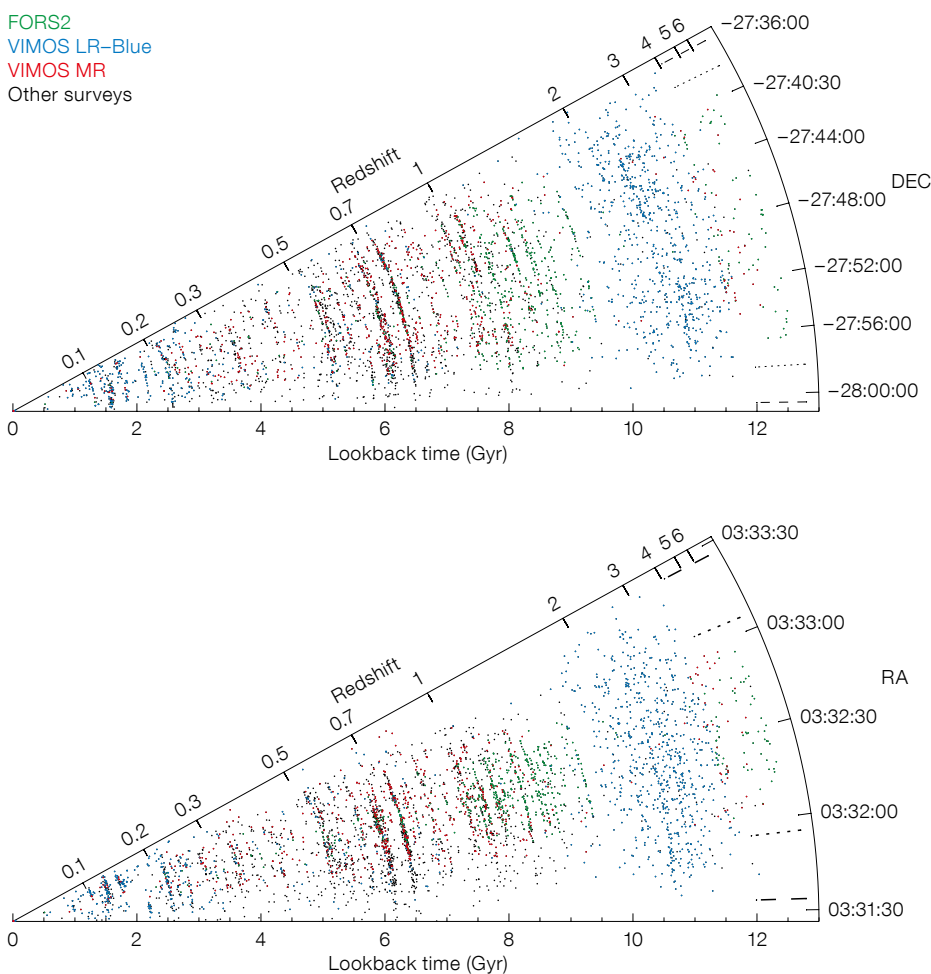
Nearly ten years ago, ESO embarked on a public project consisting of a number of observing campaigns in the CDFS field, primarily with the VLT, designed to complement the capabilities of HST prior to Servicing Mission 4. The VLT campaign was conducted under the programme, The Great Observatories Origins Deep Survey (GOODS): ESO Public Observations of the SIRTf Legacy/HST Treasury/Chandra Deep Field South, with PI Catherine Cesarsky, over the periods

P68–P77. Science-ready data products were prepared by the ESO–GOODS Team, which included members from the Space Telescope European Co-ordinating Facility (ST–ECF) and the community. The team publicly released these data into the ESO Archive in a progressive manner within 6–12 months of the conclusion of each observing run.

The ESO–GOODS programme reached the final milestone in December 2009 by completing the public release of all advanced science-ready data products consisting of (see Table 1):

1. deep near-IR coverage of the GOODS region in the *JHK* bands with ISAAC;
2. very deep *U*-band imaging of the entire CDFS area with VIMOS;
3. an extensive spectroscopic campaign with FORS2 and VIMOS which has yielded  $\sim 2700$  secure source redshifts.

Figure 1. Wedge diagrams showing two projections of the spatial distribution of galaxies with lookback time from all publicly available redshifts in the CDFS as of the end of 2009 (from Balestra et al., 2010). Different spectroscopic surveys are colour-coded as indicated. Only 4234 reliable redshifts are considered here: 2574 from ESO–GOODS (green, blue and red dots), 1660 from other surveys (black dots).



\* A number of students, post-docs and staff members have contributed to the ESO–GOODS Team over the years. These included Italo Balestra, Catherine Cesarsky, Vincenzo Mainieri, Paolo Padovani, Paola Popesso, Alvio Renzini, Jörg Retzlaff, Alessandro Rettura, Benoît Vandame from ESO; Bob Fosbury, Jonas Haase, Richard Hook, Harald Kuntschner from ESO/ST–ECF; Stefano Cristiani, Mario Nonino, Eros Vanzella at INAF–Trieste; and Mark Dickinson (NOAO) and Mauro Giavalisco (UMass) from the US GOODS collaboration.

Table 1. Summary of ESO–GOODS observations and data releases.

Campaign	Description	Observing time (hours)	Data release/date	Publications
Near-IR imaging	ISAAC in <i>J</i> -, <i>H</i> -, <i>Ks</i> -bands, 170 arcmin <sup>2</sup> to 25 AB mag ( $5\sigma$ )	476.0	ISAAC v2.0/2007-09-10	Retzlaff et al., 2010
	<i>Ks</i> -band of the HUDF <sup>1</sup> to 25.6 AB mag, 0.36" seeing	25.3	ISAAC HUDF v1.0/2010-03-02	
<i>U</i> -band imaging	VIMOS <i>U</i> - and <i>R</i> -band, 400 arcmin <sup>2</sup> , to $U \sim 29.8$	40.0	VIMOS img v1.0/2009-04-24	Nonino et al., 2009
<i>R</i> -band imaging <sup>1</sup>	and $R \sim 29$ AB ( $1\sigma$ )	16.3		
FORS2 spectroscopy	300l grism (0.55–1.0 $\mu\text{m}$ ), 1635 spectra of 1236 targets, 887 redshifts out to $z = 6.3$	130.0	FORS2 v3.0/2007-10-31	Vanzella et al., 2008
VIMOS spectroscopy	LR-B grism (0.35–0.7 $\mu\text{m}$ ), 3634 spectra of 3271 targets, 2040 redshifts ( $1.8 < z < 3.5$ )	120.0	VIMOS v2.0/2009-12-15	Popesso et al., 2008
	MR grism (0.4–1.0 $\mu\text{m}$ ), 1418 spectra of 1294 targets, 882 redshifts ( $z < 1$ and $z > 3.5$ )			Balestra et al., 2010

<sup>1</sup> Based on other programmes in the ESO Archive.

A summary of the spectroscopic effort in the CDFS is shown in Figure 1, which includes redshifts from both ESO–GOODS and a number of additional VLT programmes. To facilitate the utilisation of such a large investment of VLT spectroscopic time (over 500 hours), an up-to-date database of all publicly available spectra obtained in the GOODS/CDFS area has been constructed by ESO and the ST–ECF and made accessible with a search-engine interface. We plan to keep this spectral database up to date in the coming years, as more reduced spectra become available, including those derived from the slitless modes of HST.

The ESO–GOODS public data products have remained in great demand over the last four years and have fueled a large number of high-impact publications. While we close this book on the ESO–GOODS programme, new chapters are being opened as this rich dataset continues to stimulate several VLT follow-up programmes, which will benefit from future observations, for example with the refurbished HST, and with Chandra and Herschel.

With the deployment of the LABOCA bolometer array on the 12-metre APEX Telescope, the ESO–GOODS multi-wavelength dataset has recently been extended to the sub-mm region. A public

legacy survey has covered the  $0.5 \times 0.5$  degree Extended CDFS field at 870  $\mu\text{m}$  to a depth of  $\sim 1.2$  mJy (Weiss et al., 2009); the resulting map has also recently been released in the ESO Archive.

Detailed information and relevant links on the ESO–GOODS project can be found at <http://www.eso.org/sci/activities/projects/goods/>.

#### References

- Balestra, I. et al. 2010, A&A, 512, 12
- Nonino, M. et al. 2009, ApJS, 183, 244
- Popesso, P. et al. 2009, A&A, 494, 443
- Retzlaff, J. et al. 2010, A&A, 511, 50
- Vanzella, E. et al. 2008, A&A, 478, 83
- Weiss, A. et al. 2009, ApJ, 707, 1201



UBR colour composite image of the GOODS-South region obtained combining the deep VIMOS *U*- and *R*-band observations with a WFI *B*-band image. The contour indicates the HST-ACS original coverage. See release eso0839 for details.





An album presenting activities of the ESO Solidarity Group in support of victims of the recent earthquake in Chile. See article on p. 60 for more details.



## The Origin and Fate of the Sun: Evolution of Solar-mass Stars Observed with High Angular Resolution

held at ESO Garching, Germany, 2–5 March 2010

Markus Wittkowski<sup>1</sup>  
Leonardo Testi<sup>1</sup>

<sup>1</sup> ESO

The goal of the workshop was to review recent results on solar-mass stars obtained with infrared and millimetre interferometers, and to discuss their importance for our understanding of stellar evolution from star formation to the late stages. The workshop was preceded by a one-day ALMA+VLTI interferometry primer. A brief summary of the workshop is presented.

The workshop was organised with a focus on solar-mass stars, and the intention of following their evolution through the Hertzsprung–Russell (HR) diagram in the light of the new interferometric observations. The goals included presenting the unique results made available by interferometry, discussing the complementarity between infrared and millimetre interferometry, merging them with observations obtained with other techniques, such as spectroscopy, and discussing their impact on the details of the evolution of Sun-like stars. Another goal was a presentation of the prospects with second generation VLTI instruments and with ALMA.

Several years of observations using the VLT Interferometer (VLTI) have allowed us to gain unprecedented new insights into different stages of stellar evolution from star formation to the late stages, using the combination of high spatial and spectral resolution. Examples are discs around young stars, debris discs, stellar atmospheres and the circumstellar environment of evolved stars. Now, the upcoming dual-feed facility PRIMA on the VLTI is about to enable astrometric measurements, with one goal being the detection and characterisation of planets around stars. In the immediate future, ALMA will provide complementary observations of stars with similar angular resolution compared to the VLTI, but at sub-mm wavelengths. ALMA will observe the chemical cycle of the interstellar medium from the formation of molecules and dust in late-type stars and in molecular clouds to the



Figure 1. Participants in the interferometry primer.

formation of stars and planetary systems, and possibly probe the chemistry of pre-biotic molecules in nearby forming planetary systems and in our own Solar System.

With the first generation of VLTI instrumentation reaching maturity, the work on second generation instruments well advanced and the opening of the ALMA Early Science due on a timescale of one year, the workshop was very timely with the presentation of many new results and an overview of the future possibilities.

### Interferometry primer

The science sessions of the workshop were preceded by a one-day ALMA+VLTI interferometry primer. It was organised with the aim of enabling attendees without experience in interferometry to advance from the basics and to be able to assess the interferometric results presented during the workshop and to develop project ideas for discussion. The morning of the primer was dedicated to the principles of interferometry in general and the techniques to implement them in the infrared and radio wavelength regimes. The afternoon session focused on the practical use of ALMA and the VLTI, including the opportunities to use these facilities, the preparation of observations and the data reduction. A feedback chart showed that the vast majority of the participants in the primer (see Fig-

ure 1) were indeed highly interested in both the VLTI and ALMA, and that the primer was perceived as being useful for their work.

### From young stellar objects to main sequence stars

The science sessions started with a discussion of molecular clouds and the first stages of stellar evolution, from proto-stars to the main sequence, and the formation, detection and characterisation of planets. Recent interferometric measurements at near-infrared, mid-infrared, centimetre and millimetre wavelengths were presented. The latest results presented in these areas from the VLTI are currently transforming our understanding of the disc–star interaction and the inner regions of protoplanetary discs. The VLTI is already approaching the frontier of imaging the inner discs, an area which will flourish with the second generation instruments.

The expected impact of ALMA was emphasised with the presentation of results from the current generation of (sub)millimetre arrays. The progress expected in the areas of the structure and chemistry of clouds and the earliest phases of collapse of molecular cores is enormous, as the improved sensitivity and frequency coverage will allow detailed studies of the less abundant species. If the study of these early phases is mostly believed to be the realm of ALMA, the synergy of infrared and millimetre observations

is expected to produce a spectacular advance in our understanding of the structure of young stellar objects and protoplanetary discs (see Figure 3). The discussion focused on the continuum of disc properties from primordial discs to debris discs and planet formation and their further evolution toward giants and white dwarfs. Several unsolved questions were raised, such as, for example, how the true disc mass can be measured, how disc properties can be constrained in the areas we can't spatially resolve, how larger bodies can be traced, how pre-main sequence tracks can be better constrained, and what happens to debris discs and planets once the star leaves the main sequence. The combination of VLTI and ALMA measurements will allow us to obtain comprehensive, high angular resolution observations of the dust and gas evolution in discs, both essential ingredients for our understanding of the planet formation process.

**From the main sequence to late stages of evolution**

The session on stellar evolution from the main sequence onward started with overviews on the current state-of-the-art of stellar evolution as well as stellar atmospheres, and, in particular for evolved stars, on the latest hydrodynamic model atmospheres. The session included presentations of the newest results in the fields of red giant branch (RGB), asymptotic giant branch (AGB), post-AGB stars and planetary nebulae (PNe). Infrared interferometry with the VLTI and other interferometers has made enormous progress, in particular in studying the details of the molecular and dusty shells around AGB stars. By comparison to the latest hydrodynamic wind models, these studies address the unsolved problem of mass-loss and the dust driving mechanisms. For post-AGB stars, the emphasis of the presented results was placed on the origin and evolution of discs — connecting the session back to the first session on young stellar objects, on binarity, magnetic fields and the shaping mechanisms in general. Presented observations, using radio and millimetre interferometers, such as the Very Large Array (VLA), the Very Large Bolometric Array (VLBA), Merlin, or the Institut de Radio-



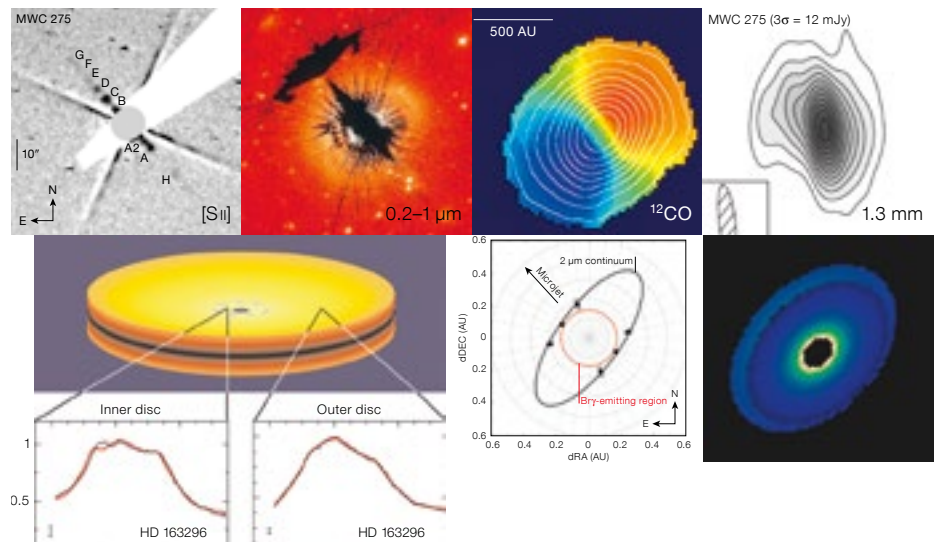
Figure 2. Participants of the workshop in the entrance hall at ESO Headquarters.

astronomie Millimétrique (IRAM) Plateau de Bure Interferometer, trace the mass-loss through the maser and dust zones in a complementary way (see Figure 4). They show an amazing chemistry and allow investigations of the nucleosynthesis in AGB stars.

The synergy of the VLTI and ALMA will again be essential in the further study of the dust production in AGB stars and their yields to the interstellar medium. The ALMA angular resolution is very well-matched with the size of the structures in AGB radio photospheres and envelopes, allowing their detailed study. Of particular interest will be the study of the millimetre transitions of water and its isotopes, especially with the ALMA Band 5 receivers, a small set of which are being built in the framework of the ALMA Enhancement project funded by the European Commis-

sion as part of the FP6 actions. During the discussions on these sessions, one question was how detailed theoretical models need to be for comparison to observations and how they can best be made readily available. Another point of discussion was that many of the presented results focused on rather extreme AGB stars, and whether we might miss the characteristics of less extreme giant stars that make up the majority in stellar populations.

Figure 3. A collection of results on HD 163296 from the presentation by Stefan Kraus. HD 163296 is a young disc very well observed in the millimetre range and with the VLTI. These results nicely illustrate the complementarity of millimetre and infrared interferometry for the same source. The figure includes results by Wassell et al., 2006; Grady et al., 2000; Isella et al., 2007, 2009; van Boekel et al., 2004; Kraus et al., 2008; Benisty et al., 2010 (from left to right and top to bottom).



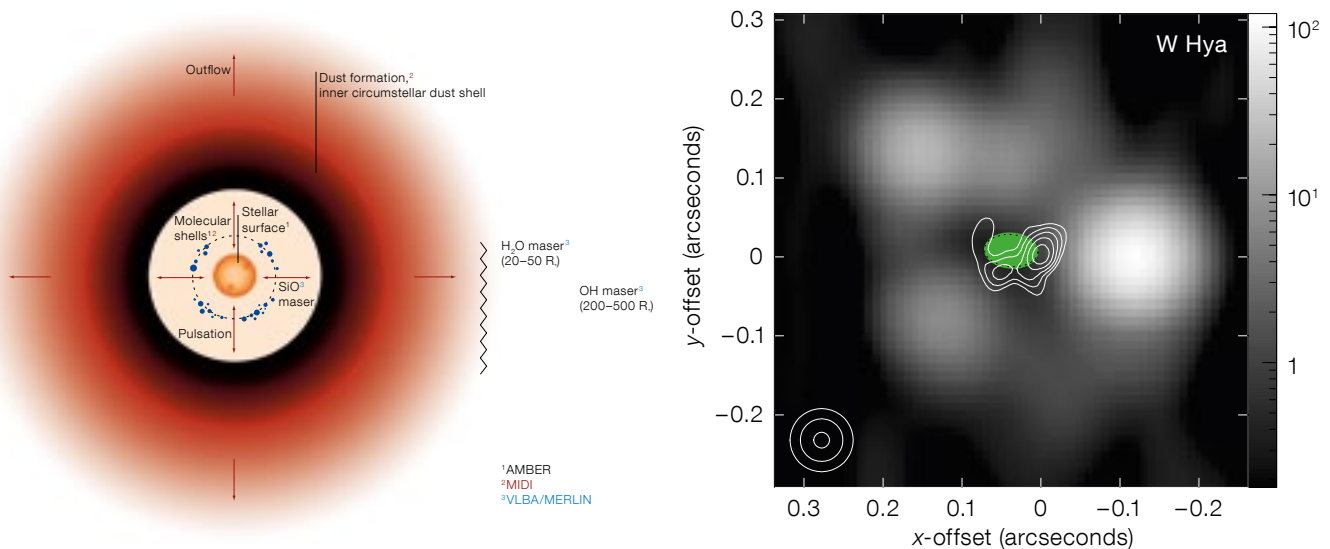


**Figure 4.** Left: A sketch of the atmosphere and circumstellar environment of AGB stars, as shown during the workshop in the presentation by Iva Karovicova (Credit: ESO/ePOD). The different regions can be studied by infrared, millimetre, and radio interferometers in a complementary way. Right: Recent simultaneous observation of the radio photosphere (green), the SiO maser shell (contours), and the H<sub>2</sub>O maser shell (gray scale) of the AGB star W Hya, from Reid & Menten (1990, 2007), as shown during the workshop in the presentation by Karl Menten.

## Facilities

The workshop ended with two presentations on the observational opportunities with the VLTI and the prospects with ALMA for solar-mass stars. Current VLTI instruments include the near-infrared instrument AMBER and the mid-infrared instrument MIDI. These instruments have already produced more than 100 refereed publications, most of which are in the field of stellar physics. First images based on VLTI data have already been obtained (cf. Kraus et al., 2009; Le Bouquin et al., 2009). The astrometric facility PRIMA (cf. van Belle, 2008) is being commissioned, and the second generation VLTI instruments MATISSE and GRAVITY are being designed. MATISSE is a four-beam mid-infrared instrument with the capability of providing reconstructed images; the main science cases are investigating star and planet formation, in particular tracing protoplanets, active galactic nuclei, evolved stars and Solar System minor bodies. GRAVITY is a four-beam near-infrared (2.2  $\mu\text{m}$ ) instrument with a spectral resolution of 20 to 4000, with

internal fringe tracking and dual-feed, with its own infrared adaptive optics, and an astrometric precision of 30 micro-arcseconds. Its main science goals include the detection of special and general relativistic effects in the cusp star orbits and other cases around the Galactic Centre, orbits of extrasolar Jupiter/Uranus mass planets, imaging jets and discs in young stellar objects, proper motions in massive star clusters and stellar motions and gas flows in galactic centres.

ALMA is designed and being built with the goal of providing, also to non-radio interferometry experts, an instrument to obtain high fidelity, high resolution and high sensitivity 3D images (cf. Haupt & Rykaczewski, 2007; Tan et al., 2009). The main science goals of ALMA cover the evolution of interstellar matter and star formation across the Universe as well as the detailed study of the chemical complexity in our own Galaxy and the Solar System. A comprehensive account of the science expected with ALMA is collected in the ALMA Design Reference Science Plan (cf. Testi, 2008). Science topics for solar-mass stars include the physical and chemical conditions of molecular clouds and the origin of the stellar initial mass function, the structure of protostars, protoplanetary disc evolution and the birth of planets, as well as the production of dust and complex molecules in the late stages of stellar evolution. ALMA is expected to announce the opportunity for Early Science observations with sixteen anten-

nas, four frequency bands and baselines up to  $\sim 1$  km by the end of 2010 or early 2011. During the early years, ALMA will constantly grow in its capabilities, eventually reaching Full Science Operations with the full complement of antennas, receivers and baseline lengths, expected for 2013.

Overall, the excellent presentations at the workshop provided an interesting and exhaustive overview on the current problems of stellar physics for solar-mass stars. Common problems in stellar evolution were discussed, such as the structure of discs for young stellar objects, Be stars and post-AGB stars. The role of infrared as well as millimetre interferometry to provide spatially resolved information was highlighted throughout the workshop. Often, the complementarity of the two was emphasised, stressing that the combination of different wavelengths can solve model ambiguities inherent in spectral energy distribution (SED) modelling and single-wavelength observations. Many presentations included comparisons with sophisticated theoretical modelling, such as hydrodynamic wind models for evolved stars, models of the disc structure around young stellar objects (YSOs), or a comparison of stellar parameters with evolutionary calculations. Presentations of the combination of interferometric techniques with other techniques, such as high resolution spectroscopy or adaptive optics imaging were also mentioned, such as for active stars or fundamental parameters of evolved



stars. On this aspect, more insights into the physical mechanisms can probably be expected when such attempts become more frequent. Although the workshop focused on solar-mass stars, many presentations also included related work on higher mass stars, such as the connection between solar-mass and high-mass young stars, or between AGB stars and supergiants.

All the talk and poster presentations, including the presentations of the interferometry primer, are available from the website of the workshop<sup>1</sup> in PDF format.

#### Acknowledgements

The organisation of this workshop would not have been possible without the dedicated help of the local organising committee members Christina Stoffer, Iva Karovicova, Eric Lagadec, Alma Ruiz Velasco, Ulf Seemann, and Paula Teixeira, and the guidance of the scientific organising committee members Rachel Akeson (Caltech), Martin Asplund (MPA), Maria-Rosa Cioni (University of Hertfordshire), Malcolm Fridlund (ESA), Andrea Richichi (ESO), Gerard van Belle (ESO) and Christoffel Waelkens (Katholieke Universiteit Leuven), who also chaired the sessions and lead the discussions. We are also grateful to all participants who travelled to Garching and presented their latest results.

#### References

Benisty, M. et al. 2010, A&A, 511, A74  
Grady, C. A. et al. 2006, ApJ, 544, 895

Haupt, C. & Rykaczewski, H. 2007, The Messenger, 128, 25  
Isella, A. et al. 2007, A&A, 469, 213  
Isella, A. et al. 2009, ApJ, 701, 260  
Kraus, S. et al. 2008, A&A, 489, 1157  
Kraus, S. et al. 2009, The Messenger, 136, 44  
Le Bouquin, J.-B. et al. 2009, The Messenger, 137, 25  
Reid, M. J. & Menten, K. M. 1990, ApJ, 360, L51  
Reid, M. J. & Menten, K. M. 2007, ApJ, 671, 2068  
Tan, G. H. et al. 2009, The Messenger, 136, 32  
Testi, L. 2008, The Messenger, 131, 46  
van Belle, G. et al. 2008, The Messenger, 134, 6  
van Boekel, R. et al. 2004, Nature, 432, 479  
Wassell, E. J. et al. 2006, ApJ, 650, 985

#### Links

<sup>1</sup> <http://www.eso.org/sci/meetings/stars2010>

Report on the ESO/ESA Workshop

## JWST and the ELTs: An Ideal Combination

held at ESO Garching, Germany, 13–16 April 2010

Markus Kissler-Patig<sup>1</sup>  
Mark McCaughrean<sup>2</sup>

<sup>1</sup> ESO

<sup>2</sup> ESA

ESA and ESO jointly organised a workshop to explore the synergies between the JWST and ground-based, extremely large telescopes (ELTs). The main goal of the workshop was to bring the JWST and ELT (GMT, TMT, E-ELT) communities together, to identify the common science cases, and to outline instrumentation/upgrade priorities for the ELTs that would maximise the scientific return in key areas of scientific research requiring both facilities, namely: The End of the Dark Ages — First Light and Re-ionisation; The Assembly of Galaxies; The Birth of Stars and Protoplanetary Systems; and Planetary Systems and the Origins of Life. A lively meeting with intense discussions brought some interesting insights.

Motivated by the advance of the three international Extremely Large Telescope (ELT) projects: the Giant Magellan Telescope (GMT), the Thirty Meter Telescope (TMT) and the European Extremely Large Telescope (E-ELT), as well as by the rapid progress towards a launch in 2014 of the James Webb Space Telescope (JWST), the European Space Agency (ESA) and ESO decided to jointly organise a meeting in order to explore the synergies between these facilities.

Astronomers can look back on two very successful decades of science dominated by the interplay between the Hubble Space Telescope and the 8–10-metre-class ground-based telescopes. The lessons learned from this powerful combination are being taken into account by the new projects. Some similarities to the past exist: JWST will lead the ground-based ELT projects by a few years and it is a facility that has its strength in imaging and low-resolution spectroscopy combined with exquisite sensitivity. The ground-based ELTs will follow with a

vastly superior photon-collecting power and a large and versatile number of scientific instruments. A few aspects will also differ. JWST will focus on longer wavelengths, with its main strength in the infrared and it will also have a limited lifetime of around 5+5 years, due to limited fuel. Also, the ELTs, assisted by adaptive optics, will provide a spatial resolution of almost an order of magnitude better than JWST. Thus, not only very high spectral, but also very high spatial, resolution might become the domain of the ground-based telescopes.

With this in mind, close to a hundred participants from Europe, North and South America as well as East Asia joined for the four day meeting held at ESO Headquarters in Garching, Germany. The sessions were not only of very high quality, thanks to very well prepared speakers, but were also very lively, with interesting and fruitful discussions. All talks can be found online on the web pages of the workshop<sup>1</sup>.

## An update on the status of the projects

The first afternoon was dedicated to an update of the various projects. Jonathan Gardner, deputy project scientist for JWST, reviewed the JWST capabilities and showed the impressive progress made in the last few years towards a launch in 2014. The large amount of flight hardware now assembled and being integrated and tested left the audience in no doubt that JWST is well on track (see Figure 1). Similarly, the four presentations on the JWST instruments — NIRSpec, NIRCам, MIRI and TFI — demonstrated the advanced stage of the instruments. All the instrument demonstration models are either on their way to, or already at, the Goddard Space Flight Centre ready to be integrated into the Integrated Science Instrument Module flight structure. Besides being reminded of the capabilities of JWST and its exquisite sensitivity in the near- and mid-infrared, the audience got, if it was still needed, the wake-up call to start planning for JWST by the middle of the decade.

The ELTs were presented in turn by Patrick McCarthy, who showed the advances of the GMT project, by David Crampton, who reviewed the progress of the TMT, and by Roberto Gilmozzi and Markus Kissler-Patig, who gave an update of the E-ELT programme. All three projects are in the process of transiting from their detailed design phase to the construction phase and aim at a first light before the end of the decade, about five years after the JWST launch. The suite of instruments investigated for these ground-based telescopes is impressive. A recurrent scheme is the support, with all possible flavours, of adaptive optics: at the diffraction limit, this capability will enable a spatial resolution between 3 and 10 milliarcseconds (depending on wavelength and telescope diameter), compared to  $> 60$  milliarcseconds for JWST, even at its shortest wavelength.

## The science sessions

The two following days were split into four topical sessions, following the main science areas of the JWST: The End of the Dark Ages — First Light and Reionisation; The Assembly of Galaxies; The



Credit: NASA/MSFC/Emmett Oivens

Birth of Stars and Protoplanetary Systems; and Planetary Systems and the Origins of Life. Each session was introduced by a review before giving room to typically five to six more focused contributions.

Avi Loeb opened the first session on First Light and Reionisation. He stressed that at high redshifts only a very small fraction of the galaxy mass had assembled and formed stars (i.e. looking at  $z > 5$  is looking at  $< 10\%$  of today's stars), and that star formation mostly proceeded in very small (and thus faint) structures, beyond the reach of the current facilities. The subsequent talks confirmed this picture and emphasised how much progress had been made most recently in exploring the properties of galaxies at redshifts of six, seven and beyond (see Figure 2). For future progress, structures of angular sizes of 100 milliarcseconds and below will have to be resolved at these high redshifts.

The topic of the Assembly of Galaxies was reviewed by Guinevere Kauffmann. A key message was the current discrepancy between some observational facts (e.g., the integrated star formation rate exceeds the stellar mass formed?!) and the associated problems of the theoreticians to connect models with data. Despite tremendous progress, our picture is still very incomplete and unsatisfactory. Subsequent talks explored how JWST

Figure 1. Six of the 18 James Webb Space Telescope mirror segments being prepared to move into the X-ray and Cryogenic Facility, at NASA's Marshall Space Flight Center.

and ELTs could help resolve these problems by investigating the properties of low- to intermediate-redshift galaxies. Detailed studies of nearby ( $z \sim 0$ ) galaxies could compete in the future with high-redshift ones when it comes to understanding the evolution of galaxies across time.

The second day started with a review by Michael Meyer on The Birth of Stars and Protoplanetary Systems. He emphasised that JWST would dominate in sensitivity and field of view, while the domain of the ELTs would be high spectral and spatial resolution. The combination of sensitivity of JWST in the infrared and the high spatial resolution of the ELTs promises fantastic progress in the study of star formation and protoplanetary discs. This theme was picked up by the other speakers of the session who expanded on the advance that would become possible in the study of star formation throughout the Local Group. It was also stressed that ALMA will of course strongly complement the JWST and ELTs. Yet, the audience was reminded that both JWST and the ELTs will all play a transformational role on their own.

Credit: NASA, ESA, G. Illingworth and R. Bouwens (University of California, Santa Cruz), and the HUDF09 Team

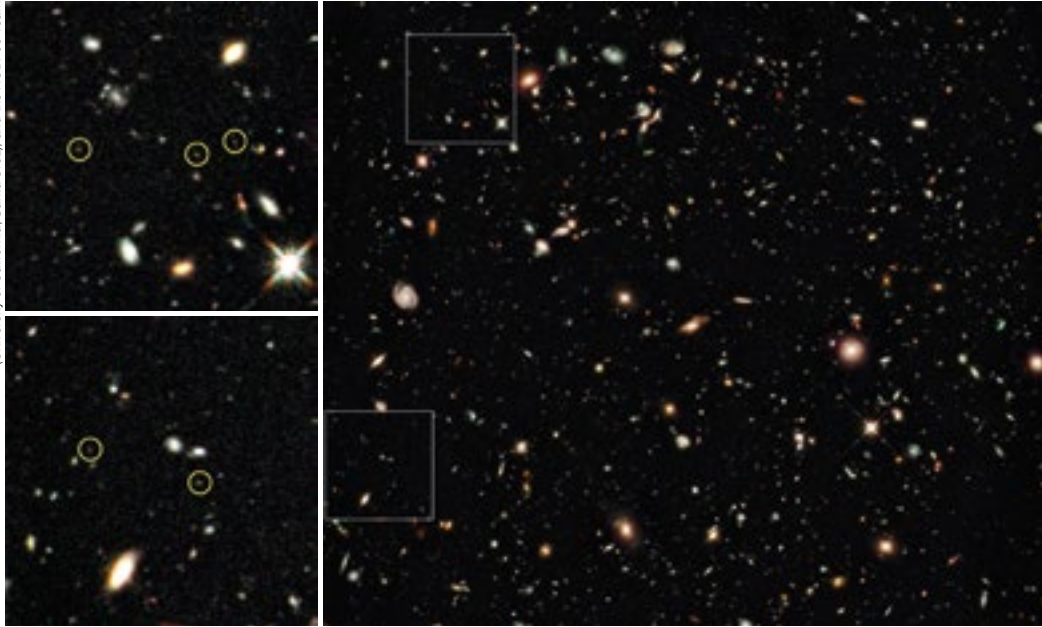


Figure 2. Early HST WFC3 near-infrared imaging observations have revealed  $z > 7$  galaxies from photometric redshifts in the Chandra Deep Field South.

The fourth session on Planetary Systems and the Origins of Life was introduced by Drake Deming. The prediction is that the race for characterising the atmosphere of a super-Earth in a habitable zone will be won by transiting planets, observed with JWST (c.f. Figure 3). Subsequently, more systematic atmospheric studies of exoplanets will probably await the planet imagers on ELTs. The advantage of JWST will be its high stability, required for precision differential work on exoplanets, while the ELTs will be able to exploit their high resolving power. The speakers agreed that the trend goes in the direction of searching for exoplanets around low-mass stars, for which planets in the habitable zone are easier to detect. Thérèse Encrenaz took the audience closer to home and provided an overview of the impressive Solar System science that the combination of JWST and ELTs would enable.

A final session on the last day peeked into a few more topics such as high time resolution and the complementarity with the Gaia mission, before moving into a long and lively general discussion.

### Discussion

The general discussion centred on a collection of questions that had been raised during the previous days. The questions

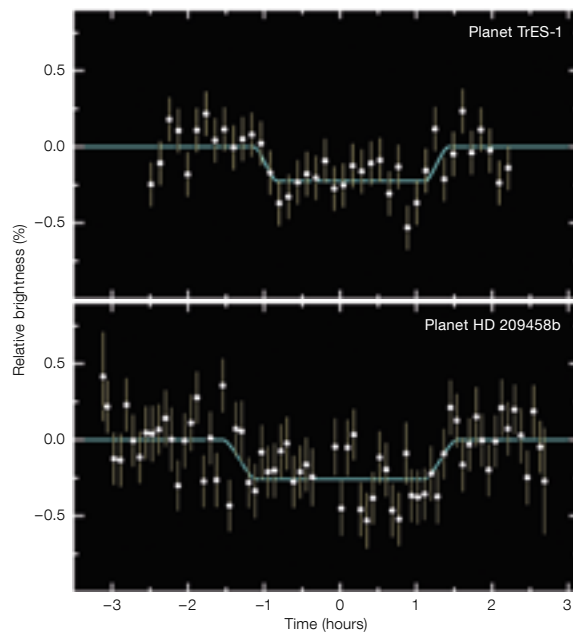


Figure 3. Two examples of light curves of exoplanet secondary eclipses (i.e. planet behind the star) observed with the Spitzer Space Telescope.

Credit: NASA/JPL-Caltech/D. Charbonneau (Harvard-Smithsonian CfA), D. Deming (Goddard Space Flight Center)

are reproduced below, followed, for some, by the strongly abridged (and subjective, for which the authors of this report apologise) answers. Rather than final answers, this should be seen a list of questions to think about further.

### Session 1

*Should JWST and/or the ELTs aim at very deep surveys to see the first galaxies?*

“Deep field” observations are conceivable, however time on these facilities will be too precious for classical surveys, which are better conducted with specialised facilities.

*What is the best strategy with JWST and ELTs to find Population III stars?*

Unclear. Serendipitous observations might be the key and slitless spectroscopy is the promising new kid on the block.



*In order to study the highest- $z$  galaxies: should we split the task into imaging with the JWST and spatially resolved spectroscopy with the ELTs?*

While the strength of each facility is recognised, enforcing a splitting does not make sense — scientists and TACs are trusted to ensure the best use of the facilities.

*Should ELTs aim at resolving  $z > 6$  objects if these are  $\ll 0.1$  arcseconds in size? If so, what is the best strategy?*

A realistic goal seems to be to resolve larger structures into 0.1-arcsecond components, but resolving the latter appears challenging even for ELTs.

## Session 2

*In order to study the “causality” in the process of galaxy formation and evolution, both gas and stars need to be understood: how can JWST and ELTs synergise?*

The “answer” was given in several talks.

*What are the physical parameters of  $z \sim 2-3$  galaxies that should be studied? “The usual suspects” and these will require spatially resolved spectroscopy.*

*Which redshift is most interesting to look at:  $z \sim 2$ , the peak of the star formation rate, or  $z \sim 6-10$  the epoch of reionisation?*

Both are equally important and JWST+ELTs will provide us with the opportunity to study  $z \sim 2-3$  galaxies in unprecedented detail, as well as for  $z \sim 6-10$  galaxies at the same level of detail as  $z \sim 2-3$  galaxies today.

## Session 3

*Should ELTs work at low spatial/spectral resolution, despite excelling at high resolution?*

Definitely. ELTs will complement JWST at short wavelengths and by having some particular modes (integral field spectroscopy, high time resolution, polarimetry).

*After five years of JWST operations (and nearly ten years of ALMA operations), what will be the most pressing questions to address with the ELTs?*

Many convincing answers were given, followed by the convincing argument that all predictions will turn out to be wrong.

*How important is the synchronicity of JWST and the ELTs?*

While iterating/bouncing between facilities (as today between HST and the 8–10-metre-class telescopes) is an advantage, no strong science case seems to call for it.

*Is the new “blue wavelength range” the near-infrared?*

It was felt that with the blue cut-off of JWST, with the push towards redder wavelengths due to adaptive optics for the ELTs, and with the strong science cases at high redshift and in star-forming regions, the science might indeed experience a push towards the red/infrared.

*Given the strong case for mid-IR instruments on ELTs — if one could put two mid-IR instruments on an ELT, which would they be? How important is low spectral resolution work from the ground given the JWST superiority?*

The mid-infrared wavelength range was indeed prominently advocated in Sessions 3 and 4 — advantages of distributing resources over the ELTs are seen and will be explored.

## Session 4

*Should the ELTs (and JWST) do any exoplanet detection work, or should they focus on their characterisation?*

Detection of many hundreds of exoplanets will have happened by the time the ELTs come online. Characterisation might then draw more attention. As stated above: long survey/detection campaigns will probably be too time-consuming to be conducted on the ELTs.

*Solar System work: do the JWST and the ELTs envisage tracking at non-sidereal rates (and at which)?*

Yes, both JWST as well as all the ELTs plan to track at non-sidereal rates, typically at rates such as to follow objects beyond the orbit of Mars.

*Biomarkers: they are challenging — should we nevertheless aim at looking for them? If so, what is the best strategy?*

Drake Deming had the final word on this question and proposed the “Zen approach”: search for life beyond the Solar System by not looking for it. In other words: life might appear in forms that our imagination is unable to grasp yet, thus a detailed study of exoplanet atmospheres and the possible detection of anomalies might be the best approach to search for biomarkers.

In Isaac Asimov’s words: “The most exciting phrase to hear in science, the one that heralds new discoveries, is not ‘Eureka!’ (I found it!) but ‘That’s funny ...’”. This workshop told us that the decade ahead of us, with the advent of the JWST and three ELTs, might become a really funny one.

## Acknowledgements

The organisers are most grateful to the SOC and the LOC (in particular to Christina Stoffer for handling the full logistics, and to Daniela Villegas for the help during the conference as well as for maintaining the web pages). The review speakers are thanked for their excellent job in introducing the topics, and all speakers for very interesting and enjoyable talks.

## Links

<sup>1</sup> <http://www.eso.org/sci/meetings/jwstelt2010/program.html>

# The ESO Solidarity Group in Support of the Earthquake Victims

## The ESO Solidarity Group\*<sup>1</sup>

<sup>1</sup> ESO

In the early morning of 27 February 2010, a devastating earthquake followed by a tsunami hit the central part of Chile. Immediate action initiated spontaneously by GEMINI and ESO employees, which was supported by the Solidarity Group, allowed around 500 kg of emergency supplies to be brought to the victims living in the countryside between Cauquenes and Pelluhue. The first-aid items were delivered on 2 March, before government help had reached these remote areas. This prompt action created the initial momentum for a series of concrete actions led by the Solidarity Group to further assist the earthquake victims. These acts of charity could be carried out thanks to the generosity of many ESO employees both in Europe and Chile who promptly answered the call for donations.

Based on requests from local communities and through on-site visits, a number of small projects were proposed. Due to limited resources, a selection was made to retain the cases where our support would be the most useful and efficient (depending on project size, condition of the potential beneficiaries, geographical

location and amount of help already received).

The main actions carried out so far have been:

- Construction of three wooden houses of area 25 m<sup>2</sup> in the village of Pichidegua (Rancagua area). This work, funded at the 50 % level by the ESO Solidarity Group, was completed by 5 April.
- Insulation of three wooden houses in the vicinity of Coinco village (Rancagua area) on the weekend of 10–11 April. In addition, 250 m<sup>2</sup> of roofing tiles to cover 20 emergency houses were bought and handed over to the administration of the Coinco Municipality.
- Construction of six wooden houses of area 30 m<sup>2</sup> in the village of Cumpeo (Talca area). This work is entirely funded by the Solidarity Group and is mainly executed by ESO volunteers. Work is currently ongoing.

A mosaic of photographs from these projects is shown on the News section page (p. 52). Other actions are planned and will be implemented as time and resources allow.

We would like to thank the ESO employees who made these actions possible through their donations and/or active participation as volunteers.

### The ESO Solidarity Group

In January 2008, inspired by the Garching Charity Group, eight ESO volunteers created the Solidarity Group in

Chile with the mission of providing support, mainly to ESO community members (employees and contractors) in emergency situations and in fund-raising for general charity work (such as donations to schools, old people's homes, non-profit organisations and handicapped individuals). By December 2009, the Solidarity Group had provided help to a contractor rebuilding her home lost in a fire, a contractor whose wife suffers from a severe illness that had to be treated with expensive medicine and an ESO staff member recovering from a heart transplant. Donations included an old, but operative, written-off science laptop to a paraplegic girl; written-off bed clothes and towels from the ESO Guesthouse to an old people's home; a wheelchair to a disabled ESO staff member; two fully filled trucks with obsolete written-off computer items to a state technical high school teaching youngsters to build and repair computers; two fully operative sets of written-off computers and printers to a primary school in Bahia Murta (an isolated distant southern Chilean village); and partial coverage of funding for specific medical treatments at the request of contractors. Since February 2010, all funds collected specifically to support the 27 February earthquake victims have been handled separately and exclusively directed to persons not belonging to the ESO community.

More information on the ESO Solidarity group can be found at <http://www.eso.org/intra/activities/charity/chile.html>.

\* The ESO Solidarity Group is composed of: Alejandra Emmerich (President), Maria Madrazo (Treasurer), Paulina Jiron (Secretary), Cecilia Ceron, Philippe Gitton, Agustin Macchino, Gianni Marconi, Francisco Olivares, Claudio Saguez, Linda Schmidtbreich

---

## ESO Participates in Germany's Girls' Day Activities

### Douglas Pierce-Price<sup>1</sup>

<sup>1</sup> ESO

On 22 April 2010, ESO participated in the Germany-wide Girls' Day activities, in which technical enterprises, universities and research organisations were invited

to organise an open day for girls, to give female school students an insight into science and technology professions and to encourage more of them to choose such careers in the future. The ESO Girls' Day, "An introduction to the work of the European Southern Observatory", was organised by a group of students and staff, with support from the education and Public Outreach Department.

Although the open day was publicised at relatively short notice, places were rapidly fully booked, and 33 students attended the event at ESO Headquarters in Garching. The students, aged between 11 and 15, came from a wide range of schools in the Munich area.

During the morning, a series of women speakers gave talks about the work of

ESO — whether in astronomy, technology, or engineering, how they had arrived at their current positions in the field, and current topics in astronomical research. After lunch, the visitors split into groups to try their hand at astrophysical exercises and calculations, observe the Sun with the help of volunteers from ESO's AGAPE group, tour the building and visit laboratories, and ask a representative from Human Resources about careers at

ESO. Finally, a live question-and-answer video connection to the VLT on Cerro Paranal let the students directly “visit” ESO's observatory site in Chile.

Girls' Day was an excellent opportunity for girls to discover the scientific, technological and engineering work of ESO. The feedback and questions asked made it clear that the students were inspired by what they saw, and many thanks are due

to the enthusiasm and hard work of the volunteers who put the Girls' Day programme together.

#### Links

Girls' Day in Germany: <http://www.girls-day.de/>

English information about Girls' Day in Germany: [http://www.girls-day.de/English\\_Information](http://www.girls-day.de/English_Information)

## New Staff at ESO

### Julien Girard

I am quite surprised to actually be writing this note for the Messenger. A couple of years ago I would never have believed I would be sitting in the VLT control room so often, understanding a lot of the stuff that's going on there, sometimes firing the laser out into the beautiful sky ...

Although my family was tremendously big, there weren't many scientists and I think I only got to look through a telescope once during my first ten years on Earth. One of my mom's uncles had a Meade 200 and we looked at the Moon. Since I showed an interest he actually wrote in his will that I should inherit the telescope. I did. But living in a city apartment, and spending most of my free time on ski slopes, sports fields and in violin classes, I am very ashamed not to have used the telescope much. Now as a professional astronomer, I have a growing amateur interest and one of these days I will definitely let my kids look through this telescope!

As I grew up — in the “middle-east of France” — I was always attracted by science and technology. I studied physics in college with a focus on physical measurement and instrumental techniques. This undergraduate experience in France fostered my interest in understanding

physical processes through measurement and mastering the instruments and methods used. I then completed a Master's degree in instrumentation physics at the University of Utah (USA), following on from my first degree. At Utah I carried out a research project for the High Energy Cosmic Ray group led by Pierre Sokolsky. Supervised by Lawrence Wiencke, I built a fiber-optic based calibration system for a giant cosmic ray observatory using the air fluorescence technique (the one that inspired the extensive air shower detectors of the Pierre Auger Observatory). This nice work and life experience motivated me to do research and study towards a PhD. Attracted by astronomy, I went for a second Master's degree in astrophysics in Grenoble (France) and learned the basics in many astronomical fields such as star formation and evolution, interstellar matter, galactic dynamics, cosmology, high angular resolution techniques, etc.

But clearly, I wanted to work closely with instruments so I chose my Master's thesis project on integrated optics component tests for interferometric beam merging (at LAOG/CEA in Grenoble). Then I was awarded a three-year scholarship to pursue full-time research in the AIRI team (Astronomy and Interferometric Resolution Imaging) at CRAL (Lyon) under the supervision of Renaud Foy. My PhD work



Julien Girard and family

was on the polychromatic laser guide star project ELPOA which aims at making diffraction-limited AO (adaptive optics) possible at visible wavelengths with full sky coverage. In fact, Renaud was the first (together with the well-known Antoine Labeyrie) to propose the artificial laser reference star concept to the astronomical community in 1985. I then worked for three years in Mexico City, first as a postdoctoral fellow at UNAM's Institute of Astronomy and then as a Professor at Instituto Politecnico Nacional (IPN). I completely embraced the country, melted in, had my wonderful “FrenXicán” daughter and got married with live musicians playing Huapangos Huastecos (songs



from the Huasteca region near the Gulf of Mexico). On the scientific side, I gravitated more towards observational astrophysics and somewhat less to instrumentation.

Since August 2009 I have been working as an Operations Staff Astronomer at ESO, spending my time between Santiago and the Paranal Observatory. I support night-time operations at UT4 (Yepun) where most adaptive optics systems are situated and recently became NACO instrument scientist. I am also trying to coordinate the activities of a revived Adaptive Optics group at ESO/Chile. The remaining time is dedicated to my personal research or R&D projects, collaborations, etc. For me, it's great to be working at the VLT where so many colleagues visit from everywhere in the world. I am trying to use my instrumental background to better serve the observatory's needs and allow the users to achieve their scientific goals. I get to learn a lot from them as well and eventually participate in some projects. The commissioning activities with Garching staff or consortia people are fun and intense work periods which I enjoy particularly. Operating such great instruments and executing OBs for these amazing programmes is thrilling. Sometimes I switch from a direct exoplanet hunt to an Einstein Cross-like lensed quasar, or zoom into the dust of the radio galaxy Centaurus A. Viewing a flare in the Galactic Centre "live" (though happening about 26 000 years ago) is also something which would move any astronomer. My astrophysical interests are broad and I am currently involved in very diverse projects involving high contrast and high angular resolution imaging and spectroscopy in the near-infrared. They range from searches for faint companions (brown dwarfs and giant exoplanets) to young stellar objects and even to AGN characterisation. I like to bring people together and motivate them to reach common goals. I think modern astronomy implies international collaborations and team work.

In Mexico I also became more and more interested in public outreach. As 2009 was the International Year of Astronomy, I produced a photographic exhibition called *Ella es Astrónoma* about women astronomers. This project was a great

success (more information can be found on my web page: [www.sc.eso.org/~jgirard/astronoma](http://www.sc.eso.org/~jgirard/astronoma)). I think that science, and astronomy in particular, isn't completely useless to society. As professionals we must pass on our knowledge and fill the young, and not-so young, public with wonder. I am also fond of photography, anthropology and traditional music from everywhere. I hope one day to bring my passions together through the organisation of popular events, why not ...

Nevertheless I think as observational astronomers we have the greatest, though most bizarre, job. We live at night in awkward places, seeking photons which we turn into intelligible (to some of us only) FITS files. I find it difficult to spend so many nights on the mountain, far away from my family in Santiago and even further away from my family in France and my wife's family in Mexico. As I am finishing this note, my eight-months pregnant wife could call anytime and ask me to rush back to Santiago if serious contractions were to start ... But I've just celebrated my 100th night at the observatory and there isn't a single day or night I spend there without having at least one "eureka moment", something that amazes me (like the clearest southern sky), or something I suddenly come to understand. This is what makes me love my job and hopefully it will keep on happening.

#### Willem-Jan de Wit

For the best part of the past decade I have held various post-doc positions in Europe. All were related to Galactic star formation and the physics of young stars, and gradually my work evolved towards high angular resolution observations and especially optical interferometry.

I started out as an astronomer performing photometry and spectroscopy on my favourite targets. I graduated from the University of Utrecht in 2001. My PhD was blessed with having two fantastic supervisors: Henny Lamers and Jean-Philippe Beaulieu. Shared supervision can sometimes lead to friction and even conflict, but not so in my case. The acute scientific insight and strong social abilities of my supervisors created a friendly



Willem-Jan de Wit

but sharp scientific atmosphere in which there was a strong sense of "teaming-up" in order to solve the open issues.

I moved to Arcetri in 2002, where I obtained a post-doc position within the European Research Training Network "Young Stellar Clusters". A better place than Florence Observatory is hard to find, either scientifically or socially. Living the Italian-style life in Tuscany is fantastic, and doing astronomy in this setting makes it even more so. Florence is special to me for another reason as it is the city where I met my wife and where we got married. In the communicative and stimulating environment of Arcetri, I continued to work on star formation issues, in particular the ones related to the formation of stellar clusters and massive stars.

In the third quarter of 2004, I traded Arcetri for LAOG in Grenoble. If Florence equals history and culture, then Grenoble equals natural Alpine beauty and all its sporting opportunities. This was not a bad trade. In those days, LAOG was abuzz because the AMBER instrument had just been successfully paralysed (first UT fringes in May 2004). My new job was dedicated part-time to the use of AMBER in the study of young stars. It was the start of my interferometric adventure that eventually would provide me with my current job as VLTI staff astronomer. My part-time involvement in AMBER convinced me, as a non-interferometrist, of the indispensable benefits of observations at (sub-)milliarcsecond resolution to

properly answer longstanding open questions related to, in particular, massive star formation. LAOG provided the opportunity to make me feel comfortable with optical interferometry and to start exploiting the VLTI to do my science. All this, while enjoying the green pastures of Le Vercors and the Belledonne.

The interest in using the VLTI to study massive star formation I shared with the astronomers at the School of Physics and Astronomy at the University of Leeds. At a conference in Catania (2005), I established first contact with that group. This eventually led to a move to England in autumn 2006. At Leeds, I took up

a post-doc position that was 100 % dedicated to doing high angular resolution observations of massive young stellar objects. The Leeds group manages to provide an ambitious scientific environment where the Friday-afternoon (or any day really) pub visit is part of a healthy standard protocol. My stay in Leeds turned out to be a very fruitful period in my career in which my interests in optical interferometry continued to develop and expand. This path went naturally hand-in-hand with an increased experience with the VLTI facility.

Last February, together with my wife and two-year old son I moved to Chile in

order to take up a position as VLTI staff astronomer. To my mind, in the last couple of years, the VLTI has shown its abilities to provide the community with unique astronomical observations at mind-boggling angular precisions, leading to impressive breakthroughs in a range of areas in stellar astrophysics. With the advent of PRIMA, the imminent arrival of PIONIER and the future second generation instruments, the impact the VLTI will continue to have on the advancement of astronomy and our understanding of astrophysics will be invaluable. I am sincerely grateful that I can be a part of this ongoing effort.

## Fellows at ESO

### Nadine Neumayer

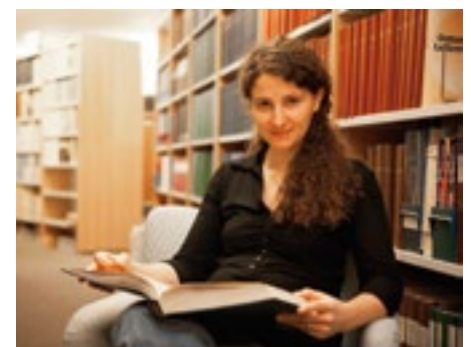
Looking at the crystal clear winter night skies I so often enjoyed – growing up in the middle of nowhere in south-west Germany – I always asked myself where all “this” comes from and where it will all go. I was fascinated by the fact that our planet Earth is just a tiny blue dot orbiting a star amongst millions of stars in a galaxy amongst billions of galaxies in a possibly endless Universe. This thought still blows my mind, and makes me want to learn more about the origin and evolution of the Universe.

After high school I wanted to find out what the life and work of an astronomer would be like. So I travelled to Chile to visit the La Silla Observatory (Paranal was still under construction at that time). Little did I know that I would end up working at ESO!

With a deep wish to become a professional astronomer, I went to the University of Heidelberg for my undergraduate studies. Afterwards I moved to Cam-

bridge, in the United Kingdom, for one year to take Part III of the Mathematical Tripos. It was during that time that my interest in black holes arose. Back in Heidelberg I finished my Diploma (MSc) with the thesis that led to my first publication – signed with my maiden name Nadine Häring. I had found my heart in Heidelberg and stayed at the Max-Planck Institute for Astronomy for my PhD, studying the nucleus of Centaurus A in great detail.

Half way through my PhD I had my first daughter, Johanna. With the great support of many people and a fellowship from the Christiane Nüsslein-Volhard-Foundation, I finished my PhD thesis at the beginning of 2007, already knowing that I would start an ESO Fellowship at the end of the year. My second daughter, Lena, was born just a few months before I started my Fellowship at ESO. Luckily, ESO contributes to a daycare unit together with the neighbouring Max-Planck Institutes, and I was more than happy to receive confirmation that both girls had a place there.



Nadine Neumayer

My research focuses on the co-evolution of black holes and galaxies and I am especially interested in how black holes get to the centres of galaxies in the first place. Along with my research I also have functional duties at ESO where I am involved with the education and Public Outreach Department, and I am part of the VISTA Science Verification Team. I am also co-organising the monthly Wine and Cheese Seminar, which has allowed me to interact with many visiting as well as ESO astronomers.

ESO is a great place to be scientifically, but also because it is a very family-friendly employer. I am happy to be part of it and to have the opportunity to live my childhood dream!

### Irina Yegorova

Like most astronomers I was fascinated by the night sky from my childhood. In addition, visiting a planetarium at the age of five, and a passion for science fiction during my school years, made me choose the profession.

I did my undergraduate studies in my home city, at the Odessa National University (Ukraine). My master's thesis was dedicated to studies of sodium enrichment of stellar atmospheres. My first observational experience at the Crimean Observatory just confirmed my desire to be an astronomer. Later I moved to Trieste, Italy, to do my PhD thesis at SISSA-ISAS (International School for Advanced Studies). My PhD project was dedicated to studies of dark and luminous matter in spiral galaxies. Although SISSA-ISAS is a theoretical institute, I always tried to expand my research towards the observational side. I remember writing a proposal for VIMOS and later reducing the data after obtaining observing time. At that time I could not imagine that only a few years in the future I would be supporting VIMOS.

I joined ESO in July 2008 as a fellow. Since my first visit to the Paranal Observatory, I have been enchanted by this place. It is so special: modern technology telescopes, the deep blue sky and the red stony landscape that gives you a feeling of being on planet Mars, rather than on Earth. For functional duties I support Melipal (UT3), and I am the instrument fellow for VISIR, the mid-infrared spectrometer and imager. Working at Paranal is challenging, but also very enthralling. It gives me an opportunity to appreciate the latest astronomical investigations, from the Solar System to redshift 8, and beyond.

When I am at Paranal I try to use any free minute to look at the stars. The southern hemisphere night sky is one of the most amazing things that I have ever seen. Looking at it reminds me of how lucky we are to uncover the secrets of the Universe. The visible sky is so beautiful and knowing that it represents only a small fraction of what can be seen makes it even more enigmatic.

Despite its geographical isolation, Chile has become a very active centre for astronomy, with such important sites as the VLT and ALMA and in the future the E-ELT. Therefore Chile offers plenty of opportunities to meet astronomers from institutes worldwide. Our science life in the Vitacura office is really vivid. Enthusiastic observers coming back from their



Irina Yegorova

campaigns are excited to share the first results of their observations. The Vitacura office is full of enthusiastic people, and you can feel at the forefront of both technology and research. This gives me inspiration for new ideas for my research. My current scientific interest covers the wide topic of galaxy formation and evolution — starting from giant spiral galaxies and finishing with tiny dwarfs. I study the dynamical properties of these objects, together with their chemical evolution history. Understanding the origin of spiral galaxies means understanding our own origin as inhabitants of the dearest disc galaxy to us, the Milky Way!



A 360-degree panorama of Paranal Observatory and the southern sky taken before morning twilight. The Moon is just rising and the zodiacal light is visible, while the Milky Way stretches across the sky.





ESO

European Organisation  
for Astronomical  
Research in the  
Southern Hemisphere



## ESO Fellowship Programme 2010/2011

The European Organisation for Astronomical Research in the Southern Hemisphere awards several postdoctoral fellowships each year. The goal of these fellowships is to offer outstanding young scientists opportunities and facilities to enhance their research programmes in close contact with the activities and staff at one of the world's foremost observatories.

In *Garching*, the fellowships start with an initial contract of one year followed by a two-year extension (three years total). The ESO Headquarters in Garching near Munich, Germany, are situated in one of the most active research areas in Europe and have among the highest concentrations of astronomers. ESO offices are adjacent to the Max-Planck Institutes for Astrophysics and for Extraterrestrial Physics and only a few kilometres away from the Observatory of the Ludwig-Maximilian University. Additionally, ESO participates in the newly formed Excellence Cluster on Astrophysics on the Garching Campus, which brings together nearly 200 scientists to explore the origin and structure of the Universe. Consequently, ESO fellows in Garching have many opportunities to interact and collaborate with astronomers at neighbouring institutes. In addition to the excellent scientific environment that will allow them to develop their scientific skills, as part of the diverse training ESO offers, Garching fellows spend up to 25 % of their time in some functional work related to instrumentation, operations support, archive/virtual observatory, VLT, ALMA, ELT, public affairs or science operations at the Observatory in Chile.

In *Chile*, the fellowships are granted for one year initially with an extension of three additional years (four years total). During the first three years, the fellows are assigned to one of the operation groups on Paranal, ALMA or APEX. Fellows contribute to the operations at a level of 80 nights per year at the Observatory. Apart from opportunities for scientific interactions within ESO, fellows have the possibility to collaborate with the rapidly growing Chilean astronomical community as well as with astronomers at other international observatories located in Chile. The addition of a new ALMA building next to ESO's Santiago offices in 2010 and the arrival of many astronomers and fellows working on the ALMA project will further enhance the stimulating scientific environment available to ESO Chile fellows. During the fourth year there is little or no functional work and several options are provided. The fellow may be hosted by a Chilean institution (and will thus have access to all telescopes in Chile via the Chilean observing time). Alternatively, she/he may choose to spend the fourth year either at ESO's Astronomy Centre in Santiago, or at the ESO Headquarters in Garching, or at any institute of astronomy/astrophysics in an ESO member state.

The programme is open to applicants who will have achieved their PhD in astronomy, physics or related discipline before 1 November 2011. Young scientists from all astrophysical fields are welcome to apply. For all fellowships, scientific excellence is the prime selection criterion.

We offer an attractive remuneration package including a competitive salary and allowances (tax-free), comprehensive social benefits, and provide financial support for relocating families.

The closing date for applications is 15 October 2010.

Candidates will be notified of the results of the selection process between December 2010 and February 2011. Fellowships begin between April and October of the year in which they are awarded.

Please apply by completing the web application form available at <http://jobs.eso.org>. Applications must include:

- your Curriculum Vitae including a list of publications (ONLY published papers, NOT papers in preparation);
- your proposed research plan (maximum two pages);
- a brief outline of your technical/observational experience (maximum one page).

In addition three letters of reference from persons familiar with your scientific work should be sent directly to ESO to [vacancy@eso.org](mailto:vacancy@eso.org) by the application deadline.

For more information about the fellowship programme and ESO's astronomical research activities please see <http://www.eso.org/sci/activities/ESOfellowship.html>. For a list of current ESO staff and fellows, and their research interests please see <http://www.eso.org/sci/activities/personnel.html>. Details of the Terms of Service for fellows including details of remuneration are available at <http://www.eso.org/public/employment/fellows.html>. For further general information about fellowship applications, please read our list of Frequently Asked Questions (FAQ) at <http://www.eso.org/sci/activities/ESOfellowship-faq.html>.

Questions not answered by the above FAQ page can be sent to: Ferdinando Patat, Tel +49 89 32006-744, e-mail: [fpatat@eso.org](mailto:fpatat@eso.org)



Announcement of the ESO Workshop on

## The Impact of Herschel Surveys on ALMA Early Science

17–19 November 2010, ESO Headquarters, Garching, Germany

The Atacama Large Millimeter/submillimeter Array (ALMA) is expected to release the call for Early Science proposals towards the end of 2010 and from 2011 will provide a huge breakthrough in exploring the “cool Universe”. ALMA will open up the study of the earliest evolutionary stages of galaxies, stars and planets that are deeply hidden within dust clouds where the optical extinction can be extremely large. However at far-infrared and submillimetre wavelengths we can directly measure physical phenomena associated with the formation process itself.

Complementary to ALMA is the Herschel Space Observatory satellite, which was successfully launched in May 2009, and is already presenting its first exciting results. By the end of 2010 Herschel will have been flying for approximately 1.5 years and it is likely that a large fraction of the key programme observations will have been completed. Data reduction and analysis will be well underway and it will be ideal timing to focus the community on the possibilities of an early follow-up of Herschel surveys with ALMA.

ALMA has a small instantaneous field of view, but allows high angular resolution images of selected sources, while Herschel has a larger field of view, with a lower angular resolution. The Herschel Spectral and Photometric Imaging Receiver (SPIRE) and Photodetector Array Camera & Spectrometer (PACS) bolometer cameras offer the opportunity to cover large areas of the sky rather quickly, providing finding lists for ALMA and allowing shorter wavelength measurements of the source emission to give complete spectral energy distributions. ALMA measurements will offer unique follow-up opportunities of the Herschel continuum and heterodyne spectroscopy surveys.

The goal of the workshop is to bring together the community of astronomers involved in Herschel Key Programmes that will be interested in proposing for ALMA Early Science. At the workshop we will discuss the early results of Herschel in the context of the Call for Proposals for ALMA Early Science, and foster possible collaborations to prepare a coordinated response to the first ALMA science from the community of Herschel users.

The potential for deep legacy-type surveys with the completed ALMA array will also be discussed.

For this workshop we are inviting contributions that present both scientific results based on Herschel surveys, and investigate the exciting possibilities of the ALMA interferometer during Early Science.

Main science topics include:

- Solar System
- Galactic low-mass star formation
- Galactic high-mass star formation
- Molecular clouds
- Protoplanetary discs
- Local Group
- Nearby galaxies
- Active galactic nuclei
- Galaxy clusters
- Cosmological background

For registration and more information please visit <http://www.eso.org/sci/meetings/almaherschel2010/>.

## Personnel Movements

### Arrivals (1 April–30 June 2010)

#### Europe

Barriga Campino, Pablo Jose (RCH)	Electronic Engineer
Brinkmann, Martin (D)	Mechanical Engineer
Manning, Alisdair (GB)	Software Engineer

#### Chile

Guieu, Sylvain (F)	Fellow
Lopez, Marcelo (RCH)	Telescope Instruments Operator
Olivares, Manuel (RCH)	Telescope Instruments Operator
Parra, Ricardo (RCH)	Mechanical Engineer
Vuckovic, Maja (SRB)	Fellow

### Departures (1 April–30 June 2010)

#### Europe

Calamida, Annalisa (I)	Post Doctoral Researcher
D’Odorico, Sandro (I)	Head of Optical Instruments
Döllinger, Michaela (D)	Fellow
Erdmann, Christopher (USA)	Librarian
Küpcü Yoldaş, Aybüke (TR)	Post Doctoral Researcher
Laaksonen, Milla (FIN)	Administrative Assistant
Moorwood, Alan (GB)	Director of Programmes
Randall, Suzanna (GB)	Applied Scientist
Sana, Hugues (B)	Fellow
Trotta, Francesco (I)	Student

#### Chile

Alquinta, Nilso (RCH)	Electrical Assistant
Huidobro, Ramon (RCH)	Technical Secretary
Le Saux, Paul (F)	Engineer
Lopez, Ignacio (RCH)	Precision Mechanic

Front Cover: A view of Cerro Armazones at sunset. Following the recommendation of the Site Selection Advisory Committee, on 26 April 2010, the ESO Council selected Cerro Armazones as the baseline site for the planned 42-metre European Extremely Large Telescope (E-ELT). The mountain is situated about 20 km from the VLT site on Cerro Paranal. (Credit: ESO/G. Lombardi)

Right: A near-infrared image of the Galactic star-forming region NGC 6334, named the Cat’s Paw Nebula. This VISTA colour-composite was composed of images in Y, J and Ks filters and the exposure time was 300 s per filter. See eso1017 for more details.







ESO, the European Southern Observatory, is the foremost intergovernmental astronomy organisation in Europe. It is supported by 14 countries: Austria, Belgium, the Czech Republic, Denmark, France, Finland, Germany, Italy, the Netherlands, Portugal, Spain, Sweden, Switzerland and the United Kingdom. ESO's programme is focused on the design, construction and operation of powerful ground-based observing facilities. ESO operates three observatories in Chile: at La Silla, at Paranal, site of the Very Large Telescope, and at Llano de Chajnantor. ESO is the European partner in the Atacama Large Millimeter/submillimeter Array (ALMA) under construction at Chajnantor. Currently ESO is engaged in the design of the 42-metre European Extremely Large Telescope.

The Messenger is published, in hard-copy and electronic form, four times a year: in March, June, September and December. ESO produces and distributes a wide variety of media connected to its activities. For further information, including postal subscription to The Messenger, contact the ESO education and Public Outreach Department at the following address:

ESO Headquarters  
Karl-Schwarzschild-Straße 2  
85748 Garching bei München  
Germany  
Phone +49 89 320 06-0  
information@eso.org  
www.eso.org

The Messenger:  
Editor: Jeremy R. Walsh  
Design: Jutta Boxheimer; Layout, Typesetting: Jutta Boxheimer and Mafalda Martins; Graphics: Roberto Duque  
www.eso.org/messenger/

Printed by Peschke Druck  
Schatzbogen 35, 81805 München  
Germany

Unless otherwise indicated, all images in The Messenger are courtesy of ESO, except authored contributions which are courtesy of the respective authors.

© ESO 2010  
ISSN 0722-6691

## Contents

### Telescopes and Instrumentation

G. Rupprecht et al. – Twenty Years of FORS Science Operations on the VLT	2
M. Kasper et al. – A New Lenslet Array for the NACO Laser Guide Star Wavefront Sensor	8
P. Martinez et al. – The High Order Test Bench: Evaluating High Contrast Imaging Concepts for SPHERE and EPICS	10

### Synopses of E-ELT Phase A and Instrument Concept Studies

S. D'Odorico et al. – An Introduction to the E-ELT Instrumentation and Post-focal Adaptive Optics Module Studies	17
T. Fusco – ATLAS: An Advanced Tomographic Laser-assisted Adaptive Optics System	18
L. Pasquini et al. – CODEX: An Ultra-stable High Resolution Spectrograph for the E-ELT	20
S. Morris, J.-G. Cuby – EAGLE: An Adaptive Optics Fed, Multiple Integral Field Unit, Near-infrared Spectrograph	22
M. Kasper, J.-L. Beuzit – EPICS: An Exoplanet Imaging Camera and Spectrograph for the E-ELT	24
N. Thatte – HARMONI: A Single Field, Visible and Near-infrared Integral Field Spectrograph for the E-ELT	26
E. Diolaiti – MAORY: A Multi-conjugate Adaptive Optics Relay for the E-ELT	28
B. Brandl et al. – METIS: A Mid-infrared E-ELT Imager and Spectrograph	30
R. Davies, R. Genzel – MICADO: The Multi-adaptive Optics Imaging Camera for Deep Observations	32
O. Le Fèvre et al. – OPTIMOS–DIORAMAS: A Wide-field Imaging and Multi-slit Spectrograph for the E-ELT	34
F. Hammer et al. – OPTIMOS–EVE: A Fibre-fed Optical–Near-infrared Multi-object Spectrograph for the E-ELT	36
L. Origlia et al. – SIMPLE: A High Resolution Near-infrared Spectrograph for the E-ELT	38

### Astronomical Science

J. Bean et al. – The CRILES Search for Planets at the Bottom of the Main Sequence	41
J. Vink – Spectropolarimetry of Wolf–Rayet Stars in the Magellanic Clouds: Constraining the Progenitors of Gamma-ray Bursts	46
P. Rosati – ESO–GOODS: Closing the Book, Opening New Chapters	50

### Astronomical News

M. Wittkowski, L. Testi – Report on the ESO Workshop “The Origin and Fate of the Sun: Evolution of Solar-mass Stars Observed with High Angular Resolution”	53
M. Kissler-Patig, M. McCaughrean – Report on the ESO/ESA Workshop “JWST and the ELTs: An Ideal Combination”	56
ESO Solidarity Group – The ESO Solidarity Group in Support of the Earthquake Victims	60
D. Pierce-Price – ESO Participates in Germany's Girls' Day Activities	60
New Staff at ESO – J. Girard, W.-J. de Wit	61
Fellows at ESO – N. Neumayer, I. Yegorova	63
ESO Fellowship Programme 2010/2011	65
Announcement of the ESO Workshop on “The Impact of Herschel Surveys on ALMA Early Science”	66
Personnel Movements	66

For caption to front cover image see page 66.